MARCUS PAURITSCH

Hydrogeology of relict rock glaciers (Niedere Tauern Range, Austria)

A dissertation submitted to the

Faculty of Natural Science

University of Graz

Austria

For the Degree of Doctor of Science

October 2016

Preface

This thesis is based on the research conducted between November 2011 and September 2016 at the Institute of Earth Sciences, NAWI Graz Geocenter, University of Graz, Austria. The work was supervised by Univ.-Prof. Dr.rer.nat. Steffen Birk and the investigations were performed in the course of a research project with the title “Wasserressourcen reliktischer Blockgletscher”-Water resources of relict rock glaciers. The project was co-funded by the European Regional Development Fund (ERDF) and the Federal Province of Styria funding program “Investitionen in Ihre Zukunft”. Principal investigator was Ass.-Prof. Mag. Dr.rer.nat. Gerfried Winkler. After the expiration of the research project, the thesis was partly funded by a scholarship of the University of Graz.

The content of this thesis is based on four papers in peer reviewed scientific journals. At the time of writing, three of them are already published and one is accepted for publication:

I:

Winkler G, Wagner T, Pauritsch M, Birk S, Kellerer-Pirklbauer A, Benischke R, Leis A, Morawetz R, Schreilechner MG, Hergarten S (2016a) Identification and assessment of groundwater flow and storage components of the relict Schöneben Rock Glacier, Niedere Tauern Range, Eastern Alps (Austria). Hydrogeology Journal, 24, 1-17, doi: 10.1007/s10040-015-1348-9.

II:

Pauritsch M, Birk S, Wagner T, Hergarten S, Winkler G (2015) Analytical approximations of discharge recessions for steeply sloping aquifers in alpine catchments. Water Resources Research, 51, 8729–8740, doi: 10.1002/2015WR017749.

III:

Pauritsch M, Wagner T, Winkler G, Birk S (accepted) Investigating groundwater flow components in an Alpine relict rock glacier (Austria) using a numerical model. Hydrogeology Journal, doi: 10.1007/s10040-016-1484-x.

IV:

Wagner T, Pauritsch M, Winkler G (2016) Impact of relict rock glaciers on spring and stream flow of alpine watersheds: Examples of the Niedere Tauern Range, Eastern Alps (Austria). Austrian Journal of Earth Sciences, 109, doi: 10.17738/ajes.2016.0006.

In this thesis, these papers are referred to by author names and the given roman numbers.

The following publications are also related to the topic of this thesis and have been co-authored during the PhD-study, but they are not included in this thesis:

Kellerer-Pirklbauer A, Pauritsch M, Winkler G (2015) Widespread occurrence of ephemeral funnel hoarfrost and related air ventilation in coarse-grained sediments of a relict rock glacier in the Seckauer Tauern Range, Austria. Geografiska Annaler A, 97 (3), 453-471, doi: 10.1111/geoa.12087

Winkler G, Pauritsch M, Wagner T, Kellerer-Pirklbauer A (2016b) Reliktische Blockgletscher als Grundwasserspeicher in alpinen Einzugsgebieten der Niederen Tauern (Relict rock glaciers as groundwater storages in alpine catchment areas in the Niedere Tauern Range). Berichte zur wasserwirtschaftlichen Planung Steiermark, 87, Graz, p. 134. http://www.wasserwirtschaft.steiermark.at/cms/dokumente/11913323_102332494/6885027d/87.pdf [Accessed 12 September 2016]

In the appendix, a selection of conference abstracts related to this work is given. They were submitted as first author and presented in the course of the PhD study at national and international conferences.

Acknowledgments

This PhD thesis would have been impossible for me to finish if it weren't for the help of my numerous colleagues and friends and I am deeply thankful to every single one of them.

First of all I want to thank my supervisor Steffen Birk for giving me the opportunity to make a PhD in hydrogeology. Thank you for your good advices, for always having an open door for me and for giving me the freedom I needed to do my research.

I am also especially grateful to Gerfried Winkler for initializing the research project which was funding my studies and for being my second, unofficial, supervisor. Gerfried, I will forever be in your debt for making all of this even possible. Thank you also for the great memories of our many field trips, the countless valuable discussions and for giving me motivation when I was in need of it.

Thanks and appreciation to Thomas Wagner. Tom, without our discussions and your general support during the preparation of the manuscripts, I would probably need a couple more years to come to this point. I also cherish the great memories of our field trips together, especially the notorious and reckless crossing of the Hirschkarlgrat at icy and snowy conditions, when I feared for my life and you were jumping around in sneakers like it was nothing.

I would also like to thank Andreas Kellerer-Pirklbauer for sharing some of his wisdom about rock glaciers with me and Michael Avian for his tips on writing a thesis. Thank you both for the memorable field trips and for making the office life much more pleasant.

I am grateful to Stefan Hergarten for helping me with the mathematical problems and for the valuable discussions about the physical correctness of my interpretations. Thank you for your physical insights and your clear and comprehensible explanations. Rainer Morawetz and Marcellus Schreilechner are thanked for their support during the performance and analysis of the geophysical investigations. I also thank Nicole Kamp for helping me to interpret the results of the ground penetrating radar survey.

Thanks to all members of the research group at the Institute of Earth Sciences and all PhD students of the UZAG doctoral school. Thanks to Erwin Kober, Franz Tscherne and Klaus Eigner for driving me safely to my field trips and also for their assistance during the field work. Thanks to Gertraud Bauer, Claudia Puschenjak and Elisabeth Gülli for the administrative support and thanks to Georg Stegmüller for keeping my computers running.

A big thank you goes out to my fellow colleagues Cyril Mayaud, Abraham Mechal Degu and Felix Thalheim with whom I shared many funny moments. Cyril, I hope we will continue to make lots of photography/hiking trips and capture some nice pictures of the moon.

I would like to thank all my good friends of the GrazConnection for letting me forget work every once in a while and I hope that they can forgive me if I have neglected them too much during the last time.

Most of all, I am thankful to Nina for her patience and support during these years and for saving me from despair more than once. xoxo

Finally I would like to thank my family and especially my parents Harry and Sylvia for their constant support and unconditional love during my whole life.

Abstract

Rock glaciers are distinctive landforms that can be found frequently in the alpine terrain of the Eastern Alps (and in alpine regions worldwide). Due to their composition of unconsolidated debris material, rock glaciers represent potential aquifer systems that might be relevant especially in crystalline regions which normally exhibit only limited groundwater storage capabilities. This study examines the groundwater storage capabilities and discharge dynamics of relict rock glaciers. More specifically, three main questions are outlined:

1) What are the hydrogeological characteristics of relict rock glaciers?
2) What are the dominant factors influencing the discharge behavior of relict rock glacier springs?
3) How important are relict rock glaciers for river discharge further downstream?

To address these questions a multidisciplinary approach was applied at the field site of the relict Schöneben Rock Glacier, located in the Niedere Tauern Range, Austria (and the catchment area of the Liesing-creek further downstream). The results of these investigations are issued in four research papers in international peer-reviewed journals. By the time of the writing of this thesis, three of them are published and one is accepted for publishing.

The first publication (Winkler et al., I) shows hydrogeological investigations at the relict Schöneben Rock Glacier using data from the draining spring as well as data resulting from a seismic refraction survey performed at several profiles along the rock glacier. The findings of this investigation show that the rock glacier has a heterogeneous internal structure and a discharge behavior with at least two flow components, a fast flow component to produce the quick responses of the spring to recharge events and a slow flow component which is responsible for the base flow. This leads to a conceptual model of the inner structure of the relict Schöneben Rock Glacier, which is defined by a thin lower layer of fine-grained sediment that is overlain by a layer of coarser material and a surface cover consisting of coarse boulders.

In the second publication (Pauritsch et al., II), the discharge recession behavior of sloping aquifers is analyzed by using three different analytical solutions of the Boussinesq equation in order to examine the influencing factor of slope angle on the discharge behavior. This is elaborated at synthetic aquifers, implemented in a numerical groundwater flow model, and applied to the relict Schöneben Rock Glacier as an example of a sloping aquifer in an alpine environment. The results of the synthetic

aquifers show that the slope angle significantly influences the discharge recession and that the analytical models can simulate the discharge recession reasonably well, depending on the slope angle and the used method. However, the data from the rock glacier suggest that several discharge-influencing factors co-exist, especially in complex alpine aquifers, which cannot be distinguished through the applied analytical models.

The third publication (Pauritsch et al., III) presents a detailed numerical groundwater model of the Schöneben Rock Glacier that is used to explore the impact of internal structures and the aquifer base topography on the discharge behavior of relict rock glaciers. Data from geophysical investigations, such as seismic refraction and ground-penetrating radar, are used to identify the aquifer geometry. The groundwater flow model is calibrated using discharge data measured at the rock glacier spring. Several versions of internal structures and two versions of aquifer base topographies are employed to verify the conceptual model of the first publication (Winkler et al., I) and to explore the possibility of other alternatives. The results show that the proposed layered structure is plausible, but alternative internal structures such as channel networks are also conceivable. Furthermore, the topography of the aquifer base influences the discharge behavior, in particular when simple, layered structures are considered.

In the final publication (Wagner et al., IV), the impact of relict rock glaciers on downstream rivers is investigated. A lumped-parameter rainfall-runoff model is employed in order to simulate the discharge of the relict Schöneben Rock Glacier. This aquifer also represents a benchmark of a watershed that is influenced by rock glaciers to 100 % as the spring is originating directly from the rock glacier front. Assuming that the rock glaciers in nearby alpine cirques have similar aquifer properties, the parameters from the Schöneben Rock Glacier are transferred. By using a semi-distributed approach, rock glacier influenced headwaters are quantified at watersheds with different areal shares of rock glaciers. The results show that the Schöneben Rock Glacier is characterized by a high storage capacity of the routing store (representing the groundwater storage) and a rather small production store (indicating the soil water store). The contribution from relict rock glacier influenced headwaters shows a distinct seasonality and applying a model with daily time steps, a high significance of rock glacier influenced headwaters further downstream is indicated by contributions of a quarter to more than four times the areal share.

Zusammenfassung

Blockgletscher sind markante Landschaftsformen, die häufig in alpinen Regionen der Ostalpen (und in alpinen Regionen weltweit) gefunden werden können. Durch ihre Zusammensetzung aus losem Schuttmaterial stellen Blockgletscher potentiell relevante Grundwasserkörper dar. Dies gilt besonders in kristallinen Regionen, die üblicherweise nur geringfügige Speicherfähigkeiten für Grundwasser aufweisen. Diese Forschungsarbeit untersucht die Grundwasserspeicherfähigkeit und Schüttungseigenschaften von reliktischen Blockgletschern. Genauer gesagt werden drei Hauptfragen formuliert:

1. Was sind die hydrogeologischen Eigenschaften von reliktischen Blockgletschern?
2. Durch welche Faktoren werden die Quellen von reliktischen Blockgletschern beeinflusst?
3. Welche Rolle spielen reliktische Blockgletscher für übergeordnete Flusssysteme?

Um diese Fragen zu beantworten, wurde ein multidisziplinärer Ansatz angewendet. Als Untersuchungsgebiet diente hierzu der reliktische Schöneben-Blockgletscher in den Niederen Tauern, Österreich (und dessen übergeordnetes Einzugsgebiet der Liesing). Die Ergebnisse dieser Untersuchungen sind in vier Forschungsbeiträgen in internationalen Fachzeitschriften publiziert. Zur Zeit des Verfassens dieser Arbeit sind drei dieser Beiträge bereits publiziert und ein Beitrag ist zur Publikation angenommen.

Die erste Publikation (Winkler et al., I) behandelt hydrogeologische Untersuchungen am reliktischen Schöneben-Blockgletscher unter Verwendung von Daten der Blockgletscherquelle und Daten einer refraktionsseismischen Untersuchung, welche entlang mehrerer Profile am Blockgletscher durchgeführt wurde. Die Ergebnisse der Untersuchungen zeigen, dass der Blockgletscher eine heterogene Struktur hat und ein Schüttungsverhalten mit zumindest zwei Fließkomponenten aufweist, eine schnellere Komponente für die schnelle Reaktion der Quelle auf Neubildungsereignisse und eine langsamere Komponente, die für den Basisabfluss verantwortlich ist. Dies führt zu einem konzeptionellen Modell über den inneren Aufbau des reliktischen Schöneben-Blockgletschers, welches durch eine dünne untere Schicht aus feinkörnigem Sediment definiert ist ,die von einer Schicht aus grobkörnigerem Material und einer Oberflächenbedeckung von Felsblöcken überlagert wird.

In der zweiten Publikation (Pauritsch et al., II) wird das Auslaufverhalten von geneigten Grundwasserkörpern analysiert, indem drei unterschiedliche analytische Lösungen der Boussinesq-

Gleichung verwendet werden, um den Einfluss der Hangneigung auf das Schüttungsverhalten zu untersuchen. Dazu wurden synthetische Grundwasserkörper, implementiert in einem numerischen Grundwassermodell, und der reliktische Schöneben-Blockgletscher als ein Beispiel eines geneigten Grundwasserkörpers in alpinem Gelände verwendet. Die Ergebnisse der synthetischen Grundwasserkörper zeigen, dass das Auslaufverhalten deutlich durch die Hangneigung beeinflusst wird und dass die analytischen Modelle das Auslaufverhalten, in Abhängigkeit der Hangneigung und der verwendeten Methode, ausreichend gut simulieren können. Die Daten des Blockgletschers deuten jedoch darauf hin, dass besonders in komplexen alpinen Grundwasserkörpern das Auslaufverhalten von mehreren koexistierenden Faktoren abhängt, welche sich durch die angewendeten analytischen Lösungen nicht differenzieren lassen.

Die dritte Publikation (Pauritsch et al., III) präsentiert ein detailliertes Grundwassermodell des Schöneben-Blockgletschers, welches dazu verwendet wird, den Einfluss der inneren Strukturen und des Reliefs der Aquiferbasis auf das Abflussverhalten des reliktischen Blockgletschers zu untersuchen. Daten von geophysikalischen Untersuchungen wie etwa Refraktionsseismik und Bodenradar werden verwendet, um die Geometrie des Grundwasserkörpers zu erfassen. Das Grundwassermodell ist unter Verwendung von Schüttungsdaten kalibriert, die an der Blockgletscherquelle aufgezeichnet werden. Mehrere Versionen von internen Strukturen und zwei Versionen der Aquiferbasis-Topographie werden verwendet, um das konzeptionelle Modell der ersten Publikation zu verifizieren und um die Möglichkeit von Alternativen zu erkunden. Die Ergebnisse zeigen, dass die Modellvorstellung einer geschichteten Struktur plausibel ist, aber auch alternative interne Strukturen wie präferenzielle Fließwege vorstellbar wären. Darüber hinaus beeinflusst die Topographie der Aquiferbasis das Auslaufverhalten besonders dann, wenn einfache, geschichtete Strukturen in Betracht gezogen werden.

In der letzten Publikation (Wagner et al., IV) wird der Einfluss reliktischer Blockgletscher auf unterstromige Flüsse untersucht. Ein „lumped-parameter“ Niederschlags-Abflussmodell wird verwendet, um die Schüttung des reliktischen Schöneben-Blockgletschers zu simulieren. Dieser Grundwasserkörper wird dann als Richtwert eines Einzugsgebietes mit hundertprozentiger Blockgletscherbeeinflussung verwendet, da die Quelle direkt aus dem Blockgletscher entspringt. Mit der Annahme, dass die Blockgletscher in den benachbarten Karen ähnliche Eigenschaften haben, können die Parameter des Schöneben-Blockgletschers transferiert werden. Unter Verwendung eines „semi-distributiven“-Ansatzes werden die blockgletscherbeeinflussten Abflussanteile in Einzugsgebieten mit flächenhaft unterschiedlichen Blockgletscheranteilen quantifiziert. Die Ergebnisse zeigen, dass der Schöneben-Blockgletscher durch eine hohe Speicherkapazität des „routing stores“ (entspricht dem Grundwasserspeicher) und einem eher kleinen „production store“

(entspricht dem Bodenspeicher) charakterisiert werden kann. Es zeigt sich, dass die blockgletscherbeeinflussten Teilabflüsse eine starke Saisonalität aufweisen. Basierend auf dem verwendeten Model auf Tagesbasis variiert der Anteil von einem Viertel bis zum Vierfachen des flächenhaften Anteils der blockgletscherbeeinflussten Einzugsgebiete wodurch Blockgletschern eine große Bedeutung für die unterstromigen Flüsse zugerechnet werden kann

Table of contents

1. Introduction

1.1. Motivation and Objectives

Rock glaciers are periglacial landforms that can be found frequently in alpine environments, but they also occur at high latitudes. For example, about 4792 rock glaciers, covering 286 km², were identified in the Austrian Alps (Kellerer-Pirklbauer et al., 2012; Krainer and Ribis, 2012). These numbers illustrate the significance of these landforms, particularly under the consideration that water draining from rock glaciers is used for local drinking water supply, hydro-electric power plants and artificial snow systems in ski resorts and might also be significant for the fragile local ecology. Nevertheless, knowledge about the hydrodynamics of rock glaciers and, especially, relict rock glaciers, which no longer contain ice, is rather limited. Research on rock glaciers is mainly focused on their distribution, movement, inner structure and ice content (e.g. Kääb and Webber, 2004; Haeberli et al., 2006; Monnier and Kinnard, 2015). In contrast, investigations about their hydrogeological properties are rare (Krainer et al., 2007; Millar et al., 2013). Research on relict rock glaciers is of particular regional importance as they comprise the highest share of the total number of rock glaciers in Austria. Moreover, their significance is expected to increase even further as currently intact rock glaciers, which are still containing ice, will at some point become relict as a result of a currently ongoing climate warming (Kern et al., 2012; Vaughan et al., 2013). To understand the prospective effect of the loss of ice on the storage capabilities of rock glaciers and the consequent changes for the local ecology and economy (e.g. energy management and natural hazards), the hydrogeology of relict rock glaciers needs to be understood. This thesis investigates the groundwater storage capabilities and discharge dynamics of relict rock glaciers as a step towards a more complete understanding of hydrogeological processes in these landforms and alpine environments in general. More specifically, three main questions are outlined:

1) What are the hydrogeological characteristics of relict rock glaciers?
2) What are the dominant factors influencing the discharge behavior of relict rock glacier springs?
3) How important are relict rock glaciers for river discharge further downstream?

To address these questions a multidisciplinary approach is applied at the field site of the relict Schöneben Rock Glacier, located in the Niedere Tauern Range, Austria (and the catchment area of the Liesing-creek further downstream).

1.2. Scientific background of rock glaciers

Rock glaciers are one of the most striking permafrost-related landforms as they can reach considerable sizes in the order of square kilometers (Fig. 1) and are usually clearly distinguishable from the surrounding environment (Gorbunov et al., 1992; Sorg et al., 2015).

The first rock glacier was described by Steenstrup (1883) in Greenland (Humlum, 1982; Barsch, 1996). Yet, the research on rock glaciers started not before about 100 years ago and. Since then, the interest in rock glaciers has been continuously rising, especially after the milestone paper of Wahrhaftig and Cox (1959).

There is an ongoing discussion about the definition of rock glaciers. The controversy is about whether to use a morphological or a genetic definition. Morphological definitions have the disadvantage that similarly looking landforms can be falsely characterized as rock glaciers, whereas genetic definitions face the problem that the genesis of individual landforms, which are suspected to be rock glaciers, is commonly unknown. Also, especially older definitions only contain periglacial considerations and neglect the possibility of debris-covered glaciers evolving into rock glaciers. A detailed discussion about this is given in the review paper of Berthling (2011).

However, a commonly used morphological definition is given by Barsch (1996): “Active rock glaciers are lobate or tongue-shaped bodies of perennially frozen unconsolidated material, supersaturated with interstitial ice and ice lenses that move downslope or downvalley by creep as a consequence of the deformation of ice contained in them and which are, thus, features of cohesive flow.“

A more recent, genetic definition is proposed by Berthling (2011): “Active rock glaciers are the visible expression of cumulative deformation by long-term creep of ice/debris mixtures under permafrost conditions”. Berthling (2011) states that with this definition the exact origin of the ice content is not needed and, thus, the problems of previous genetic definitions do not apply here.

Distribution

Rock glaciers are abundant landforms that frequently occur at mountain ranges all over the world and are even reported to exist on Mars (e.g. Head et al., 2005). For example, in South America Rangecroft et al. (2014) identified 94 rock glaciers in the Bolivian Andes. In North America, about 200 rock glaciers are known in the Alaska Range (Wahrhaftig and Cox, 1959) and 289 rock glaciers are reported in the Sierra Nevada by Millar and Westfall (2008). In Asia, more than one thousand rock glaciers (covering an area about 5000 km²) are identified in the northern Tien Shan region (Gorbunov et al., 1992; Bolch and Gorbunov, 2014; Sorg et al., 2015) and 702 rock glaciers are mapped in selected areas of the Hindu Kush Himalayan region by using Google Earth (Schmid et al., 2015). Particularly high numbers of rock glacier occurrences are reported in the European Alps. Bollmann et al. (2012) identified 1697 rock glaciers in the Italian Alps and in the Austrian Alps 4792 rock glaciers, covering 286 km², are known (Kellerer-Pirklbauer et al., 2012; Krainer and Ribis, 2012).

Genesis

Basically, the development of rock glaciers depends on three influencing factors (Barsch, 1996):

- The climate conditions have to be suitable for permafrost. Besides a low air temperature, the amount of (winter) precipitation is also essential. Humlum (1998) has shown that rock glaciers mainly exist at sites with limited snow accumulations in relation to debris supply, whereas sites with high snow accumulations and limited amount of debris exhibit normal glaciers.
- A certain slope angle to commence the movement process of the frozen debris.
- A sufficient supply of debris material which can originate either from talus slopes or glacial sediments such as moraines. Thus, rock glaciers are categorized as talus-derived or glacier-derived, respectively.

Talus-derived rock glaciers develop by debris accumulation at the talus slope (Barsch, 1996). The pores are filling up with periglacial ground ice and the rock mass starts to creep downslope at some point. Glacier-derived rock glaciers consist of debris accumulations, such as morainic sediments, that are residuals of retreating glaciers. There are often ice lenses remaining in such sediment accumulations and, together with the infiltration and freezing of water, the movement of the rock glacier can be enabled. In contrast to this, debris-covered glaciers can evolve into rock glaciers when interstitial ground ice exists additionally to buried surface ice (Haeberli et al., 2006; Harrison et al., 2008; Berthling, 2011). Thus, there is a continuum with rock glaciers as a rock mass cemented with

interstitial ice on one end and debris-covered glaciers on the other end, which particularly complicates morphological definitions of rock glaciers (Berthling, 2011).

Fig. 1: Examples of some large rock glaciers in the Tien Shan region, Kyrgyzstan that illustrate the continuum of rock glaciers and debris covered glaciers (42°54’30’’N, 77°07’00’’E; Landsat image in Google earth, ©2016 Cnes/Spot Image, Image ©2016 DigitalGlobe).

Morphology/structure

The shape of rock glaciers can be described as lobate (width is larger than length), tongue-shaped (length is larger than width) or complex (polymorph) (Wahrhaftig and Cox, 1959; Barsch, 1996). The size of rock glaciers is highly variable as rock glaciers are strongly dependent on their surroundings and environment (e.g. Ikeda and Matsuoka, 2006; Kellerer-Pirklbauer et al., 2012). An example of a large rock glacier in Austria is the relict Reichhart Rock Glacier in the Niedere Tauern Range, which covers an area of 1.78 km². However, in the Austrian Alps rock glaciers usually cover an area less than one km² (Kellerer-Pirklbauer et al., 2012; Krainer and Ribis, 2012). Generally, larger examples can be found in the Ile Ala-Tau Range, Kazakhstan and Kyrgyzstan, which shows a more continental climate (Bolch and Gorbunov, 2014).

Morphologically, rock glaciers have distinct and steep front and side boundaries and in the European Alps, the thickness is usually less than 100 m (Frehner et al., 2015). An unfrozen “active” layer with a

thickness of several meters protects the frozen core from direct sun radiation and warm air temperatures (Johnson et al., 2007). The surface of rock glaciers typically shows extensive formations of longitudinal and transversal ridges and furrows which develop as a consequence of the movement process (Kääb and Webber, 2004; Frehner et al., 2015). The surface is covered by rocks and boulders of variable sizes depending on the rockwall geology. Ikeda and Matsuoka (2006) distinguish between bouldery rock glaciers which show a surface layer of matrix-free boulders with sizes of up to several cubic meters, and pebbly rock glaciers with a surface layer composed of matrix-supported debris. The former are found in areas of crystalline rocks and massive limestones and the latter in areas with less resistant shale and stratified limestones (Ikeda and Matsuoka, 2006). The size of the debris strongly influences the morphology of rock glaciers by controlling the transport processes. As such, pebbly rock glaciers are smaller, contain less ice and have less dominant transversal ridges compared to bouldery rock glaciers (Ikeda and Matsuoka, 2006). Cheng et al. (2007) have shown that coarse blocky layers in particular have the ability to lower the temperature of the underlying material. Thus, this so-called active layer enables the existence of permafrost ice in relatively warm areas (Johnson et al., 2007). The type and distribution of the ice is dependent on the genesis of the rock glacier and can be present as interstitial ice or ice lenses (e.g. Haeberli et al., 2006). The ice content of active rock glaciers usually varies between 50 and 70 % (Haeberli et al., 2006; Hausmann et al., 2012) but can be locally significantly higher (100 % at ice lenses).

Types

Rock glaciers are classified as active, inactive and relict (also called fossil) depending on their ice content and, consequently, their movement (Barsch, 1996):

Active rock glaciers are currently moving downslope or downhill with velocities of up to a few meters per year (e.g. Krainer and Mostler, 2006). Besides of their actual movement, they can also be identified morphologically by the lack of vegetation (Fig. 2a; Fig. 3a). Furthermore, they show a steep and unstable front with a slope angle of more than 35° (Barsch, 1996). As the groundwater stored in the rock glacier is in contact with ice, the temperature of the spring water is usually low throughout the year (below 1°C (Krainer and Mostler, 2002)).

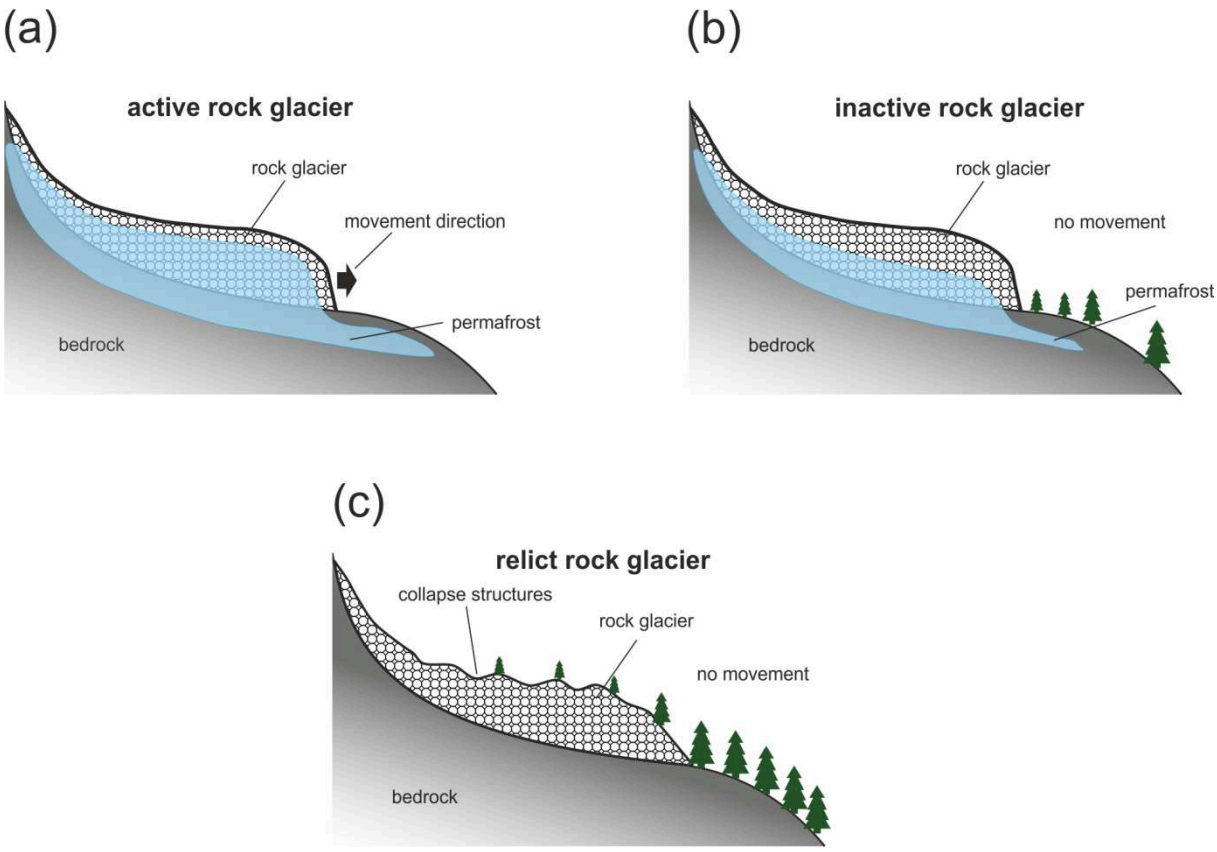

Fig. 2: Illustration of the rock glacier classification in (a) active, (b) inactive and (c) relict rock glaciers (modified after Kellerer-Pirklbauer, 2008).

Inactive rock glaciers are currently not moving but still contain ice (Fig. 2b). Because the movement has come to a halt, inactive rock glaciers are becoming covered by vegetation and the front becomes stable with a lower slope angle (Barsch, 1996). Inactivity of rock glaciers can result from melting of the frozen core as a consequence of changing climate conditions (climatic inactive). Another possibility is a shortage of debris or ice supply because the rock glacier has advanced too far from its source or has advanced to a valley floor with a lower slope angle which hampers the movement (dynamic inactivity). However, inactive rock glaciers can be reactivated by changing conditions (Barsch, 1996).

In contrast to active and inactive rock glaciers (often combined as intact rock glaciers), relict rock glaciers no longer contain ice (Fig. 2c). Distinct collapse structures are often visible at the surface as a result of the loss of volume caused by the melting of ice (Barsch, 1996). Moreover, the slopes are further stabilized and less steep and relict rock glaciers are often extensively covered by vegetation (Fig. 3b). This makes the identification of relict rock glaciers in the field sometimes challenging and it is advisable to additionally use remote sensing data such as airborne laser scanning (ALS).

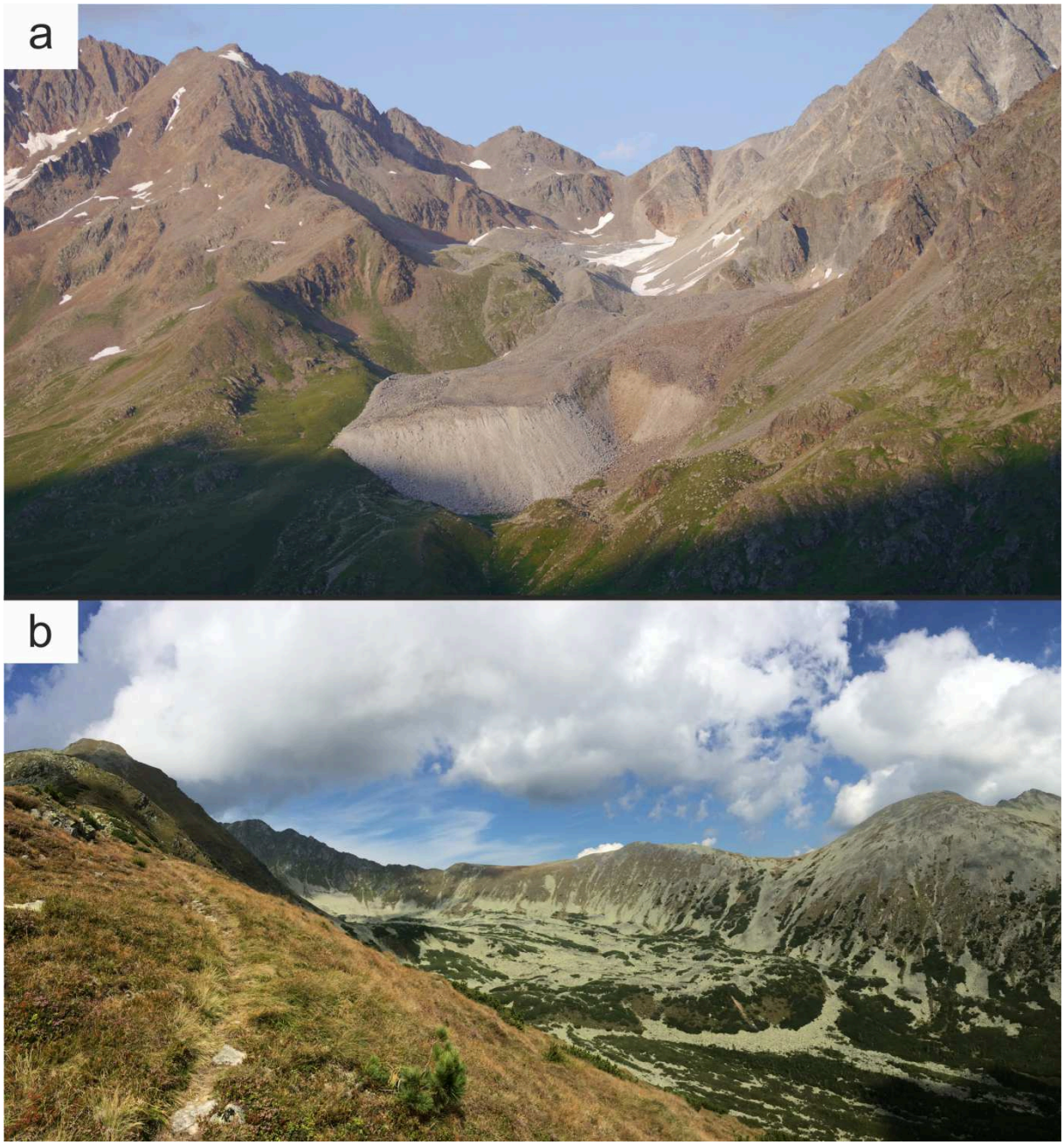

Fig. 3: Examples of (a) an active rock glacier with a steep and unstable front (Innere Ölgrube Rock Glacier, Kaunertal, Tyrol, Austria; width of front is approximately 200 m) and (b) a relict rock glacier with extensive vegetation cover and distinct collapse structures visible at the surface (Hölltal Rock Glacier, Ingeringtal, Styria, Austria; width of front is approximately 450 m; photo by courtesy of T. Wagner).

Movement process

The movement of rock glaciers is dominated by creep (Arenson et al., 2002; Haeberli et al., 2006), but basal sliding can also be significant (Hausmann et al., 2012). Furthermore, Zurawek (2002) has identified several shear planes at excavations of a relict rock glacier and therefore suggested shearing processes as the main deformation mechanism during its former active stage. The velocity of rock glaciers depends on several factors such as slope, thickness and internal composition (Haeberli et al., 2006). Moreover, cold temperate rock glaciers generally move slower than warm ones (Kääb et al., 2002). Due to the local topography of the underlying bedrock, local bulging can occur in front and thinning behind of transversal ridges, which is reflected as ridges and furrows at the surface (Kääb and Webber, 2004). However, Frehner et al. (2015) conclude that the ridges and furrow structures are an expression of buckle folding of viscous layers as a mechanical response to layer-parallel compression. Hausmann et al. (2012) suggest that the movement of rock glaciers is dependent on a combination of the ice content and the thickness of the frozen zone, as rock glaciers with low ice contents require higher thickness to overcome the internal friction.

Climate indicator/age

The age of rock glaciers in the Austrian Alps was estimated by Rode and Kellerer-Pirklbauer (2011) who used the Schmidt-hammer exposure-age dating method and showed that many rock glaciers in this area formed during the Lateglacial and Holocene (6.7-11.4ka). According to velocity data of neighboring rock glaciers, they suggest a formation period of 500-5600 years. As rock glaciers are stable at certain climatic conditions, they can be used as indicators for these conditions (Hughes et al., 2003; Paasche et al., 2007; Putnam and Putnam, 2009). Moreover, relict rock glaciers can indicate the paleoclimate of their active time period (formation and evolution) and they can contain information about air temperature, seasonal precipitation and wind (Humlum, 1998).

Hydrogeology

The hydrological significance of rock glaciers was realized early (Corte, 1976). Brenning (2005) and Azócar and Brenning (2010) investigated rock glaciers in the Chilean Andes and showed their hydrological importance in this semi-arid to arid area. They found that in some areas the storage volumes of frozen water within rock glaciers are even more important than those of normal glaciers.

An increasing importance of rock glaciers for water supplies is also predicted in Bolivia and other arid mountain ranges (Rangecroft et al., 2013).

Furthermore, the hydrological importance of rock glaciers in alpine regions was investigated by Krainer and Ribis (2009). Their results suggest that the majority of the drained water originates from precipitation events and snowmelt, whereas meltwater of the permafrost ice represents a rather small share of the total discharge. However, high concentrations of heavy metals are reported in the meltwater of active rock glaciers (Thies et al., 2013), which seem to originate from permafrost ice (Krainer et al., 2015). Yet, the processes responsible for the heavy metal enrichment of the permafrost ice are still unclear and a focus of ongoing research.

Hydrological investigations of rock glaciers primarily focus on intact forms (e.g., Harris et al., 1994; Krainer and Mostler, 2002; Krainer et al., 2007), whereas relict rock glaciers have been almost neglected. Nevertheless, Gödel (1993) and Untersweg and Schwendt (1995; 1996) investigated the hydrological importance of relict rock glaciers in the Niedere Tauern Range. They showed that even though the rock glaciers are relict forms, they are significant for water management issues as they are often coupled to large springs that stand out of the neighboring springs in crystalline regions.

1.3. Investigation area

The investigation area of the studies included in this thesis is located in the Styrian part of the Niedere Tauern Range, Austria. This mountain range consists of the following subunits (from west to east): Schladminger Tauern Range, Wölzer Tauern Range, Rottenmanner Tauern Range and the Seckauer Tauern Range. The highest mountain is the Hochgolling (2862 m a.s.l.) located in the Schladminger Tauern Range and, generally, the elevation of the mountain peaks is decreasing from west to east. Moreover, as the climate becomes more continental towards east (Nagl, 1976; Wakonigg, 1978), the eastern subunits of the Niedere Tauern Range were less affected by glaciers of the last glaciation maximum (LGM) (Van Husen, 1987; Ehlers et al., 2011). The glaciers in the Seckauer Tauern Range did not reach the main valleys (Fig. 4) and after the LGM, this area became free of glaciers at an early stage (Untersweg and Schwendt, 1996). Thus, rock glaciers were able to develop earlier and reach larger dimensions in the eastern subunits compared to the western subunits, where only small examples can be found (Untersweg and Schwendt, 1996).

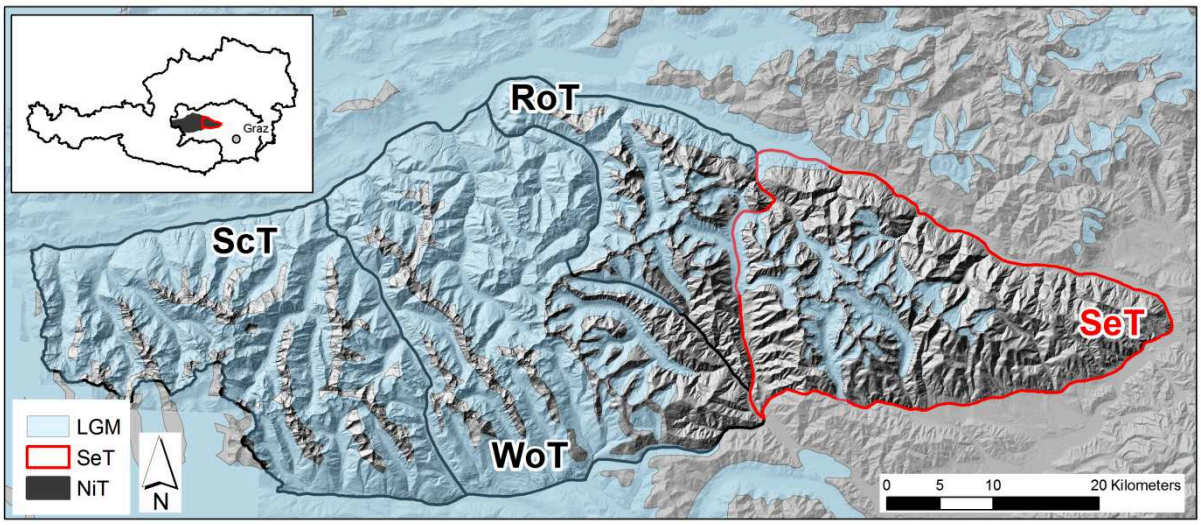

Fig. 4: Map of the last glaciation maximum (LGM) of the Styrian part of the Niedere Tauern Range (NiT). ScT = Schladminger Tauern Range; WoT = Wölzer Tauern Range; RoT = Rottenmanner Tauern Range; SeT = Seckauer Tauern Range (modified after Ehlers et al., 2011). GIS data were provided by the Federal Government of Styria (© GIS-Steiermark).

The geology of the Niedere Tauern Range is part of the Austroalpine Unit which is a complex nappe stack that can be subdivided into the Upper- and Lower Austroalpine Subunits (Schmid et al., 2004; Froitzheim et al., 2008). The Lower Austroalpine Subunit represents the continental margin of the Penninic Ocean, lies on top of the Penninic Nappes and can be found in the western part of the Niedere Tauern Range (Pfingstl et al., 2015). The Upper Austroalpine Subunit covers most parts of the Niedere Tauern Range and contains a series of nappes. The lowermost nappe is the Silvretta-Seckau Nappe System which mainly covers the Seckauer Tauern Range. It is overlain in the North by the metamorphic Paleozoic sequences of the Greywacke zone and in succession by the Juvavic, Tirolic-Noric and Bajuvaric Nappe Systems of the Northern Calcareous Alps (Pfingstl et al., 2015). Towards South, the Silvretta-Seckau Nappe System is covered in order by the Koralpe-Wölz Nappe System (metamorphic basement), the Ötztal-Bundschuh Nappe System (basement-cover sequence) and the Drauzug-Gurktal Nappe System (Variscan basement and Permo-Mesozoic cover sequence)(Schuster and Kurz, 2005; Pfingstl et al., 2015).

The Silvretta-Seckau Nappe System contains the catchment area of the Schöneben Rock Glacier that is studied in detail within this thesis. The nappe system consists of a pre-alpine basement (dominated by paragneisses) covered by Permo-Mesozoic metasediments (Schuster and Kurz, 2005). However, in the catchment of the Schöneben Rock Glacier only the Pre-Alpine Basement is present (Fig. 5).

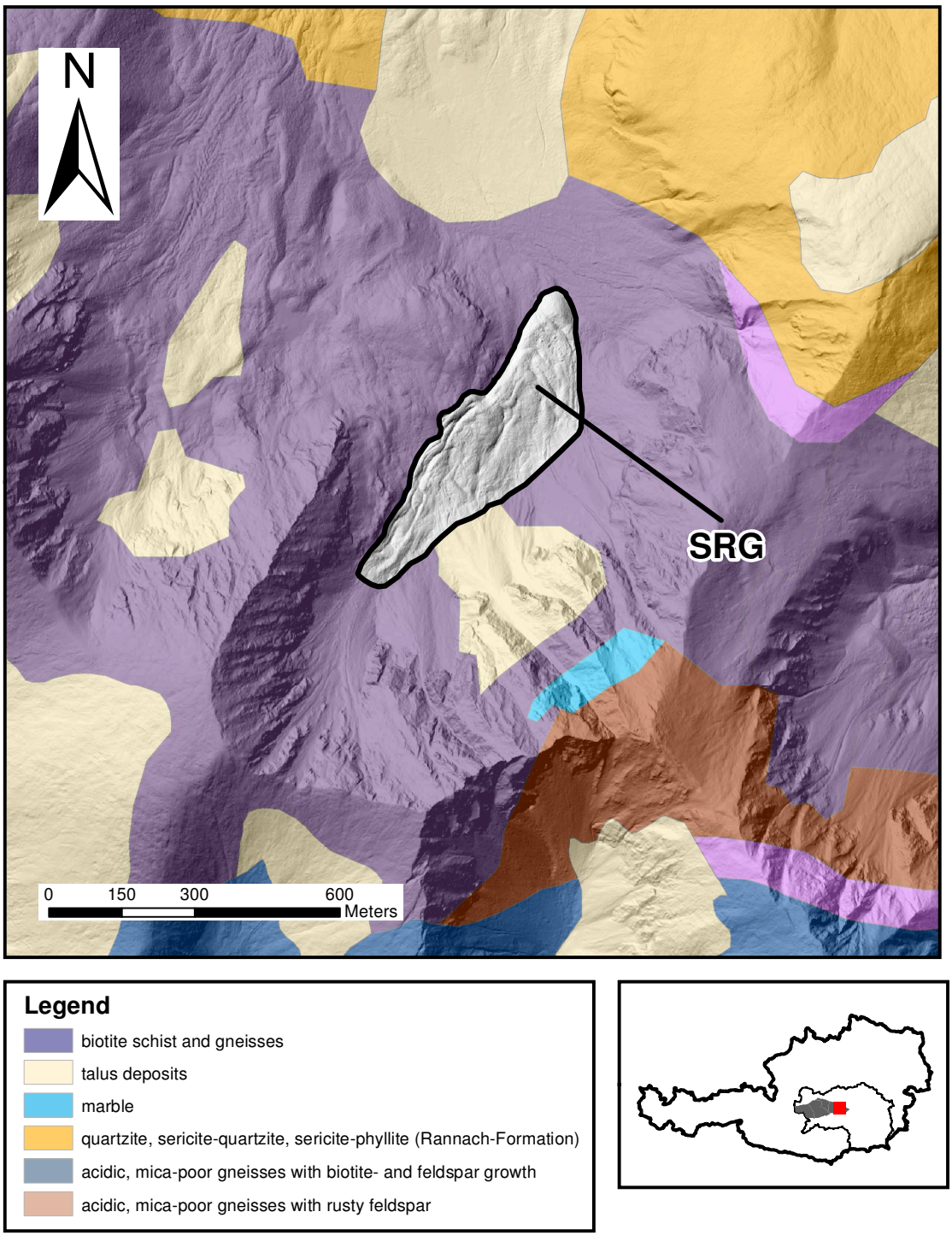

Fig. 5: Geological map of the surroundings of the Schöneben Rock Glacier (SRG). The position of the presented are within Austria is indicated in the inlet. The Styrian part of the Niedere Tauern Range is highlighted as dark polygon in the inlet. Geological and GIS data were provided by the Federal Government of Styria (© GIS-Steiermark).

The relict Schöneben Rock Glacier is located at E14°40’25’’, N47°22’39’’ (see Fig. 6), has a length of about 750 m, a maximum width of about 250 m and covers an area of 0.11 km². The front is at an elevation of 1715 m (a.s.l.) and the root of the tongue-shaped rock glacier is at an elevation of 1912 m (a.s.l.). The surface consists of coarse rocks and boulders of sizes up to several cubic meters and is partly covered by vegetation. Moreover, the surface morphology is characterized by distinct ridge and furrow structures and the slope of the front is stable and relatively flat. Therefore, the Schöneben Rock Glacier is characterized as a relict form and significant permafrost occurrences are not to be expected. The Schöneben Rock Glacier is drained by a single spring located at the front of the rock glacier. This spring is part of the official spring network of the Hydrographic Service of Styria (HZB-number 396762) and the water stage is continuously monitored at a notch weir located 40 m below the actual spring. Additionally, water temperature and electric conductivity are continuously measured directly at the spring and an automatic weather station was installed directly on the Schöneben Rock Glacier (at 1823 m a.s.l.). More details about the available data are given in Winkler et al. (I), Pauritsch et al. (III), Wagner et al. (IV), Kellerer-Pirklbauer et al. (2015) and Winkler et al. (2016b). Due to the compact gneissic rocks and the steep relief of the catchment area, major water exchange between adjacent cirques is assumed to be negligible.

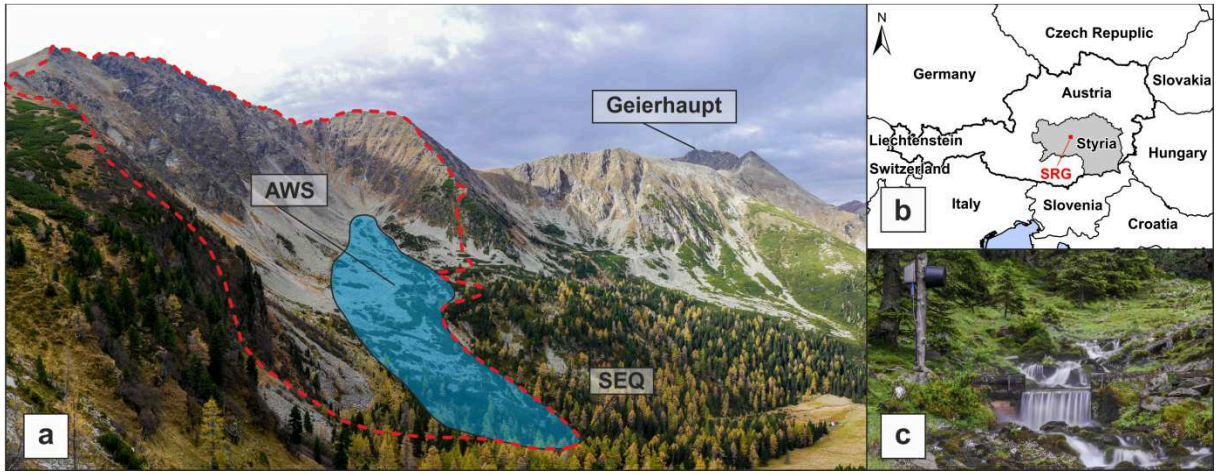

Fig. 6: (a) Schöneben Rock Glacier highlighted as a blue polygon and the catchment area delineated with a red dashed line; Geierhaupt = highest peak in the Seckauer Tauern Range (2417 m a.s.l.); AWS = automatic weather station; SEQ = rock glacier spring; (b) location of the Schöneben Rock Glacier (SRG) within Austria and Styria; (c) rectangular notch weir situated about 40 m downstream of SEQ (Pauritsch et al., III).

2. Methods

Discharge/recession analysis

To investigate the hydrogeological characteristics of relict rock glaciers, the discharge recession of the Schöneben Rock Glacier spring is analyzed as a representative example of rock glacier springs in general. For these investigations the winter base flow is used because during this time the aquifer is mostly unaffected by interrupting recharge processes, as precipitation commonly occurs in the form of snow during that time and, therefore, is stored in the snow cover. There are several mathematical models that can be used to describe the discharge recession of an aquifer. In Winkler et al. (I) the discharge recession of the Schöneben Rock Glacier is investigated using two analytical models. The first, simple model represents a linear storage and results in a discharge recession following an exponential function (Maillet, 1905). More complex aquifers can be approximated using a superposition of several linear storages, which are active during different times of the recession and thus result in several exponential functions. Using the recession coefficient of the base flow (latest time period of the recession), the remaining volume of stored groundwater can be estimated (Kresic, 2007). Moreover, using an assumed storage coefficient and the areal extent of the aquifer, the thickness of the saturated zone can be computed. The second, more sophisticated model simulates the discharge recession after a finite recharge pulse as a power law function (Birk and Hergarten, 2010) and is regarded as a more precise representation of particularly the early stage runoff (Rorabaugh, 1964). The equations and a more detailed description of the applied models can be found in Winkler et al. (I).

However, both models assume a horizontal aquifer base, but that might not be appropriate for the Schöneben Rock Glacier as it is situated in alpine terrain and has an average surface slope of about 16°. Therefore, the influence of slope angle on the discharge recession is investigated in Pauritsch et al. (II) by using analytical approximations of the Bousssinesq equation for sloping aquifers. The investigated analytical models contain the Brutsaert solution (Brutsaert, 1994), the Hogarth approximation (Hogarth et al., 2014) and the Parlange approximation (Parlange et al., 2001). The latter is actually an approximation for horizontal aquifers but has also shown to work reasonably well at sloping aquifers (Mendoza et al., 2003). The models simulate the drainage of an initially fully saturated aquifer, which is compared to a numerical groundwater model implemented in MODFLOW (McDonald and Harbaugh, 1988) as a reference.

Furthermore, the analytical approximations of sloping aquifers are also used to estimate the aquifer properties of the Schöneben Rock Glacier and the results are compared to the models applied in Winkler et al. (I). The equations and a more detailed description of the applied analytical approximations can be found in Pauritsch et al. (II).

Natural/artificial tracers

Natural tracers such as water temperature, electric conductivity and stable isotopes ($\delta^{18}O$ and $\delta^{2}H$) are used to analyze the storage and discharge dynamics of the Schöneben Rock Glacier. However, water temperature has to be regarded as a reactive tracer as it is adjusting to the thermal conditions of the ground. The stable isotopes are conservative tracers and electric conductivity can be assumed to be also conservative because of the negligible water-rock interaction in crystalline rocks. The time lag between the hydraulic recharge pulse and the measured breakthrough of recharge water at the spring is analyzed to estimate the travel time of recharge water. Moreover, electric conductivity and stable isotopes are used in two-component mixing models (Wels et al., 1991) to separate and quantify pre-event water and recharge water. Differences of the isotopic signature of the spring water to the meteoric water line gives information about the storage and mixing processes within the aquifer and as $\delta^{18}O$ shows seasonal variations, it is used to estimate the mean residence time of the groundwater. A more detailed description of the mixing model and the applied methods using the natural tracers is given in Winkler et al. (I).

Using the chemical compounds fluorescein sodium, sulforhodamine B and eosin Y as artificial tracers, a tracer test was performed in 2012 in addition to a previously conducted tracer experiment in 2009 (Pauritsch, 2011). The tracers were injected simultaneously at two injection points, fluorescein sodium at the rooting zone of the rock glacier in a horizontal distance of 670 m from the spring and sulforhodamine B and eosin Y at a location in the proximity of a prominent gully at the southern side of the rock glacier in a horizontal distance of 350 m from the spring (Fig. 2 in Winkler et al., I). The tracers are detected at the spring using a field fluorometer (Albillia GGun-FL30; Schnegg, 2002) and the data are used in Winkler et al. (I) to estimate the pore velocity and hydraulic conductivity of the rock glacier. A more detailed description of the tracer tests is given in Winkler et al. (I).

Geophysics

The motivation for the geophysical investigations is to determine the thickness and internal structure of the rock glacier (e.g., layering) as well as the relief of the underlying bedrock, which is assumed to represent the aquifer base. Moreover, relatively thick saturated zones should become visible in the surveys. The data are then used to specify the aquifer geometry used in the numerical groundwater model presented in Pauritsch et al. (III).

The geophysical investigations performed in the course of this study contain a seismic refraction survey (hereinafter referred to as RS) and a ground-penetrating radar survey (hereinafter referred to as GPR). A detailed description about the applied GPR is given in this chapter as it is only partly described in the publications featured herein. In contrast, the RS is already described in detail in Winkler et al., (I) and therefore only a short description is presented here.

Three profiles (one longitudinal and two transversal profiles; see Fig. 7) were investigated in the RS survey. The seismic energy was partly induced using a sledge hammer and partly by using explosive charges, planted into the voids of the blocky surface of the rock glacier. The acoustic waves, which were refracted at layer boundaries, separating layers with different material properties, were recorded by geophones that were situated on the surface in 5 m distance to each other along the investigated profiles.

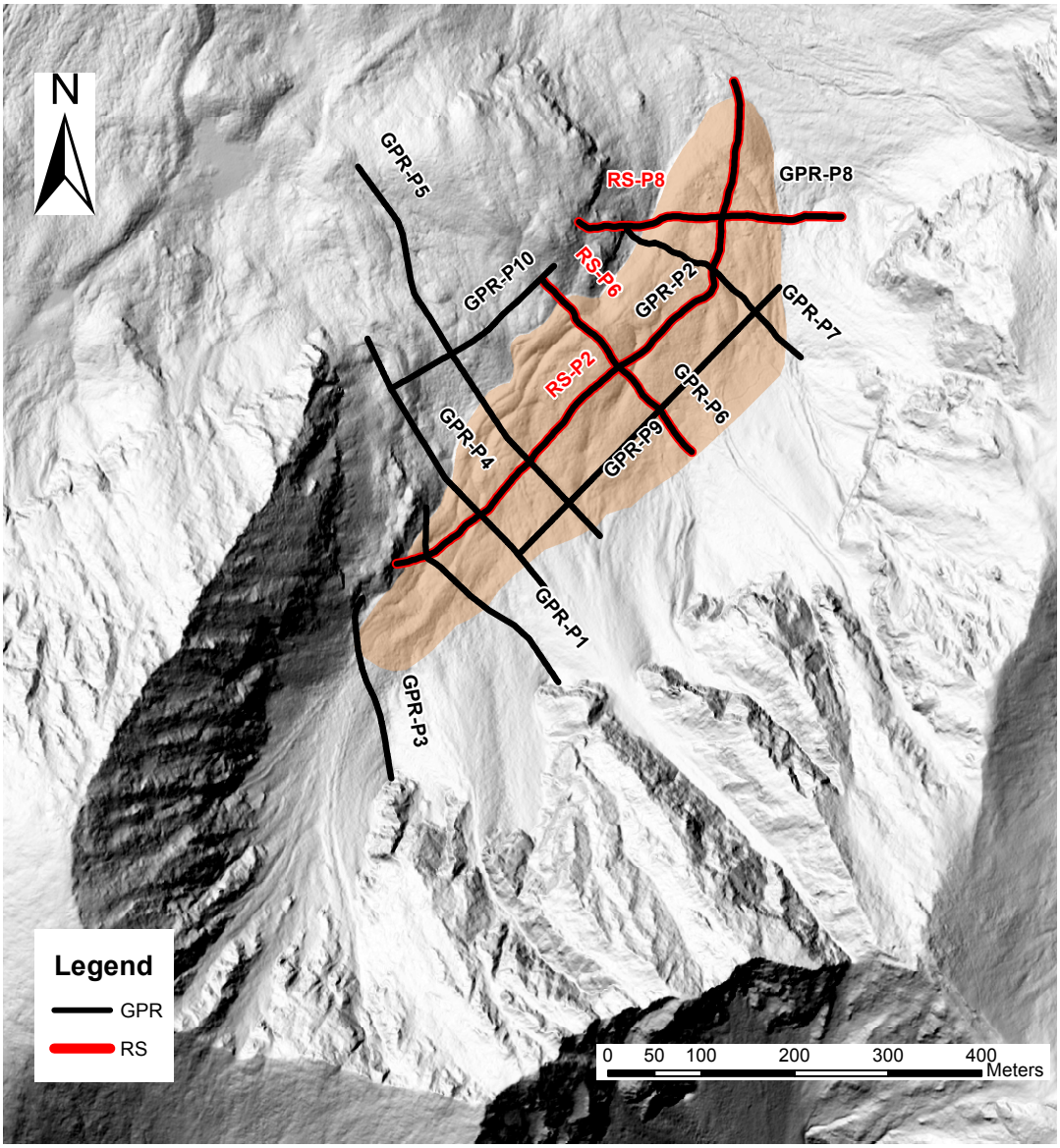

Fig. 7: Positions of the ground penetrating radar (GPR) profiles and seismic refraction (RS) profiles. GIS data were provided by the Federal Government of Styria (© GIS-Steiermark).

The GPR method is based on electromagnetic waves that are emitted into the ground by an antenna. The waves are partly reflected at boundaries, separating different materials, and are finally received again at the surface using an antenna. The reflection at the boundaries is dependent on the material differences and is strong at distinct differences (Annan, 2009). The penetration depth and resolution are dependent on the frequency of the antenna (Annan, 2009). In the conducted GPR survey ten profiles were investigated, three of them coinciding with the RS profiles for comparison (Fig. 7). The

profiles cover the actual rock glacier as well as some of the surrounding areas. The profiles were extended in the north-western part to investigate possible groundwater flow towards the neighboring catchment which was indicated by tracer tests conducted earlier (Pauritsch, 2011; Winkler et al., I). An antenna with a frequency of 100 MHz was used, leading to an estimated penetration depth of 25 m and a resolution of 0.6 m (estimated values are for dry sand; Cassidy, 2009). The survey was conducted during winter time in order to efficiently pull the antenna on the snow cover along the profiles (Fig. 8). The post processing and analysis of the data was performed using the software Reflexw (v7.2.2; ©Sandmeier geophysical research).

Fig. 8: Field impression of the ground-penetrating radar measurements on the Schöneben Rock Glacier in March 2012 (photo by courtesy of A. Kellerer-Pirklbauer)

Numerical groundwater model

A numerical groundwater model of the relict Schöneben Rock Glacier is elaborated to investigate the dominating aquifer features influencing the discharge of relict rock glacier springs (Pauritsch et al., III). Therefore, several model scenarios with differences in the internal structure and the aquifer base

topography are compared to each other. The focus lies on the respective discharge behavior of scenarios containing layered structures as opposed to preferential flow through channels, because the possibility of both types of internal structures is indicated by observations at other rock glaciers (Untersweg and Proske, 1996; Krainer et al., 2015). The aquifer geometry is determined through the geophysical investigations and the applied input data consist of recharge, which is estimated using a simple soil water balance model using measured precipitation data (from the automatic weather station), and estimated evapotranspiration. The models are calibrated and verified using the discharge which is measured at the spring of the Schöneben Rock Glacier. A more detailed description of the applied model scenarios and the model setup can be found in Pauritsch et al. (III).

Lumped-parameter model

An extended version of the lumped-parameter rainfall-runoff model GR4J (Perrin et al., 2003) is used to simulate the discharge of the Schöneben Rock Glacier. The model consists of four parameters (x_1 [mm]: maximum capacity of soil moisture accounting store; x_2 [mm]: water exchange coefficient; x_3 [mm]: maximum capacity of routing store; x_4 [days]: time parameter) that are free for calibration. In order to simulate multi-annual time periods, a degree-day snow module (Majone et al., 2010) is added to the model (GR4J+). Potential evapotranspiration is computed based on the findings of Oudin et al. (2005). Although no direct aquifer parameters such as hydraulic conductivity or specific yield can be derived from this model, it allows a verification of the conceptual understanding of relict rock glaciers by examination of the calibrated parameters. Furthermore, the parameter set of the Schöneben Rock Glacier catchment is used for similar neighboring rock glacier catchments in a semi-distributed model. The discharge of the rock glaciers is then added as external input to subordinate catchment areas where discharge measurement stations are available (Finsterliesing and Unterwald, see Fig. 1b in Wagner et al., IV). As the catchments have different areal shares of rock glacier influenced headwaters, the impact of the rock glaciers on the discharge behavior of the downstream rivers can be investigated. A more detailed description of the lumped-parameter rainfall-runoff model and the catchment areas used for the semi-distributed approach can be found in Wagner et al. (IV).

3. Main results and discussion

This chapter summarizes the main results of the investigations performed for this thesis. For a more detailed description and discussion of the results, the reader is referred to the respective publications in the appendices.

Discharge/recession analysis

The analysis of the winter recession of the discharge shows that the Schöneben Rock Glacier is not a single linear storage (Winkler et al., I). However, the recession can be approximated by a superposition of at least three exponential functions (Maillet, 1905) with recession coefficients of 0.028 to 0.047 1/d, 0.005 to 0.01 1/d, and 0.002 1/d for the early, intermediate and base flow recession, respectively (see Fig. 5 and Table 2 in Winkler et al., I).

The estimated volume of groundwater stored in the aquifer at the beginning of the recession is estimated to be at least 2.7×10^5 m³. With an assumed storage coefficient of 0.2 the estimated thickness of the saturated zone is approximately 10 m (Winkler et al., I).

The exponent of the power law function of Birk and Hergarten (2010) results in a value of 0.38. As a homogeneous aquifer would result in a value of 0.5, this result suggests some multi-scale aquifer structures such as fractal storage or scale-invariant flow patterns (Winkler et al., I).

The discharge recession analysis of sloping aquifers reveals that there are considerable differences between the applied analytical approximations (Pauritsch et al., II). As the Parlange approximation (Parlange et al., 2001) is actually designed for horizontal aquifers, the deviations to the numerical reference model naturally increases at larger slope angles. The Hogarth approximation (Hogarth et al., 2014) performs well at moderate slope angles of up to 5° and the Brutsaert solution (Brutsaert, 1994) is preferable for steeper slope angles because of the best representation of the kinematic wave that occurs at steep and/or hydraulically highly conductive aquifers at the transition from the early to the late time period. Furthermore, the initial condition seems to have a considerable impact on the early time period and therefore it is suggested to use the transition point for parameter estimations.

Applying these analytical models at the data of the Schöneben Rock Glacier shows that, when only the winter recession data is considered, the resulting estimations of aquifer thickness and hydraulic conductivity are in good agreement with the other results herein (Winkler et al., I). However, differences can be observed between the results of the individual models. The aquifer thickness is 10, 15 and 12 m and the hydraulic conductivity is $7x10^{-4}$, $1.4x10^{-5}$ and $1.7x10^{-5}$ m/s for the Parlange approximation, Hogarth approximation and Brutsaert solution, respectively (Pauritsch et al., II).

Although the occurrence of a kinematic wave is suggested by the Hogarth approximation and Brutsaert solution at a slope of 15°, which is approximately the average surface slope of the Schöneben Rock Glacier, no kinematic wave can be observed in the measured discharge data of the Schöneben Rock Glacier. This suggests that the aquifer is not homogeneous and also other factors are influencing the spring discharge, which are not included in the strongly simplified analytical models (Pauritsch et al., II).

Natural/artificial tracers

The investigations in Winkler et al. (I) show that a time lag of about 4 h can be observed at the rock glacier spring between the maximum recharge and the peaks of the natural tracers (electric conductivity and water temperature). The tailing of these parameters appears different as water temperature recovers to its pre-event value within hours whereas the electric conductivity requires several days. This can be attributed to the fact that water temperature is a reactive tracer that quickly adjusts to the ground temperature, whereas electric conductivity is assumed to be a conservative tracer as the water-rock interaction in crystalline rocks is negligible. Applying a two-component mixing model (Wels et al., 1991) under usage of the electric conductivity shows that during a recharge event only about 20 % of the total discharge is actual recharge water whereas 80 % is older (longer stored) groundwater. Using the same model with the isotope data results in a ratio of 13 and 87 %, respectively, and is thus in good agreement. The mean residence time of the groundwater is estimated to be 7 months and the low scattering of the data suggests a good storage capacity and mixing processes of the recharge within the rock glacier.

The results of the artificial tracer test (performed in 2012) are presented in detail in Winkler et al. (I) and show that fluorescein sodium was not detected at the spring for the entire measurement period, even though the tracer was injected at the same location as in the prior tracer test in 2009, where the tracer was detected at the spring after approximately 100 days. One likely possibility is that in

2012 the fluorescein sodium was preliminarily stored in the unsaturated zone and only little by little passed on to the saturated zone. Thus, the concentration at the spring remained below the detection limit. However, the other tracers were already detected after a short period of 2-3 hours. Moreover, the recorded tracer signals of sulforhodamine B and eosin Y suggest that a plume of the tracers remained at the position of the injection point because the time lag of the tracer peaks, triggered by recharge events, remained the same. Using these data, the pore velocity is estimated at 3.2×10^{-2} m/s. With an estimated hydraulic gradient of 0.14 and a drainable porosity of 0.2, the hydraulic conductivity results in 4.6×10^{-2} m/s.

Geophysics

The results of the RS survey clearly show the boundary of the bedrock and the overlying sediment cover in an average depth of 20-30 m (Winkler et al., I). While profiles RS-P02 and RS-P08 (Fig. 7) indicate a relatively homogeneous thickness of the sediment cover, profile RS-P06 shows a submerging of the bedrock topography in the southeastern part. This suggests that the Schöneben Rock Glacier is located on an asymmetrically shaped cirque. The surface topography is ascending towards Southeast because of the significant talus slopes located in this area. This leads to a high sediment thickness of more than 60 m (Pauritsch et al., III; Winkler et al., I).

A layered structure consisting of two layers can be observed within the debris cover over large parts of the profiles. In the profiles RS-P02 and RS-P08 the lower layer has an average thickness of 10-25 m and is characterized by p-wave velocities of less than 1000 m/s, thereby indicating unsaturated sediments with variable fine-grained material (Winkler et al., I). On top of this layer is an up to a few meters thick sediment cover consisting of blocky material with characteristic p-wave velocities of 330-990 m/s. At the profile RS-P06, a maximum thickness of 50 and 15 m for the lower and upper layer is respectively indicated in the southeastern part of the profile (Winkler et al., I).

A saturated zone was not detected in any of the RS profiles. However, due to the applied setup of the RS survey (geophone spacing of 5 m) and the velocity contrast of the layers, a blind zone of 14±5 m is possible (Winkler et al., I). As a saturated zone is required as a source of the base flow of the spring, it can therefore be assumed that it is limited to a maximum thickness of 19 m (Pauritsch et al., III).

The results of the GPR survey exhibit a high level of noise, which results among other things presumably from diffraction from the boulders near the surface (Merz et al., 2015). Because of the low quality of the data, identification of the bedrock boundary was challenging and internal

structures of the rock glacier were not possible to derive (Winkler et al., 2016b). However, the data of the RS survey were used to support the process of bedrock identification at coinciding sections with the RS profiles and intersections of the profiles. As a result, the bedrock boundary was indicated in most GPR profiles except GPR-P09, where no layer boundary was visible. Thus, this profile was discarded from further post-processing and interpretation.

The bedrock topography is determined with the software Surfer 8 (Version 8.06.39, ©1993-2006, Golden Software, Inc) using kriging of the data of the RS and GPR survey. However, as profile RS-P06 indicates a submerging of the bedrock topography and the profiles of the geophysical investigations are not covering the talus slopes in the southeast of the Schöneben Rock Glacier, this area is interpolated using additional anchor-points (Pauritsch et al., III). Two different approaches are applied to estimate the sediment thickness in this area (Fig. 9). First, the average slopes of the rock cliffs above the talus slopes are extrapolated down into the talus slopes and intersected with the elevation of the last known points of the nearest profile (Fig. 9a). Alternatively, the depth is linearly increasing from zero at the top of the talus slopes towards the elevation of the last known points of the nearest geophysics profile (Fig. 9b). The former results in steep sides and a nearly horizontal bedrock topography with a high sediment thickness in the area of the talus slopes. Opposing to this, the latter indicates more gentle slopes and only a relatively thin sediment cover in this area (Pauritsch et al., III).

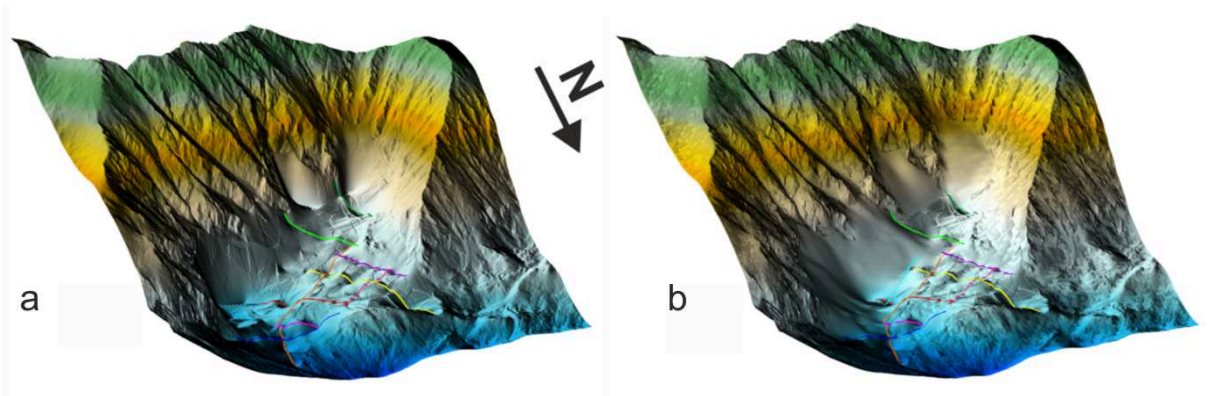

Fig. 9: Digital elevation model of the estimated bedrock topography. The colored lines represent the profiles of the geophysical survey; (a) shows the approach using extrapolated slopes of the rock cliffs above the talus slopes; (b) presents the alternative approach using a linearly increasing depth towards the rock glacier

Numerical groundwater model

The numerical groundwater models show that a homogeneous model fails to reproduce the discharge behavior of the Schöneben Rock Glacier, which supports the previous findings and indicates that the rock glacier is a more complex, heterogeneous aquifer (Pauritsch et al., III). The discharge behavior of the spring can be reasonably simulated by models with layers and/or preferential flow structures such as channel networks. The estimated hydraulic conductivity is in the order of 10^{-2} – 10^{-3} m/s for the parts controlling the fast flow component and 10^{-5} – 10^{-6} m/s for the parts controlling the slow flow component. Thus, the results are in good agreement with the results of the tracer experiment and the analytical models (see Winkler et al., I and Pauritsch et al., II).

However, with the lack of information about the water table within the rock glacier and as the models are therefore solely calibrated on the spring discharge time series, the results are ambiguous and the layering or the presence of preferential flow channels as the origin of the heterogeneity cannot be clearly distinguished (Pauritsch et al., III). This ambiguity, resulting from the spatially integrative spring discharge time series, also afflicts the effect of the aquifer base topography. However, the numerical groundwater models show that the topography of the aquifer base influences the discharge behavior especially when simple model structures with few adjustable parameters are considered. In contrast, in more complex models the effect of the aquifer base topography is minimized in the course of the calibration.

Lumped-parameter model

The discharge behavior of the Schöneben Rock Glacier can be simulated accurately using the GR4J+ lumped-parameter model (Wagner et al., IV). Using data of the automatic weather station on the Schöneben Rock Glacier, the calibrated parameters result in a small maximum capacity of the soil moisture accounting store (x_1=90 mm) and a significant maximum capacity of the routing store (x_3=303 mm), representative for the soil and the groundwater storage, respectively. These results are in good agreement with the natural tracers, which show that the majority of the spring water after recharge events is long stored groundwater with only small amounts of event water and little influence of the soil cover (which is almost negligible).

The short value of 1.15 d for the time parameter x_4 indicates that the vadose zone is quickly passed and plays a negligible role (Wagner et al., IV), which is in good agreement with the results of the

artificial tracer experiment (see Winkler et al., I). Moreover, the positive value of 9.4 mm for the water exchange coefficient (x_2) shows that additional water is required to equalize the water balance, which can be explained by general measurement uncertainties of precipitation in alpine terrain and snow drifts over the ridges.

The application of the semi-distributed model also shows that rock glacier-free areas of the catchments are calibrated with high values for the maximum capacity of the routing store. This indicates the occurrence of additional aquifers other than rock glaciers, such as for example moraine deposits and scree slopes. However, on a daily time step the maximum runoff contribution of rock glaciers in the investigated catchment areas is 63 and 52 % at respective areal shares of rock glaciers of 15 and 12 %. The contribution of the rock glacier influenced headwaters varies seasonally and shows the maximum contribution of rock glaciers in the late snow melt period and late summer time.

4. Conclusions

The individual investigations of this thesis are in good agreement with each other and suggest that the relict Schöneben Rock Glacier is a heterogeneous aquifer with hydrogeological characteristics similar to karst aquifers. As such, the discharge analysis, natural tracers and artificial tracer experiment reveal a rather quick response of the spring to recharge events. The observed time shift between the actual recharge event and the response of the spring appears to be only a few hours. Contrasting to this, the base flow recession analysis suggests a large storage component, which enables the spring to have a considerable base flow during dry periods. This is also supported by the lumped-parameter model, which is suggesting a significant groundwater storage, whereas the percentage of the quick flow component is relatively small (consistent with event water separation).

The discharge behavior of the rock glacier spring is influenced by a variety of factors. First, the investigated analytical models show that the slope of the aquifer base is decisive for the discharge behavior of the base flow and, consequently, for the estimated aquifer parameters. However, the analyses show that heterogeneous aquifers such as the investigated rock glacier are challenging to simulate with such strongly simplified analytical models. Nevertheless, reasonable ranges of aquifer properties can be provided by using more than one method (multimethod approach) and by focusing solely on the winter recessions. Second, the numerical model demonstrates that the topography of the aquifer base can also have important implications on the discharge dynamics. Third, the numerical model also shows that the internal structure obviously has a strong influence on the discharge behavior. Layered structures as well as a network of draining channels or a combination of both are conceivable. However, to determine the actual internal structure of the Schöneben Rock Glacier additional information about the spatial and temporal variation of the water table is needed. An interpretation that is solely dependent on the spring discharge yields a strong ambiguity as these data are highly spatially integrative.

The results of the semi-distributed approach of the lumped parameter model suggest that discharge from relict rock glaciers is an important contribution to the downstream rivers. The contribution seasonally varies and a maximum impact can be observed during the late snow melt period and late summer time. During these times, the contributed discharge of the rock glaciers ranges up to a multiple of their areal share and therefore indicates a significant importance of relict rock glaciers.

The results of this thesis show that relict rock glaciers represent complex, heterogeneous aquifers that can have significant influence on the downstream rivers under current climate conditions and

moreover might gain further importance in the course of climate warming. Thus, they should be taken into account for water management issues such as human water supply, hydroelectric power plants and flood preventions.

5. Perspectives

The characterization of the hydrogeological properties and functioning of rock glaciers is a significant task because rock glaciers represent important aquifers in high alpine catchments and thus are the source of many headwaters that are significant contributions for lower elevated water basins (e.g., Wagner et al., IV). Knowledge about the hydrodynamics of rock glaciers is also essential to evaluate the vulnerability of rock glacier springs regarding their usability for human water supply and may help to determine the source of heavy metals, which were recently observed in the melt water of active rock glaciers (Krainer et al., 2015).

In order to enhance the knowledge of the hydrogeological properties and functioning of relict rock glaciers, further information about the spatial and temporal variations of the water table is required. These data may introduce additional constraints to the numerical model and therefore reduce the ambiguity of the results. However, the acquisition of these data is a challenging task, because the installation of observation wells is cost-expensive and technically difficult due to the rough terrain and the coarse blocky material at the rock glacier surface. Thus, it seems more beneficial to use additional geophysical investigations. In particular the application of airborne methods such as frequency-domain or time-domain electromagnetics or (airborne) ground-penetrating radar seems promising (see Pauritsch et al., III).

Furthermore, the consequences of changing climate conditions on rock glaciers and their springs should be investigated with special regards to the seasonality of the contribution of rock glaciers, which may adjust in the course of changing climatic conditions. Moreover, the transition from active to relict rock glaciers may result in a changed discharge behavior and therefore can also influence the hydrology and ecology of downstream rivers. However, the coarse blocky materials covering the rock glaciers have a cooling effect on the permafrost ice below (Johnson et al., 2007), which can delay melting processes and make the time estimation of the melting of rock glacier-related ice not straight forward.

6. References

Annan AP (2009) Electromagnetic principles of Ground Penetrating Radar. In: Jol HM (Ed.), Ground Penetrating Radar: Theory and Applications. Elsevier Science, Amsterdam (The Netherlands), pp. 3–40.

Arenson L, Hoelzle M, Springman S, (2002) Borehole deformation measurements and internal structure of some rock glaciers in Switzerland. Permafrost and Periglacial Processes, 13 (2), 117–135, doi: 10.1002/ppp.414.

Azócar GF, Brenning A (2010) Hydrological and geomorphological significance of rock glaciers in the dry Andes, Chile (27°–33°S). Permafrost and Periglacial Processes, 21 (1), 42–53, doi: 10.1002/ppp.669 .

Barsch D (1996): Rockglaciers: Indicators for the Present and Former Geoecology in High Mountain Environments. Springer Series in Physical Environment 16. Springer Verlag, Berlin, 331 pp.

Berthling I (2011) Beyond confusion: rock glaciers as cryo-conditioned landforms. Geomorphology, 131 (3–4), 98–106, doi: 10.1016/j.geomorph.2011.05.002

Birk S, Hergarten S (2010) Early recession behaviour of spring hydrographs. Journal of Hydrology, 387 (1-2), 24-32, doi:10.1016/ j.jhydrol.2010.03.026

Bolch T, Gorbunov AP (2014) Characteristics and origin of the rock glaciers in northern Tien Shan (Kazakhstan/Kyrgyzstan). Permafrost and Periglacial Processes, 25, 320–332, doi: 10.1002/ppp.1825

Bollmann E, Rieg L, Spross M, Sailer R, Bucher K, Maukisch M, Monreal M, Zischg A, Mair V, Lang K, Stötter J (2012) Blockgletscherkataster Südtirol – Erstellung und Analyse [Rock glacier registry Southern Tyrol – creation and analysis]. In: Stötter J, Sailer R (Eds) Permafrost in Südtirol. Innsbrucker Geographische Studien, 39, 147-171

Brenning A (2005) Geomorphological, hydrological and climatic significance of rock glaciers in the Andes of Central Chile (33–35°S). Permafrost and Periglacial Processes, 16, 231–240, doi: 10.1002/ppp.528.

Brutsaert W (1994) The unit response of groundwater outflow from a hillslope. Water Resources Research, 30, 2759– 2763, doi: 10.1029/94WR01396.

Cassidy NJ (2009) Electrical and Magnetic Properties of Rocks, Soils and Fluids. In: Jol, H.M. (Ed.), Ground Penetrating Radar: Theory and Applications. Elsevier Science, Amsterdam (The Netherlands), pp. 41–72.

Cheng GD, Lai YM, Sun ZZ., Jiang F (2007) The 'thermal semi-conductor' effect of crushed rocks. Permafrost and Periglacial Processes, 18 (2), 151–160, doi: 10.1002/ppp.575.

Corte AE (1976) Rock glaciers. Biul Peryglacjalny26, pp. 175–197.

Ehlers J, Gibbard PL, Hughes PD (2011) Quaternary glaciations—extent and chronology: a closer look. In: van der Meer JJM (Ed.). Developments in quaternary science. Heidelberg (Germany): Springer. p. 1–1108.

Frehner M, Ling AHM, Gärtner-Roer I (2015) Furrow-and-Ridge Morphology on Rockglaciers Explained by Gravity-Driven Buckle Folding: A Case Study From the Murtèl Rockglacier (Switzerland). Permafrost and Periglacial Processes, 10, 57–66, doi: 10.1002/ppp.1831.

Froitzheim N, Plasienka D, Schuster R (2008) Alpine tectonics of the Alps and Western Carpathians. In: McCann T (Ed.) The Geology of Central Europe, Volume 2: Mesozoic and Cenozoic. 1141-1232. Geological Society of London.

Gödel S (1993) Geohydrologie der Blockgletscher im Hochreichhart-Gebiet (Seckauer Tauern, Steiermark) [Geohydrology of rock glaciers in the Hochreichhart-area (Seckauer Tauern Range, Styria)]. MSc thesis, University of Vienna

Gorbunov AP, Titkov SN, Polyakov VG (1992) Dynamics of rock glaciers of the Northern Tien Shan and the Djungar Ala Tau, Kazakhstan. Permafrost and Periglacial Processes, 3, 29–39, doi:10.1002/ppp.3430030105

Haeberli W, Hallet B, Arenson L, Elconin R, Humlum O, Kääb A, et al. (2006) Permafrost Creep and Rock Glacier Dynamics. Permafrost and Periglacial Processes, 17, 189–214, doi: 10.1002/ppp.561.

Harris SA, Wayne K, Blumenstengel D, Cook H, Krouse R, Whitley G (1994) Comparison of the water drainage from an active near slope rock glacier and a glacier, St. Elias Mountains, Yukon Territory. Erdkunde, 48, 81-91

Harrison S, Whalley B, Anderson E (2008) Relict rock glaciers and protalus lobes in the British Isles: implications for Late Pleistocene mountain geomorphology and palaeoclimate. Journal of Quaternary Science, 23, 287–304, doi: 10.1002/jqs.1148.

Hausmann H, Krainer K, Brückl E, Ullrich C (2012) Internal structure, ice content and dynamics of Ölgrube and Kaiserberg rock glaciers (Ötztal Alps, Austria) determined from geophysical surveys. Austrian Journal of Earth Sciences, 105 (2), 12–31.

Head JW, Neukum G, Jaumann R, Hiesinger H, Hauber E, Carr M, et al. (2005) Tropical to mid-latitude snow and ice accumulation, flow and glaciation on Mars. Nature, 434, 346–351, doi: 10.1038/nature03359.

Hogarth WL, Li L, Lockington DA, Stagnitti F, Parlange MB, Barry DA, Steenhuis TS, and Parlange JY (2014) Analytical approximation for the recession of a sloping aquifer. Water Resources Research, 50, 8564–8570, doi: 10.1002/2014WR016084.

Hughes PD, Gibbard PL, Woodward JC (2003) Relict rock glaciers as indicators of Mediterranean palaeoclimate during the Last Glacial Maximum (Late Würmian) of northwest Greece. Journal of Quaternary Science, 18, 431–440, doi: 10.1002/jqs.764.

Humlum O (1982) Rock glacier types on Disko, Central West Greenland. Geografisk Tidsskrift, 82, 59-66.

Humlum O (1998) The climatic significance of rock glaciers. Permafrost and Periglacial Processes, 9, 375–395, doi: 10.1002/(SICI)1099-1530(199810/12)9:4<375::AID-PPP301>3.0.CO;2-0.

Ikeda A, Matsuoka N (2006) Pebbly versus boulder rock glaciers: Morphology, structure and processes. Geomorphology, 73 (3–4), 279–296, doi: 10.1016/j.geomorph.2005.07.015

Johnson BG, Thackray GD, Van Kirk R (2007) The effect of topography, latitude, and lithology on rock glacier distribution in the Lemhi Range, central Idaho, USA. Geomorphology, 91, 38–50, doi: 10.1016/j.geomorph.2007.01.023.

Kääb A, Weber M (2004) Development of transverse ridges on rock glaciers: field measurements and laboratory experiments. Permafrost and Periglacial Processes, 15 (4), 379–391, doi: 10.1002/ppp.506.

Kääb A, Isaksen K, Eiken T, Farbrot H (2002) Geometry and dynamics of two lobe-shaped rock glaciers in the permafrost of Svalbard. Norwegian Journal of Geography, 56, 152–160.

Kellerer-Pirklbauer A (2008) Aspects of glacial, paraglacial and periglacial processes and landforms of the Tauern Range, Austria. PhD thesis, University of Graz.

Kellerer-Pirklbauer A, Lieb GK, Kleinferchner H (2012) A new rock glacier inventory in the eastern European Alps. Austrian Journal of Earth Sciences, 105 (2), 78-93.

Kellerer-Pirklbauer A, Pauritsch M, Winkler G (2015) Widespread occurrence of ephemeral funnel hoarfrost and related air ventilation in coarse-grained sediments of a relict rock glacier in the Seckauer Tauern Range, Austria. Geografiska Annaler A, 97 (3): 453-471, doi:10.1111/geoa.12087

Kern K, Lieb GK, Seier G, Kellerer-Pirklbauer A (2012) Modelling geomorphological hazards to assess the vulnerability of alpine infrastructure: The example of the Großglockner-Pasterze area, Austria. Austrian Journal of Earth Sciences, 105 (2), 113-127.

Krainer K, Mostler W (2002) The discharge of active rock glaciers: examples from the Eastern Alps (Austria). Arctic, Antarctic and Alpine Research, 34 (2), 142-149.

Krainer K, Mostler W (2006) Flow velocities of active rock glaciers in the Austrian Alps. Geografiska Annaler A, 88 (4), 267–280, doi: 10.1111/j.0435-3676.2006.00300.x.

Krainer K, Ribis M (2009) Blockgletscher und ihre hydrologische Bedeutung im Hochgebirge [Rock glacier and their hydrological importance in high mountains]. – Mitteilungsblatt des hydrographischen Dienstes in Österreich, 86, 65-78

Krainer K, Ribis M (2012) A rock glacier inventory of the Tyrolean Alps (Austria), Austrian Journal of Earth Sciences, 105 (2),32-47

Krainer K, Mostler W, Spoetl C (2007) Discharge from active rock glaciers, Austrian Alps; a stable isotope approach. Mitteilungen der Österreichischen Geologischen Gesellschaft, 100, 102-112.

Krainer K, Bressan D, Dietre B, Haas JN, Hajdas I, Lang K, Mair V, Nickus U, Reidl D, Thies H, Tonidandel D (2015) A 10,300-year-old permafrost core from the active rock glacier Lazaun, southern Ötztal Alps (South Tyrol, northern Italy). Quaternary Research 83 (2), 324-335, doi:10.1016/j.yqres.2014.12.005

Kresic N (2007) Hydrogeology and Groundwater Modeling, Second Edition. Boca Raton, Florida, (CRC Press, Taylor & Francis)

Maillet E (1905) Mécanique et physique du globe. Essai d'hydraulique souterraine et fluviale (Mechanics and physiques of the world. An essay of subterranean and fluviatile hydraulics) [Mechanics and physics of the globe. Groundwater and river hydraulic test (Mechanics and physical of the world. An essay of subterranean and fluvial hydraulics)]. Paris

Majone B, Bertagnoli A, Bellin A (2010) A non-linear runoff generation model in small Alpine catchments. Journal of Hydrology, 385, 300-312, doi: 10.1016/j.jhydrol.2010.02.033.

McDonald MG, Harbaugh AW (1988) A modular three-dimensional finite-difference ground-water flow model. In: U.S. Geological Survey Techniques of Water-Resources Investigations, Book 6, A1, 586 p

Mendoza GF, Steenhuis TS, Walter MT, Parlange JY (2003) Estimating basin-wide hydraulic parameters of a semi-arid mountainous watershed by recession-flow analysis. Journal of Hydrology, 279 (1-4), 57–69, doi: 10.1016/S0022-1694(03)00174-4.

Merz K, Maurer H, Buchli T, Horstmeyer H, Green AG, Springman SM (2015) Evaluation of Ground-Based and Helicopter Ground-Penetrating Radar Data Acquired Across an Alpine Rock Glacier. Permafrost and Periglacial Processes, 26, 13–27, doi:10.1002/ppp.1836.

Millar CI, Westfall RD (2008) Rock glaciers and periglacial rock-ice features in the Sierra Nevada; classification, distribution, and climate relationships. Quaternary International, 188, 90-104.

Millar CI, Westfall RD, Delany DL (2013) Thermal and hydrologic attributes of rock glaciers and periglacial talus landforms: Sierra Nevada, California, USA. Quaternary International, 310, 169-180, doi: 10.1016/j.quaint.2012.07.019.

Monnier S, Kinnard C (2015) Internal Structure and Composition of a Rock Glacier in the Dry Andes, Inferred from Ground-penetrating Radar Data and its Artefacts. Permafrost and Periglacial Processes, 26 (4), 335-346, doi: 10.1002/ppp.1846.

Nagl H (1976) Die Raum-Zeit-Verteilung der Blockgletscher in den Niederen Tauern und die eizeitliche Vergletscherung der Seckauer Tauern [The spatial-temporal-distribution of rock glaciers in the Niedere Tauern Range and the ice-age glaciation oft he Seckauer Tauern Range]. Mitteilungen naturwissenschaftlicher Verein der Steiermark, 106, 95–118.

Oudin L, Hervieu F, Michel C, Perrin C, Andréassian V, Anctil F, Loumagne C (2005) Which potential evapotranspiration input for a lumped rainfall-runoff model? Part 2 – Towards a simple and efficient potential evapotranspiration model for rainfall-runoff modeling. Journal of Hydrology, 303, 290–306, doi: 10.1016/j.jhydrol.2004.08.026

Paasche Ø, Dahl SO, Løvlie R, Bakke J, Nesje A (2007) Rockglacier activity during the Last Glacial–Interglacial transition and Holocene spring snowmelting. Quaternary Science Reviews, 26, 793–807, doi: 10.1016/j.quascirev.2006.11.017.

Pauritsch M (2011) Die Hydrodynamik reliktischer Blockgletscher am Beispiel des Schönebenblockgletschers (Seckauer Tauern, Steiermark) [The hydrodynamics of relict rock glaciers at the example oft he Schöneben Rock Glacier (Seckaer Tauern Range, Styria)]. MSc thesis, University of Graz.

Pauritsch M, Birk S, Wagner T, Hergarten S, Winkler G (2015) Analytical approximations of discharge recessions for steeply sloping aquifers in alpine catchments. Water Resources Research, 51, 8729–8740, doi: 10.1002/2015WR017749

Pauritsch M, Wagner T, Winkler G, Birk S (accepted) Investigating groundwater flow components in an Alpine relict rock glacier (Austria) using a numerical model. Hydrogeology Journal, doi: 10.1007/s10040-016-1484-x.

Parlange JY, Parlange MB, Steenhuis TS, Hogarth WL, Barry DA, Li L, Stagnitti F, Heilig A, Szilagyi J (2001) Sudden drawdown and drainage of a horizontal aquifer. Water Resources Research, 37, 2097–2101, doi: 10.1029/2000WR000189.

Perrin C, Michel C, Andréassian V (2003) Improvement of a parsimonious model for streamflow simulation. Journal of Hydrology, 279 (1-4), 275-289, doi: 10.1016/S0022-1694(03)00225-7.

Pfingstl S, Kurz W, Schuster R, Hauzenberger C (2015) Geochronological constraints on the exhumation of the Austroalpine Seckau Nappe (Eastern Alps). Austrian Journal of Earth Sciences, 108, 172–185.

Putnam AE, Putnam DE (2009) Inactive and relict rock glaciers of the Deboullie Lakes Ecological Reserve, northern Maine, USA. Journal of Quaternary Science, 24, 773–784, doi: 10.1002/jqs.1252.

Rangecroft S, Harrison S, Anderson K, Magrath J, Castel AP, Pacheco P (2014) A first rock glacier inventory for the Bolivian Andes. Permafrost and Periglacial Processes, 25, 333-343, doi: 10.1002/ppp.1816.

Rode M, Kellerer-Pirklbauer A (2012) Schmidt-hammer exposure-age dating (SHD) of rock glaciers in the Schöderkogel-Eisenhut area, Schladminger Tauern Range, Austria.The Holocene, 22, 761-771, doi: 10.1177/0959683611430410.

Rorabaugh MI (1964) Estimating changes in bank storage and ground-water contribution to streamflow. IAHS Publication, 63, 432-441.

Schmid SM, Fügenschuh B, Kissling E, Schuster R (2004) Tectonic map and overall architecture of the Alpine orogen. Eclogae Geologicae Helvetiae, 97 (1), 93-117, doi: 10.1007/s00015-004-1113-x.

Schmid MO, Baral P, Gruber S, Shahi S, Shrestha T, Stumm D, Wester P (2015) Assessment of permafrost distribution maps in the Hindu Kush Himalayan region using rock glaciers mapped in Google Earth. The Cryosphere, 9, 1089-2099, doi: 10.5194/tc-9-2089-2015.

Schnegg PA (2002) An inexpensive field fluorometer for hydrogeological tracer tests with three tracers and turbidity measurement. In: Bovanegra E, Martinez D, Massone H (eds) XXXII IAH and ALHSUD Congress Groundwater and Human Development, Mar del Plata, Argentina, October 2002.

Schuster R, Kurz W (2005) Eclogites in the Eastern Alps: High Pressure Metamorphism in the context of the Alpine Orogeny. Mitteilungen der Österreichischen Mineralogischen Gesellschaft, 150, 183-198.

Sorg A, Kääb A, Roesch A, Bigler C, Stoffel M (2015) Contrasting responses of Central Asian rock glaciers to global warming. Scientific Reports, 5, 8228, doi: 10.1038/srep08228

Steenstrup KJV (1883) Bidrag til Kjendskab til Bræerne og Bræ-Isen i Nord-Grønland. Meddelelser om Grønland, 4 (2), 69-112.

Thies H, Nickus U, Tolotti M, Tessadri R, Krainer K (2013) Evidence of rock glacier melt impacts on water chemistry and diatoms in high mountain streams. Cold Regions Science and Technology, 96, 77–85, doi: 10.1016/j.coldregions.2013.06.006.

Untersweg T, Proske H (1996) Untersuchungen an einem fossilen Blockgletscher im Hochreichhartgebiet (Niedere Tauern, Steiermark) [Investigations at a fossil rock glacier in the Hochreichhart-area (Niedere Tauern Range, Styria)]. Grazer Schriften der Geographie und Raumforschung, 33, 201–207.

Untersweg T, Schwendt A (1995) Die Quellen der Blockgletscher in den Niederen Tauern [The springs of rock glaciers in the Niedere Tauern Range]. Bericht der wasserwirtschaftlichen Planung, 78, pp. 110.

Untersweg T, Schwendt A (1996) Blockgletscher und Quellen in den Niederen Tauern [Rock glacier and springs in the Niedere Tauern Range]. Mitteilungen der Österreichischen Geologischen Gesellschaft, 87, 47-55.

Van Husen D (1987) Die Ostalpen in den Eiszeiten [The Eastern Alps in the ice-ages]. Geologische Bundesanstalt, Vienna, 24 pp.

Vaughan DG, Comiso JC, Allison I, Carrasco J, Kaser G, Kwok R, Mote P, Murray T, Paul F, Ren J, Rignot E, Solomina O, Steffen K, Zhang T (2013) Observations: Cryosphere. In: Stocker TF, Qin D, Plattner GK, Tignor M, Allen SK, Boschung J, Nauels A, Xia Y, Bex V, Midgley PM (Eds.) Climate Change 2013: The Physical Science Basis. Contribution of Working Group I to the Fifth Assessment Report of the Intergovernmental Panel on Climate Change . Cambridge University Press, Cambridge, United Kingdom and New York, NY, USA.

Wagner T, Pauritsch M, Winkler G (2016) Impact of relict rock glaciers on spring and stream flow of alpine watersheds: Examples of the Niedere Tauern Range, Eastern Alps (Austria). Austrian Journal of Earth Sciences, 109, doi: 10.17738/ajes.2016.0006

Wahrhaftig C, Cox A (1959) Rock glaciers in the Alaska Range. Geological Society of America Bulletin, 70, 383–436, doi: 10.1130/0016-7606(1959)70[383:RGITAR]2.0.CO;2.

Wakonigg H (1978) Witterung und Klima in der Steiermark [Weather and climate in Styria]. Arbeiten aus dem Institut für Geographie in Graz, 23, 473 pp.

Wels C, Cornett RJ, Lazarete BD (1991) Hydrograph separation: A comparison of geochemical and isotopic tracers. Journal of Hydrology, 122, 253-274, doi: 10.1016/0022-1694(91)90181-G.

Winkler G, Wagner T, Pauritsch M, Birk S, Kellerer-Pirklbauer A, Benischke R, Leis A, Morawetz R, Schreilechner MG, Hergarten S (2016a) Identification and assessment of groundwater flow and storage components of the relict Schöneben Rock Glacier, Niedere Tauern Range, Eastern Alps (Austria). Hydrogeology Journal, 24, 1-17, doi: 10.1007/s10040-015-1348-9

Winkler G, Pauritsch M, Wagner T, Kellerer-Pirklbauer A (2016b) Reliktische Blockgletscher als Grundwasserspeicher in alpinen Einzugsgebieten der Niederen Tauern [Relict rock glaciers as groundwater storages in alpine catchment areas in the Niedere Tauern Range]. Berichte zur wasserwirtschaftlichen Planung Steiermark, 87, pp. 134. http://www.wasserwirtschaft.steiermark.at/cms/dokumente/11913323_102332494/6885027d/87.pdf [Accessed 12 September 2016]

Zurawek R (2002) Internal Structure of a Relict Rock Glacier, Sleza Massif, Southwest Poland. Permafrost and Periglacial Processes, 13, 29–42, doi: 10.1002/ppp.403.

7. Publications

7.1. Publication I

Winkler G, Wagner T, Pauritsch M, Birk S, Kellerer-Pirklbauer A, Benischke R, Leis A, Morawetz R, Schreilechner MG, Hergarten S (2016a) Identification and assessment of groundwater flow and storage components of the relict Schöneben Rock Glacier, Niedere Tauern Range, Eastern Alps (Austria). Hydrogeology Journal 24: 1-17. doi: 10.1007/s10040-015-1348-9

Hydrogeol J (2016) 24:937–953
DOI 10.1007/s10040-015-1348-9

PAPER

Identification and assessment of groundwater flow and storage components of the relict Schöneben Rock Glacier, Niedere Tauern Range, Eastern Alps (Austria)

Gerfried Winkler[1] · Thomas Wagner[1] · Marcus Pauritsch[1] · Steffen Birk[1] · Andreas Kellerer-Pirklbauer[2] · Ralf Benischke[3] · Albrecht Leis[3] · Rainer Morawetz[3,4] · Marcellus G. Schreilechner[3,4] · Stefan Hergarten[5]

Received: 15 April 2015 / Accepted: 29 November 2015 / Published online: 6 January 2016

Abstract More than 2,600 relict rock glaciers are known in the Austrian Alps but the knowledge of their hydraulic properties is severely limited. The relict Schöneben Rock Glacier (Niedere Tauern Range, Austria), with an extension of 0.17 km^2, was investigated based on spring data (2006–2014) and seismic refraction survey. Spring-discharge hydrographs and natural and artificial tracer data suggest a heterogeneous aquifer with a layered internal structure for the relict rock glacier. The discharge behavior exhibits a fast and a delayed flow component. The spring discharge responds to recharge events within a few hours but a mean residence time of several months can also be observed. The internal structure of the rock glacier (up to several tens of meters thick) consists of: an upper blocky layer with a few meters of thickness, which lacks fine-grained sediments; a main middle layer with coarse and finer-grained sediments, allowing for fast flow; and an approximately 10-m-thick basal till layer as the main aquifer body responsible for the base flow. The base-flow component is controlled by (fine) sandy to silty sediments with low hydraulic conductivity and high storage capacity, exhibiting a difference in hydraulic conductivity to the upper layer of about three orders of magnitude. The high storage capacity of relict rock glaciers has an impact on water resources management in alpine catchments and potentially regulates the risk of natural hazards such as floods and related debris flows. Thus, the results highlight the importance of such aquifer systems in alpine catchments.

Electronic supplementary material The online version of this article (doi:10.1007/s10040-015-1348-9) contains supplementary material, which is available to authorized users.

✉ Gerfried Winkler
gerfried.winkler@uni-graz.at

Thomas Wagner
thomas.wagner@uni-graz.at

Marcus Pauritsch
marcus.pauritsch@uni-graz.at

Steffen Birk
steffen.birk@uni-graz.at

Andreas Kellerer-Pirklbauer
andreas.kellerer@uni-graz.at

Ralf Benischke
ralf.benischke@joanneum.at

Albrecht Leis
albrecht.leis@joanneum.at

Rainer Morawetz
rainer.morawetz@geo-5.at

Marcellus G. Schreilechner
marcellus.schreilechner@geo-5.at

Stefan Hergarten
stefan.hergarten@geologie.uni-freiburg.de

[1] Institute of Earth Sciences, NAWI Graz, University of Graz, Heinrichstrasse 26, 8010 Graz, Austria

[2] Department of Geography and Regional Science, University of Graz, Heinrichstrasse 36, 8010 Graz, Austria

[3] Resources – Institute for Water, Energy and Sustainability, JOANNEUM RESEARCH, Elisabethstrasse 18/II, 8010 Graz, Austria

[4] Current employer: Geo5 GmbH, Roseggerstrasse 17, 8700 Leoben, Austria

[5] Institute of Earth and Environmental Sciences, University of Freiburg, Albertstrasse 23-B, 79104 Freiburg, Germany

Keywords Groundwater flow · Conceptual models · Storage capacity · Austria · Relict rock glacier

Introduction

Climate change and the related increase of average air temperature have an important impact on the hydrological cycle particularly in alpine watersheds where the runoff is currently dominated by melting snow or ice (Barnett et al. 2005). It is predicted that the contribution of snow to winter precipitation will decrease, and that the winter snow cover will melt earlier. As a consequence, the peak river runoff will be shifted from summer and autumn to winter and early spring (e.g., Jasper et al. 2004; Stewart et al. 2004; Barnett et al. 2005; Tague and Grant 2009). This has a high significance, as alpine watersheds are important for water supply for human consumption and for sensitive ecosystems, also influencing areas further downstream. The importance of alpine groundwater contribution to stream flow has been shown by numerous studies in the last two decades (e.g., Campbell et al. 1995; Clow et al. 2003; Liu et al. 2004; Roy and Hayashi 2009; Tague and Grant 2009).

The decisive impact on seasonal stream flow patterns in alpine catchments is dominantly affected by the subsurface drainage processes of soils and sediment accumulation such as moraines, scree slopes or rock glaciers and subordinately of the subjacent bedrock. These processes are related to the topography and the subsurface properties such as porosity, transmissivity and storage capacity. Thus, one key challenge in the hydrological modeling of alpine watersheds is the quantification of these properties regulating the groundwater flow.

Moraines, scree slopes and active rock glaciers have been hydrogeologically characterized in recent studies, especially in the North American Rocky Mountains and the European Alps. Hydrological, hydrochemical and isotopic investigation methods have been applied to identify and determine the drainage processes, and surface geophysical investigations have been conducted to gain information about the geometry of these alpine aquifers and their internal structure. Clow et al. (2003) pointed out the importance of talus and debris-bound frozen water storage related to permafrost in an alpine catchment in the Colorado Rocky Mountains (USA). Roy and Hayashi (2009) and Langston et al. (2011) characterized the complex heterogeneous water flow and the internal structure of a moraine-talus feature. Their studies suggest that unconsolidated sediment landforms can provide multiple and possibly disconnected water flow paths with unique geochemical characteristics. They conclude that such sediment accumulations cannot be treated as a single, homogeneous groundwater system in hydrological modeling of alpine watersheds. The hydrology and the hydrological importance of active rock glaciers as water storages in alpine catchments have been investigated in particular during the last two decades. Rock glaciers are landforms indicating permafrost conditions during their genesis and evolution. These landforms are frequently characterized by distinct flow structures with ridges and furrows at the surface. Rock glaciers can be divided into intact (active and inactive) and relict ones. Active rock glaciers are frozen debris bodies with interstitial ice or ice lenses and move gravitationally down-slope or down-valley in the order of usually decimeters to a few meters per year (e.g., Barsch 1996; Haeberli et al. 2006). When movement comes to an end but ice is still present within the rock glacier, they are classified as inactive (but still intact); relict rock glaciers no longer have any ice.

Azócar and Brenning (2010) and Brenning (2005) estimated the water equivalent of frozen water stored in rock glaciers of the Chilean Andes, and showed that rock glaciers are even more important in storing frozen water than glaciers. Millar and Westfall (2008) and Millar et al. (2013) characterized the hydrologic and thermal behavior of rock glaciers and related landforms in the Californian Sierra Nevada (USA). Krainer and Mostler (2002) and Krainer et al. (2007) separated the run-off components snow and ice-melt water, rainwater and longer stored groundwater at the active Reichenkar Rock Glacier in the Austrian Alps using stable isotopes and hydrographs. The transition from active rock glaciers to, first, inactive and, later, relict rock glaciers is strongly affected by the lower limit of mountain permafrost, as the retreat of permafrost causes ice melting within the rock glaciers. Climate warming causes an upward shift of the lower limit of mountain permafrost (e.g., Haeberli and Beniston 1998), which will accelerate the transformation of active to relict rock glaciers in the future. In the Austrian Alps, for instance, already more than 2,600 relict rock glaciers exist covering a total area of about 150 km^2 (Kellerer-Pirklbauer et al. 2012; Krainer and Ribis 2012). Research on relict rock glaciers is mainly focused on their distribution (e.g., Harrison et al. 2008; Kellerer-Pirklbauer et al. 2012; Krainer and Ribis 2012; Onaca et al. 2013) or on their relevance as markers of sudden climate changes during the late glacial period (e.g., Hughes et al. 2003; Paasche et al. 2007; Putnam and Putnam 2009). In the 1990s, water resources studies documented the importance of relict rock glacier springs for the water supply of human consumption and the ecosystem in the Niedere Tauern Range, Austria (Untersweg and Schwendt 1995, 1996). Recent studies in the easternmost subunit of the Niedere Tauern Range (i.e., Seckauer Tauern Range) show that more than 50 % of the total area above 2,000 m above sea level (a.s.l.) and almost 22 % of the total area above 1,500 m a.s.l. are drained through relict rock glaciers or related landforms (Winkler et al. 2012; Winkler et al., University of Graz, unpublished report, 2014). However, knowledge about their genesis (e.g., Ballantyne et al. 2009), internal structure, hydraulic properties and impact on the hydrology of alpine catchments is still very limited.

The objective of this paper is the identification and assessment of the flow and storage components of a relict rock glacier and in a further consequence to provide a conceptual model of its internal structure and drainage processes. This is achieved by applying a multi-disciplinary approach combining analyses of the hydrograph and natural and artificial tracers. The aquifer geometry and internal structure were additionally investigated using geophysics. The results contribute to a better understanding as to whether such sediment accumulations should be treated as homogeneous or heterogeneous aquifers and moreover to what extent such aquifers act as relevant storages and/or provide groundwater contributions to Alpine stream flow, affecting also the sensitive Alpine ecosystem (e.g., Muir et al. 2011).

Investigation area

The investigation area is located in the Seckauer Tauern Range (SeT, 626 km^2), being the eastern most subunit of the Styrian part of the Niedere Tauern Range (NiT, 2,440 km^2) in the Austrian Eastern Alps (Fig. 1). In the NiT, 561 rock glaciers (including protalus ramparts) and related rock glacier catchments were identified based on a recent rock glacier inventory (Winkler et al., University of Graz, unpublished report, 2014). The subunit SeT contains 101 rock glaciers and 27 protalus ramparts (i.e., embryonal rock glaciers) and belongs geologically to the Upper Austroalpine subunit, more precisely to the Silvretta-Seckau nappe system and its Mesozoic cover. It consists of varying types of gneisses of the pre-alpine basement and post-variszic clastic metasediments of the cover series (Scharbert 1980, 1981; Mair 2002; Schmid et al. 2004) being comparable to most of the other regions in the Austrian Alps where rock glaciers occur.

The hydrogeological investigations presented in this paper were conducted at the relict Schöneben Rock Glacier (SRG) in the SeT (E14°40′26″, N47°22′31″, Fig. 1). The SRG covers an area of about 0.17 km^2, extending between 1,715 and 1,912 m a.s.l. with a distinct spring at the rock glacier front (SEQ, Figs. 1 and 2a,b). The SRG consists predominantly of coarse-grained gneissic sediments at the surface with blocks up to the size of a few cubic meters. The southeastern part of the rock glacier forms the rooting zone of the rock glacier with typical talus slopes partially overlaying the rock glacier and causing some uncertainty of the rock glacier's areal extent (indicated by the dot-dashed line in Fig. 1). The entire spring catchment (Schöneben cirque) covers 0.67 km^2 with a maximum elevation of 2,295 m a.s.l. The rock glacier covers about 17 % of the total catchment; 27 % is covered by talus slopes with a slope angle of up to 35°, and 56 % of the area consists of bare rock cliffs up to 200 m high (Figs. 1 and 2a).

The discharge of SEQ has been recorded since 2002, measuring continuously the stage at a weir with a rectangular notch (Fig. 2b,d). The spring belongs to the official spring network of the Hydrographic Service of Styria (HZB No. 396762). The stage-discharge equation applicable for a rectangular notch weir (e.g., Morgenschweis 2010) is verified by monthly individual discharge measurements using the salt dilution method. In addition, electrical conductivity and water temperature have been measured since 2008 directly at the spring. In December 2011 an automatic weather station (S-AWS) was installed at SRG at an elevation of 1,822 m a.s.l. In May 2012 an automatic remote digital camera (S-RDC) was placed at the opposite mountain ridge of SRG, approximately 500 m to the northeast at an elevation of 1,960 m a.s.l. to monitor visually the snow cover. Figure 2a,c show the rock glacier at summer time and at late wintertime, respectively.

Methods

Seismic refraction survey

The seismic refraction investigations were carried out at two transversal profiles RS-P06 and RS-P08 with lengths of 250 and 295 m and one longitudinal profile RS-P02 with a length of 714 m (Fig. 1; Table 1). The average spacing of the seismic geophones (sensor type PE2 4SB-10-458, one geophone at each position) was 5 m for RS-P06 and RS-P08 and 6 m for RS-P02 along a survey line. The seismic energy was generated by two different sources. First, an 8-kg sledge hammer (SH) was used to hit against a plastic plate (multiple blows) to generate seismic signals (first breaks) on the geophones near the shot point (minimum 20–30 positions left and right). Second, a minor amount of blasting agent (BA) with a maximum load of 250 g dynamite per single shot was used in order to detect the deeper layers and the bedrock. This source was essential for the check shot positions out of both sides of the seismic line. The data acquisition in the field was done with a seismic acquisition system Summit II Plus (DMT) where up to 120 geophones were active simultaneously. Processing and analyzing of the first arrival times was done with the software package SDM v2.2 (developed by JOANNEUM RESEARCH). The software is based on the generalized reciprocal method (GRM) of Palmer (1980) and is especially useful for geological situations where layers with different p-wave velocities appear (e.g., debris layer above bedrock). However, there are basically three possibilities in seismic refraction which might cause undetected layers. The layer is of lower velocity than the overlying medium or it is too thin and has insufficient velocity contrast to provide a discernible arrival or a travel time graph may be missed

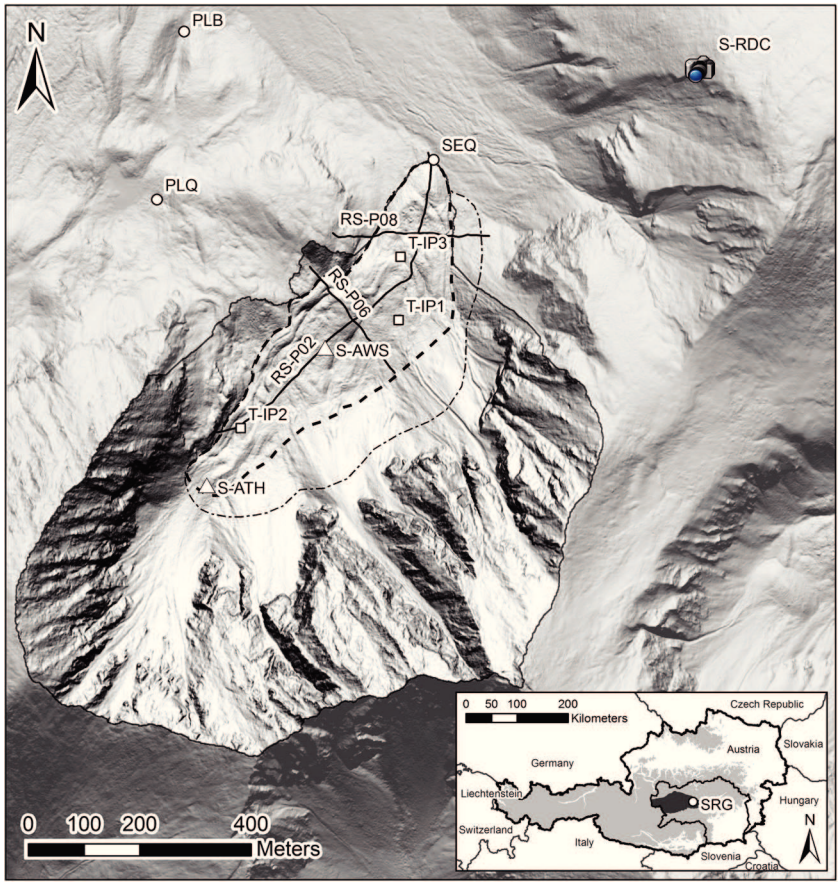

Fig. 1 Map delineating the relict Schöneben Rock Glacier (SRG) and its hydrological catchment based on airborne laser scan data with a resolution of 1 m. The delineation of the *SRG* is shown as a *thick black dashed* polygon; a possible extend to the south-east is indicated by a *thin dot-dashed* polygon. The refraction seismic profiles *RS-P02*, *-P06* and *-P08* are shown by *solid black lines*. Tracer injection points are shown as *white rectangles* (*T-IP1*, *-IP2* and *-IP3*), the weather station *S-AWS* and the air temperature and humidity station *S-ATH* as *white triangles*, the remote camera (S-RDC) with a *camera symbol*; the springs *SEQ* and *PLQ* as well as the *PLB* sampling location are indicated as *white circles*. The inset shows the SRG within the Styrian part of the Niedere Tauern Range (*dark grey*). Elevations above 600 m are highlighted in *light grey* within the national border of Austria (also including the boundaries of the federal state of Styria)

with sparse geophone coverage (e.g., Banerjee and Gupta 1975; Greenhalgh 1977; Schmöller 1978, 1982).

Recession analysis

First studies of rock glacier springs in the Seckauer Tauern Range in the 1990s (Gödel 1993; Untersweg and Schwendt 1995, 1996) indicated a discharge behavior similar to that of karst springs with discharge ratios of maximum to minimum discharge (Q_{max}/Q_{min}) per hydrologic year of about 10. Spring discharge is controlled by permeability and storage of the aquifer as well as by the areal extent of the catchment draining into the rock glacier. This catchment can be several times larger than the rock glacier aquifer itself, providing thus higher discharge. Discharge ratios (Q_{max}/Q_{min}) can be influenced by the hydrometeorological conditions and thus cannot easily be interpreted in terms of aquifer properties. In contrast, the base flow recession of spring hydrographs is supposed to be the drainage from the aquifer storage and therefore unaffected by recharge processes; thus, base flow recession provides information about the aquifer properties as intensely discussed in the literature (e.g., Brutsaert and Nieber 1977; Dewandel et al. 2003; Birk and Hergarten 2010; Kresic and Bonacci 2010).

One of the simplest approximations of the flow recession is a linear storage, assuming the water volume $V(t)$ [L^3] still stored in the aquifer above spring level at time t is proportional to the discharge $Q(t)$ [L^3/T] at that time (e.g., Kresic 2007):

$$V(t) = \frac{Q(t)}{\alpha} \tag{1}$$

where α [1/T] is a constant termed recession coefficient. If the recession coefficient is known, this equation can be employed to calculate the groundwater volume remaining at time t. Assuming the absence of any additional recharge or evaporation (Eq. 1) leads to the well-known exponential recession function (Maillet 1905):

$$Q(t) = Q_0 \, e^{-\alpha t} \tag{2}$$

where Q_0 is the discharge at time $t = 0$.

However, the linear relationship between discharge Q and stored volume V (Eq. 1) does not hold for the vast majority of the aquifer, predominantly due to spatially non-uniform changes of the water table. Therefore, recession curves do not follow the simple exponential function (Eq. 2) over the entire range for most springs. The most widespread extension of the linear storage model to overcome this limitation is an

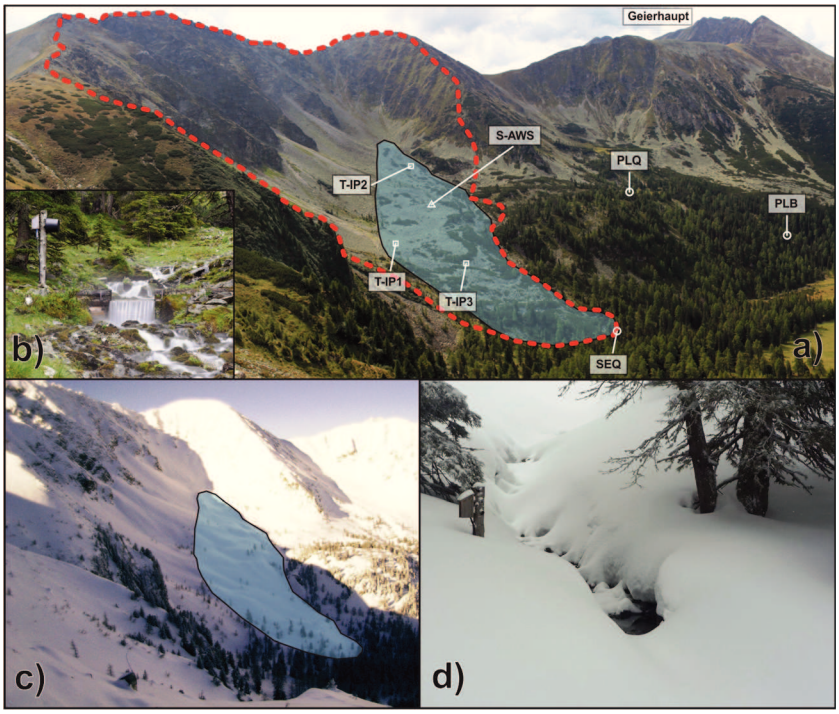

Fig. 2 Field impressions of the SRG catchment area and its surrounding. **a** The SRG is *highlighted in blue* and its catchment is surrounded by the *dashed red line*. View point from the automatic remote digital camera (S-RDC) that is installed at a distance of approximately 500 m in the north-east of the rock glacier at an elevation of 1,960 m a.s.l. In the *upper right* is Mount Geierhaupt (2,417 m a.s.l.), which is the highest peak in the Seckauer Tauern Range. *SEQ* = spring of the rock glacier (1,715 m a.s.l.; *S-AWS* = automatic weather station (1,822 m a.s.l.). For descriptions of *T-IP1*, *-IP2* and *-IP3*, *PLQ* and *PLB* see Fig. 1. **b** Gauging station, located a few tens of meters downstream of the actual spring SEQ, **c**–**d** the SRG catchment and the gauging station in wintertime with extensive snow coverage

approximation of the overall recession curve by a discrete set of exponential functions with different recession coefficients where each exponential function holds over a certain range of discharge. Conceptually, this is often interpreted in terms of different aquifer components (e.g., Sauter 1992; Baedke and Krothe 2001). Yet, closer analysis of the groundwater flow equation reveals that even the recession of a homogenous aquifer does not follow the linear storage model, but involves an infinite series of exponential functions (e.g., Nutbrown and Downing 1976; Sahuquillo and Gómez-Hernández 2003). Rorabaugh (1964) showed that the recession after an instantaneous water-table rise (due to a short recharge pulse) in a homogenous aquifer with parallel flow obeys a power law

$$Q(t) \propto t^{-b} \tag{3}$$

with a slope of −0.5 at the early stage and is approximated by a single exponential function only at large times $t > 0.5/\alpha$. Birk and Hergarten (2010) extended the Rorabough model to the recession after finite recharge pulses of length t_0 yielding:

$$Q(t) = \frac{8}{\pi^2} Q_0 \left\{ \sum_{i=1}^{\infty} \frac{1}{(2i-1)^2} \exp\left[-(2i-1)^2 \alpha t\right] - \sum_{i=1}^{\infty} \frac{1}{(2i-1)^2} \exp\left[-(2i-1)^2 \alpha (t+t_0)\right] \right\} \tag{4}$$

While an exponential recession is characterized by

$$\frac{dQ(t)}{dt} = -\alpha Q(t) \tag{5}$$

where the recession coefficient α is constant, a power-law recession (Eq. 3) obeys the relation

$$\frac{dQ(t)}{dt} = -\frac{b}{t} Q(t) \tag{6}$$

In this sense a power-law recession can be interpreted in terms of a recession coefficient

$$\alpha(t) = \frac{b}{t} \tag{7}$$

continuously decreasing through time, while multiple exponential functions correspond to discrete recharge regimes where the recession coefficient remains constant over some

Table 1 Details of the shot and receiver configurations and the spread of the seismic profiles. *SH* sledgehammer, *BA* blasting agent

Profile	Direction	Length [m]	Geophone spacing [m]	No. of geophones	Shots
RS-P02	N–S/NE–SW	714	6	120	30SH/10BA
RS-P06	NW–SE	250	5	51	14SH/5BA
RS-P08	W–E	295	5	60	13SH/5BA

range. Within this work, it is attempted to match the observed hydrograph recession using the exponential function given by Eq. (2) with a superposition of several exponential functions, and the model given by Eq. (4).

Natural tracers

Physico–chemical parameters such as water temperature and electrical conductivity (EC) in addition to stable isotope data of $\delta^{18}O$ und $\delta^{2}H$ were used as natural tracers to characterize the storage and the flow dynamics of the aquifer. Water temperature will be altered due to temperature differences between infiltrating water and the subsurface (rock/sediments), and thus can be considered as a reactive tracer. However, the stable isotopes of water are supposed to be unaffected from rock–water interaction and therefore the isotope signature is regarded as a conservative tracer. In addition, EC was also defined as a conservative tracer as the rock–water interaction in crystalline rocks is assumed to be negligible considering short residence times of a few hours to a few days. To estimate travel times of fast flow components, the time lags between the recharge pulses after precipitation events and the respective breakthrough of event water at the spring were calculated. The highest recharge rate is assumed to coincide with the inflection point of the rising limb of the hydrograph (e.g., Kovács et al. 2005). The breakthrough of event water is indicated by the maximum deviation of the physico–chemical parameters from their pre-event values (e.g., Sauter 1992; Birk et al. 2004). Furthermore, the use of the EC as a geochemical tracer allows for the separation of event water with lower solute content from pre-event water with higher solute content based on a two-component mixing model (Wels et al. 1991). The short-term variation of the EC is caused by the mixing of the event water component (Q_n) and the pre-event water, neglecting any dissolution reactions along the flow paths (which is an appropriate assumption in crystalline rocks). Q_n [L^3/T] can be calculated by the equation

$$Q_n \approx Q_s - \frac{EC_s - EC_p}{EC_{old} - EC_p} Q_s \quad (8)$$

where Q_s [L^3/T] is the total discharge, EC_s [M^{-1} L^{-2} T^3 I^2] the electrical conductivity of the spring water (measured in µS/cm), EC_p the electrical conductivity of the precipitation water and EC_{old} denotes the electrical conductivity of the pre-event water. Cumulative rainwater samples (SEN) were taken in 100-ml bottles placed in the blocky subsurface near the weather station (S-AWS), protected against evaporation and replaced about every month during the periods June to October 2012 and May to July 2013. EC_p measured in the laboratory yielded an average value of 16 µS/cm. In addition, the two-component mixing model can also be applied analyzing the change of the isotopic composition of spring water ($\delta^{18}O$ and $\delta^{2}H$) during a precipitation event knowing the isotopic signatures of the rainwater and the pre-event water. Therefore, the isotopic signature of spring water was analyzed in samples that were taken every 15 h for 1 week before, during and after a precipitation event in August/September 2012. Based on a cumulative rainwater sample (SEN), collecting the rainwater over a period of 10 days prior to the event, the isotopic signature (representing the rainwater component) was determined with −7.89 ‰ for $\delta^{18}O$ and −49.49 ‰ for $\delta^{2}H$. Mean residence time (MRT) was estimated for SEQ applying a simple sine function approach to data from the stable isotope $\delta^{18}O$ (e.g., Stichler and Herrmann 1983; McGuire and McDonnell 2006). Based on the fact that $\delta^{18}O$ in precipitation usually shows a pronounced seasonal variation due to the seasonally varying air temperature, this should also be seen at the spring, where the aquifer acts as a dampening element (dispersion and mixing in the aquifer). This dampening can be used to calculate a MRT of fast flow component, considering that a precipitation event will be reflected by a peak in the isotopic signature, and thus the time lag between precipitation event and peak can be quantified. This MRT should not be confused with a depletion time calculated from runoff recession analysis. The input function was calculated from isotope data of the Planneralm Station, assuming that the station SEN shows a similar behavior in absolute values as well as in the total variation (refer to Fig. 7). The Planneralm Station is the nearest official measuring station of the Environmental Agency of Austria (ANIP 2007) located about 35 km to the west at 1,605 m a.s.l. The output function was based on the isotope data of SEQ.

Artificial tracers

Two artificial tracer tests were performed (in 2009 and 2012) in order to investigate the storage and flow dynamics in detail. In 2009, fluorescein sodium (Uranin; UR) and sodium naphtionate (NA) were injected on the surface of the rock glacier at the injection points T-IP2 and T-IP3, respectively (Fig. 1). T-IP2 is located near the rooting zone of the rock

glacier about 670 m (horizontal distance) above SEQ at 1,870 m a.s.l. and T-IP3 at 1,770 m a.s.l. with a distance of 200 m from SEQ. The injection date of the tracer test in 2009 was the 16th of June. At each injection location, 1 kg of the dye was dissolved in a 100-l water tank and then rinsed with 200 l of water and additionally by rainfall during the days after injection. In the first 2 weeks after the injection, water samples were taken at regular intervals and after 6 weeks, small carbon bags with activated carbon were used to sample for an additional 6.5 months at a monthly time interval until December. The carbon bags consist of perforated material allowing water to flow through them, and are filled with fine-grained activated carbon. If there is injected dye tracer in the water, the tracer will be adsorbed cumulatively over the time period in which the bag has been exposed to the water. The analysis of the carbon sample will give a qualitative result and allows for the detection of traces of the injected dye below the usual detection limit (0.002 ppb) for water samples. The two last carbon samples were taken on the 24th of June and 21st of July 2010 after the snowmelt. On the 13th of June 2012, UR was again injected at T-IP2 and sulforhodamine B (SRB) and eosin Y (EO) simultaneously at T-IP1 with a distance of 350 m from SEQ at 1,820 m a.s.l. (Fig. 1). Two kilograms of UR were dissolved in a 100-l water tank and then rinsed with 200 l at T-IP2, and at T-IP1, 1 kg each of SRB and EO were separately dissolved in 50-l water tanks and rinsed with 100 l. Tracer detection at the spring was recorded using a field fluorometer (Albillia GGun-FL30; Schnegg 2002) with a recording rate of 2 min until the 8th of December. Afterwards, the recording rate was changed to 15 min until the end of the automatic observation on the 29th of May 2013. In addition, water samples were taken using an automated sample collector (Maxx TP 4 C) at time intervals of one to 15 h during the first 2 months. Furthermore, carbon bags were used for sampling at the spring SEQ and the Postlleiten Creek (PLQ, PLB; Fig. 1). Sampling intervals of the carbon bags ranged from 4 days to 16 weeks until the end of October 2013.

Results

Seismic refraction survey

The seismic refraction results (Figs. 3 and 4) show three layers, representing the bedrock (as layer 1) and an overburden of the bedrock with variable fine grain content (layer 2) covered with blocky coarse-grained sediments (layer 3) (Lichtenegger et al., Joanneum Research, unpublished report, 2014; Kellerer-Pirklbauer et al. 2014). The bedrock is characterized by p-wave velocities between 3,860 and 4,890 m/s consistent with results from metamorphic rocks at other investigation areas. At the longitudinal profile RS-P02 (for location see Fig. 1) the bedrock was identified in an average depth between 20 and 30 m below surface except for the lower and upper endings where the bedrock strikes out near the surface. Figure 3 shows a selected seismic refraction field record at shot point position 36.5 of profile RS-P02. Based on the manual picking of the first breaks, the individual discrete layers were identified along the three profiles. In the southeastern part of RS-P06, the bedrock top dips down to a depth of more than 60 m below surface (Fig. 4). At RS-P08 the bedrock top in the eastern part is about 30 m below surface. Both transversal profiles unfortunately end within the sediment accumulation and do not reveal the entire geometry of the aquifer in the eastern part; however, the results suggest an asymmetric shape of the bedrock top being much deeper towards the east of the rock glacier. The p-wave velocities of the overburden (layer 2) in RS-P02 and RS-P08 are mostly below 1,000 m/s and indicate unsaturated sediments with variable finer grained material. The layer thickness ranges from 10 to 25 m extending approximately parallel to the topography in RS-P02. The westernmost 60 m of RS-P08 are characterized by bedrock up to the ground surface, while layer 2 exhibits a thickness up to 25 m further in the east. A more differentiated internal structure is shown at profile RS-P06 (Fig. 4). The debris body above the bedrock in RS-P06 is characterized by p-wave velocities between 1,090 and 1,690 m/s. The velocities of layer 2 indicate an unsaturated finer grained, sometimes higher consolidated loose material reaching a layer thickness of about 50 m which is only detected in the southeastern part of the profile. The upper most layer (layer 3) consists of a coarse-grained blocky material with low p-wave velocities between 330 and 990 m/s at all three profiles and an averaged thickness of a few meters. The maximum thickness of about 15 m was observed in RS-P06 (Fig. 4). In total, the results suggest an asymmetrical cirque filled with rock-glacier and talus sediments with a maximum thickness exceeding 60 m and with a nearly horizontal aquifer base for most of the lower half of the rock glacier. According to the encountered velocity contrasts of the unconsolidated sediments and the bedrock, the detection of a potential groundwater saturated layer within the debris accumulation with an assumed velocity of 1,700 m/s is limited to a minimum thickness of about 14 ± 5 m using several first break picks and the approach proposed by Schmöller (1978). As no larger groundwater saturated layer was observable in the seismic refraction data, it was concluded that the saturated aquifer thickness at the time of investigation (average discharge conditions) seems to be smaller than about 15 m, and the material properties of this layer remain unknown.

Hydrograph analysis

The discharge ratios (Q_{max}/Q_{min}) of the hydrologic years from November 2005 to October 2013 range from approximately

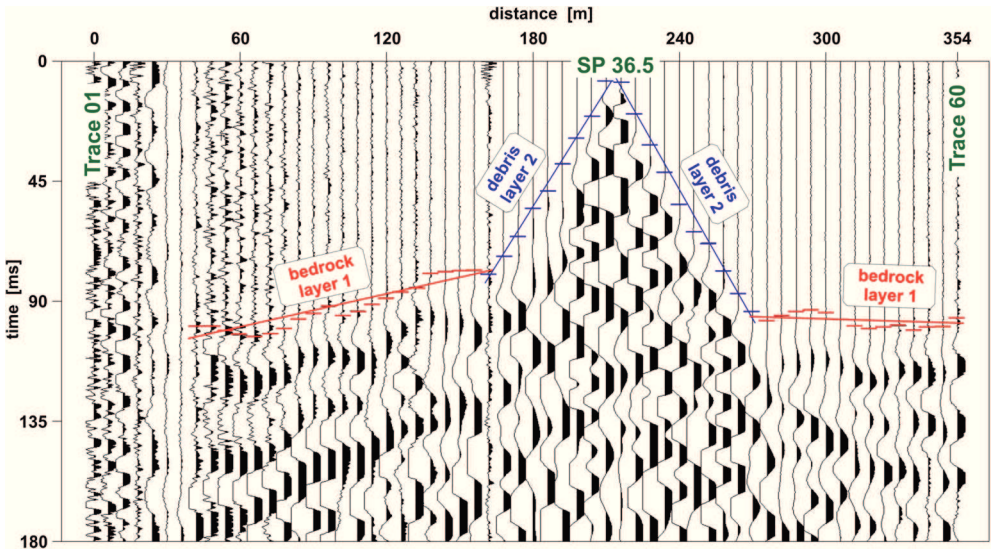

Fig. 3 The field record of first break picks of the traces *1–60* at position *36.5* of the seismic refraction profile RS-P02

20 to 100. The long-term recession curves of seven subsequent winter periods (2006–2013) are shown in Fig. 5a. Three of these periods (E5, E6 and E7) are free of significant intermediate recharge events related to warmer periods and subsequent snowmelt or rainfall. The other four recessions indicate temporary recharge events and are therefore not further analyzed. However, their recession behavior after recharge pulses still corresponds reasonably well to the recession coefficients of E5, E6 and E7—see Fig. S1 of the electronic supplementary material (ESM).

The semilogarithmic plot in Fig. 5b reveals that the aquifer cannot be considered as a single linear storage. The recession curves can, however, be approximated by a superposition of three (or more) exponential functions suggesting that the aquifer may contain at least three storage coefficients with different recession coefficients similar to observations from karst systems (e.g., Sauter 1992; Baedke and Krothe 2001). The recession coefficient (α) of the early flow recession (first 25 days) ranges from 0.028 to 0.047 1/d, the intermediate α from 0.005 to 0.01 1/d, and the base flow recession after approximately 90 days yields an α of 0.002 1/d (Table 2). The fitting of the coefficients was done by a least-square minimization for each hydrograph section.

However, applying Eq. (3), the double-logarithmic plot (Fig. 5c) reveals that the discharge follows a power law with exponent $b = 0.38$. Figure 5c displays an example of a recession curve given by Eq. (4) assuming a length of the recharge period of 20 days and a (long-term) recession coefficient of 0.002 1/d.

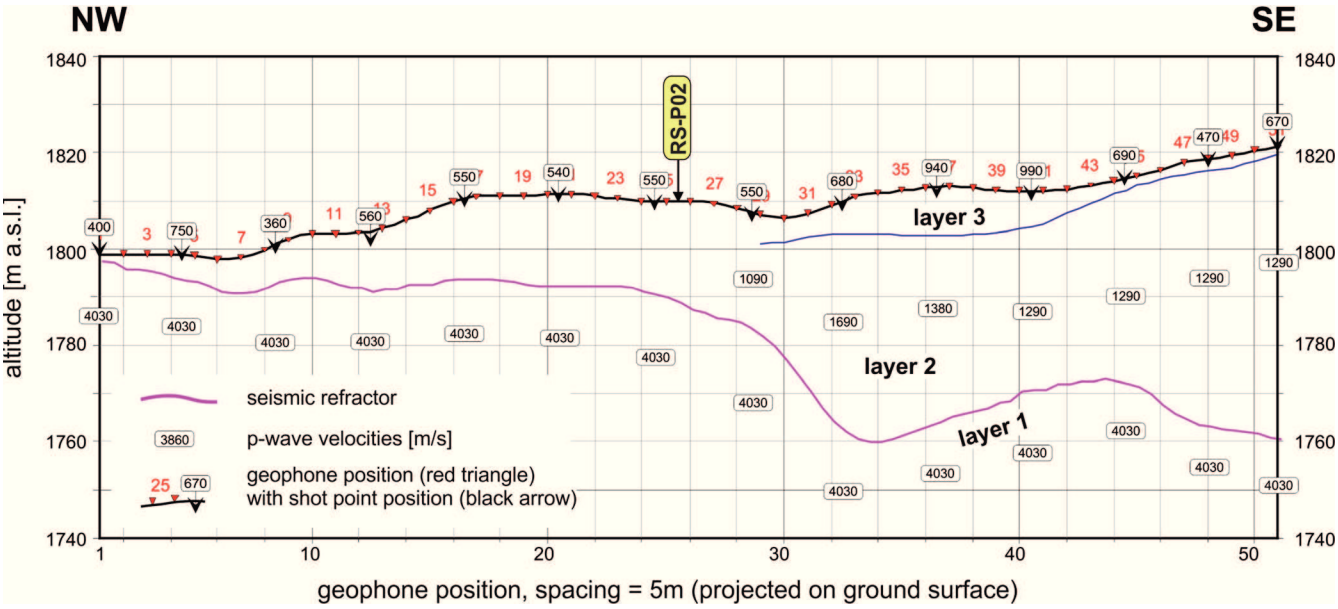

Fig. 4 Seismic refraction profile RS-P06, intersection point with profile *RS-P02* in the middle of the profile. Note the thickness of layer 2 in the SE part of the profile. *Blue line* represents the seismic refractor between *layer 2* (*upper* limit) and *layer 3* (*lower* limit)

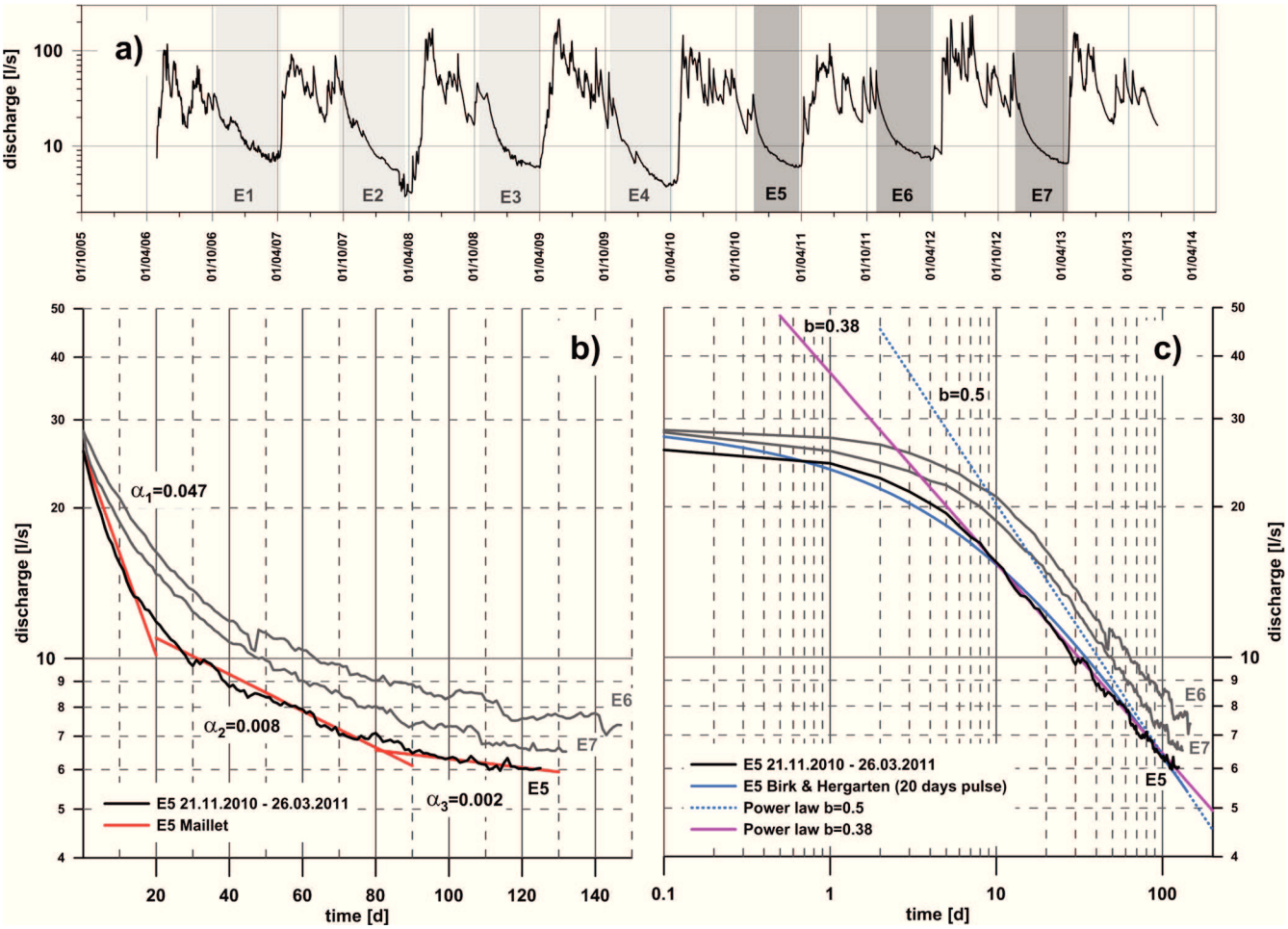

Fig. 5 **a** Hydrograph of SEQ between April 2006 and January 2014. Long-term recessions over the winter periods without (*in dark grey*) and with (*in light grey*) intermediate recharge events. **b** Semi-logarithmic plot of the long-term recessions without intermediate recharge events; the *red lines* indicate fitted recession functions based on the exponential model (Maillet 1905) with the recession coefficients (α) given next to the *lines*. **c** Log-log plot of the long-term recessions over the winter periods without intermediate recharge events; the *solid blue line* shows the recession function of a 20-days recharge pulse according to Eq. (4) (Birk and Hergarten 2010) and a power law fit is shown in *pink* ($b = 0.38$); in addition a power law with $b = 0.5$ (representing a homogeneous aquifer) is plotted as a *dotted blue line*

This analytic recession curve approaches a power law after approximately 80 days. The observed recession curves, however, exhibit a power-law behavior already from approximately 10 days onwards. Even more important, the power-law exponent (b) of a homogeneous aquifer is 0.5 (Eq. 3), while the exponent $b = 0.38$ found here is significantly lower. An exponent different from 0.5 suggests some multi-scale aquifer structure. This may be related to, e.g., a scale-invariant (fractal) size distribution of storage elements (Hergarten and Birk 2007) or to a scale-invariant flow pattern (Hergarten et al. 2014).

Table 2 Long-term recessions of three winter periods (Fig. 5) with the related recession coefficients and water volumes based on Maillet (1905) and measured discharges. *MM* = millions, t_r for the recession time, Q_0 for the initial discharges of the recessions at time $t = 0$, Q_{re} for the residual (lowest) discharge before snowmelt, α_1 for the early recession coefficient, α_2 for the intermediate recession coefficient and α_3 for the base flow recession coefficient, V_{out} for the total water volume flowing out during the recession (measured), V_{reM} for the remaining water volume calculated from Q_{re} and α_3, V_{TM} for the sum of V_{out} and V_{reM}, V_{reR} for the remaining water volume calculated with $\alpha_b = 0.003$, V_{TR} for the sum of V_{out} and V_{reR}

Recession	Time [d]	Discharge [l/s]		Recession coefficient – Maillet [1/d]			Water volume [MM m^3]				
	t_r	Q_0	Q_{re}	α_1	α_2	α_3	V_{out}	V_{reM}	V_{TM}	V_{reR}	V_{TR}
E5: 21.11.2010–26.03.2011	125	26.0	6.0	0.047	0.008	0.002	0.10	0.26	0.36	0.17	0.27
E6: 05.11.2011–27.03.2012	143	28.5	7.3	0.028	0.005	0.002	0.14	0.32	0.46	0.21	0.35
E7: 29.11.2012–10.04.2013	132	28.2	6.5	0.038	0.007	0.002	0.12	0.28	0.40	0.18	0.30

Due to the limited total capacity of the aquifer, the power-law recession must turn into an exponential decay at large times, although this transition is not observed during the winter periods considered in this study. Therefore, only an upper limit for the long-term (base flow) recession coefficient can be given. If the transition to an exponential recession occurred at $t = 125$ days (the length of the shortest recession curve in Fig. 5b,c, E5; Table 2), Eq. (7) yields the respective recession coefficient of 0.003 1/d, so that the base flow recession coefficient α_b must be smaller than 0.003 1/d.

Adopting the lowest residual discharge rate at the end of the long term recessions of 6 l/s (Table 2) and $\alpha_b = 0.003$ 1/d in Eq. (2), the remaining water volume in the rock glacier must be at least 1.7×10^5 m^3 (E5). All water volumes calculated with the base flow recession coefficient based on Maillet (1905), $\alpha_3 = 0.002$ 1/d in Table 2, yield larger values. The sum of the water volume during the recession (V_{out}) and the remaining water (V_{reR}) exhibit a total water volume in the aquifer of at least 2.7×10^{-5} m^3 at the beginning of the recession (for E5). Assuming a storage coefficient (drainable porosity) S [−] of 0.2 over the whole rock glacier area of 0.17 km^2 results in a saturated aquifer thickness of about 10 m.

Natural tracers

The water temperature exhibits a mean temperature of 2.2 °C (2008–2014, standard deviation 0.12 °C) with a seasonal variation between 1.9 and 2.5 °C. The highest temperatures are in late summer and the lowest in late winter. The seasonal variation of the water temperature shows a phase shift of approximately 60–110 days towards the air temperature over the observation period from 2011 to 2014. For this period, the mean water temperature of 2.2 °C is very similar to the mean air temperature of the catchment (2.1 °C). The mean air temperature of the catchment is calculated by the mean (air temperature at mean elevation) of S-AWS and S-ATH which is further corrected for the mean catchment elevation by the air temperature gradient of 0.57 °C/100 m valid for the SeT based on ten meteorological stations nearby (Taucher 2010). The EC ranges between 34 and 76 μS/cm with the highest values in late winter representing the base flow and the lowest values in summer. A closer look at individual recharge events (Fig. 6) reveals that after precipitation events both EC and water temperature exhibit their peaks up to 4 h after the maximum recharge (inflection point on the rising discharge limb). Applying Eq. (8) to 23 events yields a mean of 20 % (individual events up to 30 %) event water, whereas about 80 % of the discharge is found to be pre-event water with longer residence times (Fig. 6). The highest percentage of event water is found approximately 1 h after the highest discharge and reaches up to 56 % of the discharge (mean of 30 %).

It is important to point out that the tailing of the breakthrough curves of water temperature and EC are different. Whereas the water temperature reaches its pre-event value after approximately half a day, the recovery of the EC takes up to 9 days. The different recovery times of the two natural tracers after a precipitation event can be explained by the different behavior of conservative and reactive tracers. The EC (in this type of setting) is predominantly affected by the mixing of pre-event water with higher solute content and event water with lower solute content. Water temperature as a reactive tracer is influenced by both the mixing and the thermal exchange with the subsurface. Both tracer results and in particular the decrease of the water temperature after precipitation events will be discussed in more detail in the 'Discussion' section.

The isotopic signature of the precipitation (SEN) and the spring water (SEQ) follows the same meteoric water line (MWL) which corresponds well with the global MWL (Fig. 7). The data set was completed with data of the Planneralm Station to show the yearly variability, as the isotopic variation of the precipitation (SEN) at S-AWS represents only the summer period. The isotope data set of SEQ scatters much less than that of the precipitation and confirms that recharge is stored and mixed in the aquifer indicating a good storage capacity. The calculated MRT is 0.6 y (about 7 months). From the availability of isotope data from SEQ it was clear that the data density during the summer (by intense event sampling) is much higher than during wintertime; therefore, the weighting of the summer data is much higher than those of the wintertime. The analysis of one precipitation event, monitored in August/September 2012 allowed the separation of discharge components by adopting Eq. (8) (Fig. 6). For this event, the isotope data indicate about 13 % of event water, which is in good agreement with the results of EC with about 17 % (Fig. 6).

Artificial tracer

The artificial tracer UR injected on the 16th of June 2009 was first detected at the spring at the beginning of August 2009, yielding a time lag between injection and first detection of approximately 50 days. No tracers were detected in the water samples after this time period, carbon bags were used as cumulative samples allowing only qualitative interpretations. The estimated peak of the breakthrough curve was in September 2009 approximately 100 days (±15 days) after the injection. Another tracer breakthrough peak was caused by the hydraulic pulse of the subsequent snowmelt. Applying the time lag of the tracer peak with 100 days and the distance of the tracer injection point to the spring with about 670 m, the pore velocity (v_p) was determined with 7.8×10^{-5} m/s. Assuming an average effective (drainable) porosity S [−] of 0.2 and applying Darcy's law (with the Darcy velocity v_f obtained by multiplying pore velocity and effective porosity) using a hydraulic gradient of 0.224, resulting from the elevation difference of 150 m and the distance of 670 m between injection point and spring, yields a hydraulic conductivity of about 7×10^{-5} m/s. The first detection of NA (injected at T-IP3) at the spring was more than 10 months after the injection during

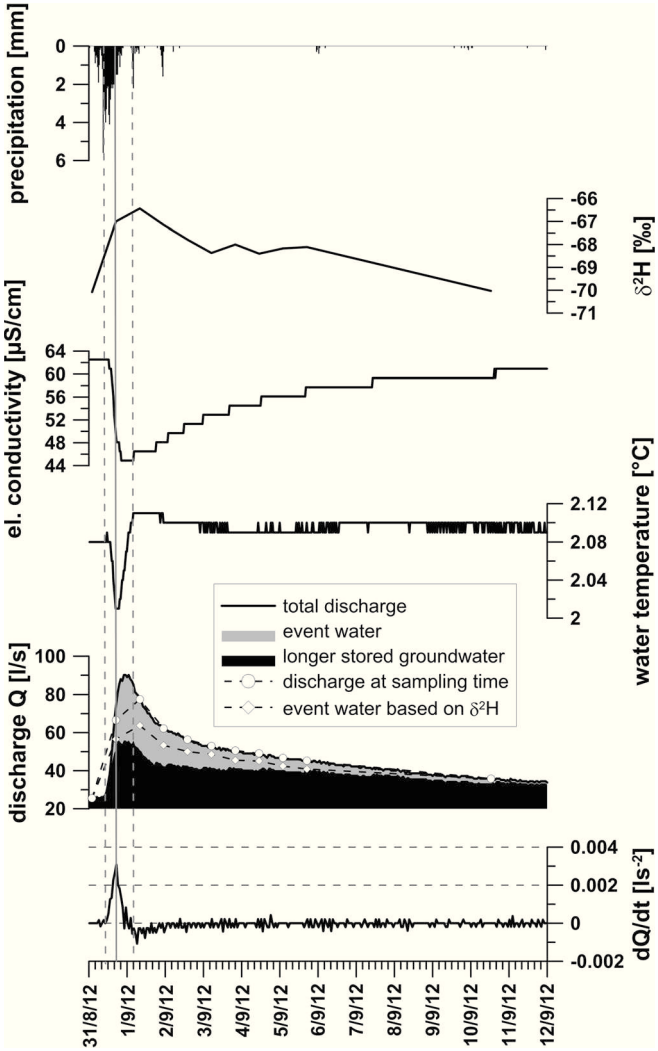

Fig. 6 Single recharge event in summer 2012 illustrating the change of recharge (d*Q*/d*t*), discharge components derived from a separation by a two-component mixing model based on electrical conductivity and isotopic signature, the time series of water temperature, electrical conductivity and isotopic signature (delta-values of deuterium) as well as precipitation recorded at the S-AWS. Event water is water with a residence time of a few days; longer stored groundwater is water with a residence time of several days and longer, up to several months. *Dashed vertical lines* mark the start of the recharge pulse and the end of water temperature recovery; the *vertical solid line* represents the highest recharge

the snowmelt period of 2010. This delay might be caused by a thick unsaturated zone at the injection point, which is in accordance with the seismic refraction data. The tracer might have reached the saturated zone delayed and/or was highly diluted and therefore the tracer intensity at the spring was below detection limit within the first 10 months. Possibly, during the subsequent snowmelt, the bulk tracer mass was remobilized by the hydraulic pulse. In addition, the tracer UR was also found at the neighboring Postlleiten Creek (PLB in Fig. 1) after more than 120 days, indicating that a small part of the Schöneben catchment drains toward the neighboring valley.

Based on the findings of the test in 2009, an additional tracer test was performed in 2012 with the injection date 13th of June 2012. The injection of UR at T-IP2 was repeated but no tracer could be detected at SEQ, although there was a positive result during the injection at the same point in 2009. This might be explained due to a long residence time in the unsaturated zone and consequently a slow release resulting in concentrations below the detection limit. The tracer concentration of SRB and EO injected at T-IP1 was monitored until the end of the snowmelt in 2013. Unfortunately, there was a data gap during the winter recession (8th of December to 10th of April) until the beginning of the snowmelt. Possibly, this was caused by a low water level that cannot provide the required water flow through the fluorometer. During the subsequent snowmelt, about 2 % recovery of SRB and about 10 % of EO were detected. In total, the tracer recovery was about 22 and 70 % of SRB and EO, respectively. The difference in recovery of the two tracers can be explained by the reactiveness of SRB mainly due to sorption effects, as SRB is inferred to be more absorptive than EO found out with batch and column experiments. Charged surfaces and the size of mineral grains, pH of the water and intraparticle diffusion can affect the tracer breakthrough significantly (Klotz 1982; Kasnavia et al. 1999; Sabatini 2000). Although, the rock glacier shows partly coarse material up to big boulders on the surface, which would normally guide the dye tracers rapidly through the underground, it can be assumed that a significant fraction of fine-grained material (sand, clay minerals, etc.) is in contact with the tracers, absorbing them temporarily or even permanently.

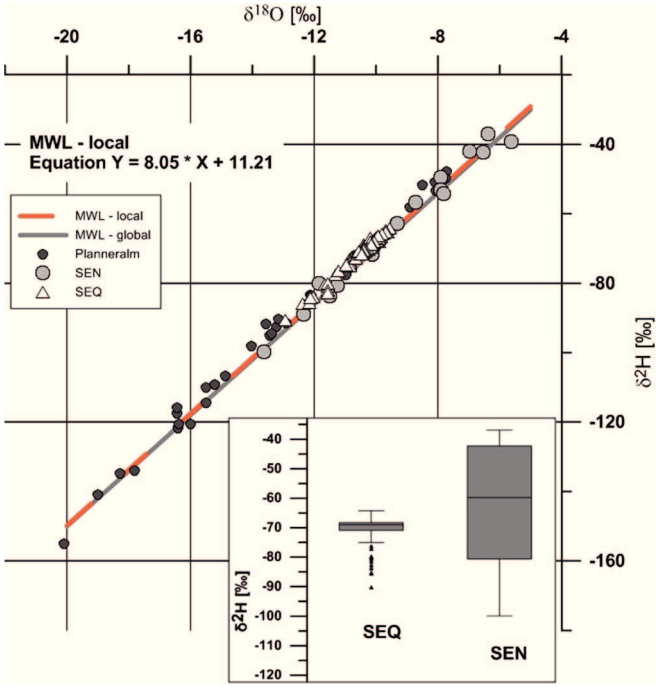

Fig. 7 Isotope data of the precipitation water (*SEN*) sampled near the S-AWS, of the spring water (*SEQ*) and the local and the global meteoric water lines. In addition the precipitation data of the nearest long-term monitoring site *Planneralm* (ANIP 2007) is shown to include the complete annual variability. The *inset* shows box and whisker plots of the SEQ and the SEN isotope data. Note the small variation in the SEQ data compared to the one of the SEN

However, first detection of the tracers was 2–3 h after injection only. The maximal change of tracer concentrations (dC/dt) occurred with a time lag of 2–4 h after the maximum change of discharge (dQ/dt) throughout the whole monitoring period (Fig. 8). This suggests a hydraulic stimulus of the tracer, being stored in a constant distance to the spring, still being located, e.g., in the subsurface at the injection point T-IP1 that would correspond to the longest distance to SEQ. An average time lag of 3 h combined with the distance of about 350 m (distance T-IP1 to SEQ) would result in an average pore velocity of about 0.032 m/s. The seismic refraction profile RS-P06 indicates the bedrock in a depth of several tens of meters in this part of the rock glacier (Fig. 4). Thus, the depth of the tracer storage is assumed to be about 50 m above SEQ, based on the elevation difference of 100 m between T-IP1 at 1,820 m a.s.l. and SEQ at 1,720 m a.s.l., resulting in a hydraulic gradient of 0.14. Adopting again a drainable porosity S [−] of 0.2 and the aforementioned hydraulic gradient, applying Darcy's law yields a hydraulic conductivity of 4.6×10^{-2} m/s. This value has to be regarded as an approximation based on the uncertainties of the input parameters. However, it provides an order of magnitude of this flow component which corresponds to unconsolidated sediments with grain sizes like that of gravel and coarser.

Discussion

The understanding of the hydrogeological system and the internal structure of relict rock glaciers such as the SRG requires an interdisciplinary approach combining hydrogeological and geophysical investigation methods. The seismic refraction survey clearly shows a layered structure of the relict rock glacier, where the measured p-wave velocity of the bedrock and coarse blocky layer (the two velocity end members) corresponds well with other test site observations (e.g., Clow et al. 2003; Schön 2011; Langston et al. 2011; Hausmann et al. 2012). The observed recession behavior of the rock glacier spring may be interpreted as a heterogeneous aquifer with multiple components. The additional results of artificial tracer tests and the evaluation of natural tracers support these findings and enable a more specific interpretation discussed in the following.

Recharge events (indicated by increasing spring discharge) are found to cause a rapid decrease of the EC of the spring water. As for an assumed conservative tracer, this is dominated by the mixing of event water with lower solute content and pre-event water with higher solute content. Based on the EC data and confirmed with the stable isotope data, the discharge separation results in about 80 % pre-event water being pushed out by a fast infiltrating recharge pulse. The remaining 20 % of the discharge is event water with short residence times, which is supported by a fast response of the spring after recharge events, pushing out the stored artificial tracer (tracer test 2012). Adopting the results of this tracer test, the fast draining aquifer component can be related to a hydraulic conductivity corresponding to dominating grain sizes of gravel and coarser material which is in good agreement with the p-wave velocities of layer 2 (main debris accumulation) observed in the seismic refraction. During the construction period of the capture of a rock glacier spring located about 2.5 km east of the

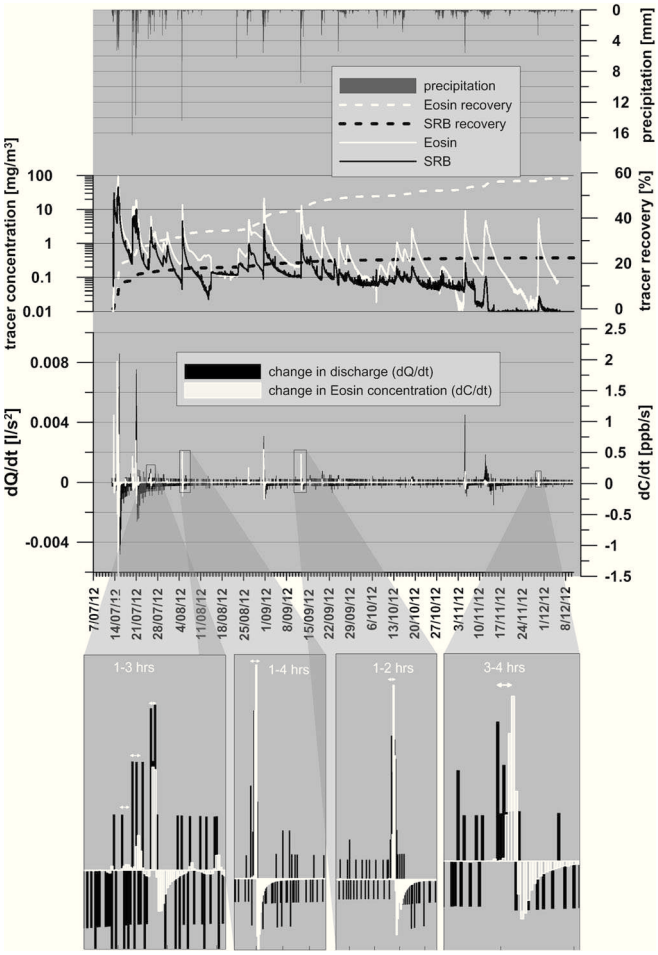

Fig. 8 Spring data of the SEQ following the tracer injection 2012 until winter base flow where a gap in the tracer data has been observed. Change in discharge (d*Q*/d*t*) and in concentration (d*C*/d*t*) of eosin based on one-hourly data, tracer concentrations and tracer recovery of eosin and sulforhodamine B, and precipitation at the S-AWS

investigation area, Untersweg and Proske (1996) were able to record a grain-size-distribution profile with a height of 6.5 m at the exposed front of the relict rock glacier. They observed a layered structure dominated by sandy, gravelly sediments including blocks up to a size of 60 cm. Similar findings were observed in drill cores at an active rock glacier in the Italian Alps (Krainer et al. 2014). Nevertheless, during summertime, the fast decrease and recovery of the water temperature appears to be in contradiction to the idea of a considerable percentage of event water. Given that the fast flow component originates from the rapid infiltration of rainwater, an increase of the water temperature would be expected after a recharge event during summertime, since the temperature of the recharge in the warm season is expected to be higher than that of the pre-event groundwater. Thus, some process that enables a rapid cooling of the event water during infiltration is needed to cause the observed decrease of the water temperature. One potential cooling source might be some remaining ice lenses in the lower part of the rock glacier. Compared to the SRG data, Clow et al. (2003) and Millar et al. (2013) measured lower mean annual water temperatures with often higher seasonal temperature variability at their intact rock-glacier- and permafrost-influenced springs. They explained the low water temperatures with remaining ice and permafrost in the subsurface. Their findings are similar to observations at springs draining active rock glaciers in the Eastern Alps (Krainer and Mostler 2002). Another explanation is provided by the findings of Harris and Pederson (1998), who investigated the thermal regime beneath coarse blocky materials at a comparable alpine study site in south-west Alberta (Canada). Their results show that blocky material reacts as an isolating layer and that the mean annual ground temperature in blocky material is several degrees Celsius cooler than that in nearby mineral soils. Such a layer would also cause a cooling of the event water during infiltration. The existence of circulating air in larger void systems at SRG is likely (Kellerer-Pirklbauer et al. 2015); however, the identification of the cooling source requires additional research in the future.

As opposed to the rapid response of the natural tracers and the tracer test of 2012 (EO and SRB), the peak of the UR breakthrough in the tracer test of 2009 was recorded after approximately 100 days. Moreover, the small variation in isotope data at SEQ compared to precipitation at SEN and the calculated MRT indicate a good mixing within the aquifer and a mean residence time of about 7 months. Based on the artificial tracer test of 2009, the hydraulic conductivity of this

aquifer component can be estimated as 7×10^{-5} m/s, which can be related to sediments with grain sizes of fine sand to silt (e.g., Bear 1972; Schwartz and Zhang 2003). This hydraulic conductivity has to be considered as an upper limit as the tracer transport may partly be influenced by the fast flow component, indicating an even finer-grained material that can be related to a layer of basal till being some remnants of a ground moraine or fine debris material, formed by the movement of the rock glacier itself during its active phase, which fits well to observations related to geophysical investigations (Hausmann et al. 2012) and drill cores (Krainer et al. 2014) at active rock glaciers. The fine grain sizes of this aquifer component are additionally in agreement with the findings of the internal structure of an exposed relict rock glacier in Poland. Zurawek (2002) identified a very heterogeneous small-scale structure with (fine) sand-dominated and silty layers. The related hydraulic conductivity of this aquifer component at SRG is comparable to the results published by Clow et al. (2003). These authors exhibit hydraulic conductivities in the range of 8×10^{-6} to 4.4×10^{-4} m/s for an aquifer system dominated by talus deposits in an alpine catchment in Colorado (Andrew Spring).

A saturated fine-grained layer thickness of about 10 m at SRG over the entire rock glacier area is estimated based on the water volume stored at the beginning of the winter recession period. Unfortunately this layer could not be observed in the seismic refractions (hidden layer, blind zone) due to the velocity contrasts and thickness of the encountered layers but is assumed to be extended at the bottom of the rock glacier which is consistent with observations at active rock glaciers (Hausmann et al. 2012; Krainer et al. 2014).

All these findings support the conceptual model of a heterogeneous layered aquifer with at least two aquifer components (Fig. 9); a rather thin (about 10 m) and low-conductivity layer with considerable storage capacity and responsible for the delayed/base flow probably extended at the rock glacier base; and a coarser grained and higher conductive layer with little storage capacity, enabling a fast response to recharge events representing the main sediment accumulation. This layer might be active not only as soon as the lower fine-grained layer is fully saturated, but also when recharge is rather intense and the relative difference in hydraulic conductivity is sufficient to create a lateral flow component. The difference in hydraulic conductivity of these two layers seems to be about three orders of magnitude.

This internal structure might be an explanation for the fast natural (EC) and artificial (EO and SRB during the tracer experiment 2012 after injection at T-IP1) tracer responses at the spring to almost every recharge event over the whole observation period. As the response time of EO and SRB seems to be constant over the whole period, it can be concluded that the tracer is stored at a certain distance to the spring, probably at the contact of these two layers. Related to the recharge pulse intensity, some of the tracer is mobilized with each event and transported to the spring by the fast, maybe lateral, flow component. Moreover, as event water is usually about 20 % of the

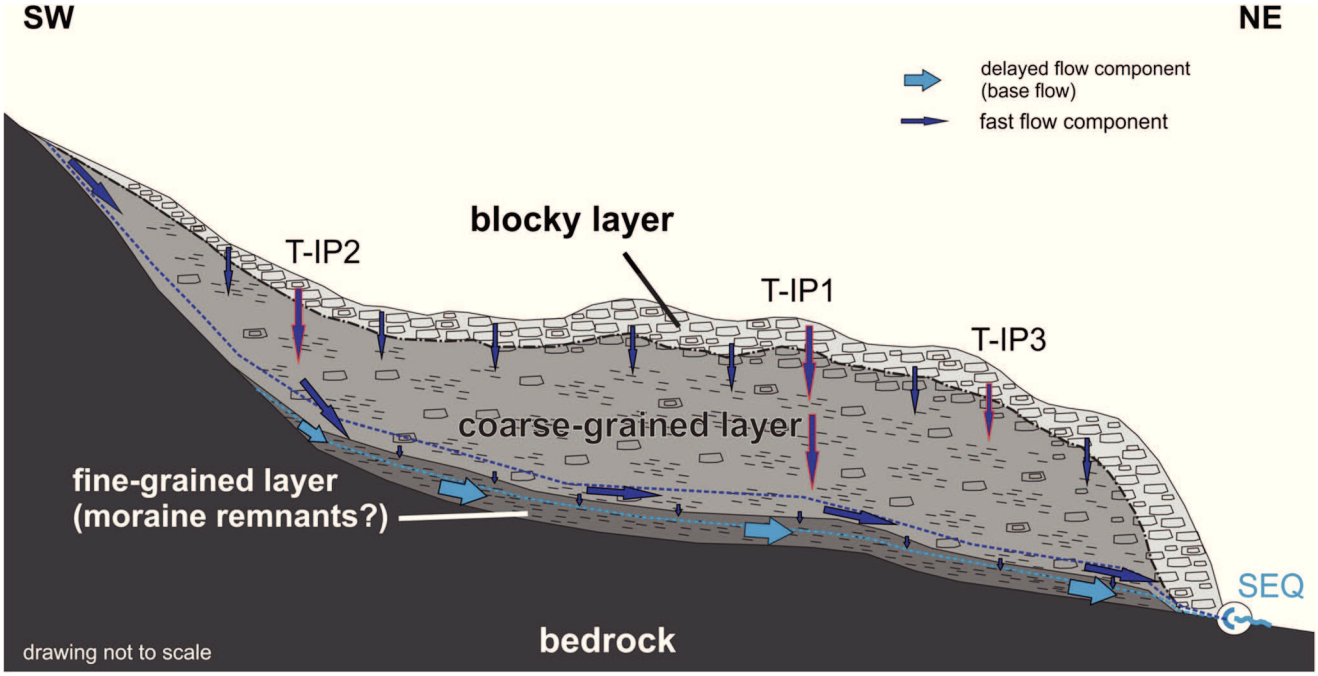

Fig. 9 Conceptual model (longitudinal section) of the relict SRG. *Dark blue arrows* represent the fast flow component, *light blue arrows* the delayed flow component. *Red* edging of the arrows indicates tracer injection at T-IP1–T-IP3. *x*-axis or length of SRG in the order of 700 m, *y*-axis or thickness of SRG from several meters up to several tens of meters

spring discharge, only some parts of the catchment need to contribute directly (fast) to the spring discharge after recharge events. The remaining recharge (80 %) will reach the spring considerably delayed. That means that e.g., the nearest sub-catchment (about 20 % of the entire catchment) in the south-east to the spring would contribute enough recharge water for the fast flow component. The response time of only a few hours on rain events can be explained based on the very steep relief of the sub-catchment, the obvious gully in the talus slope (see Fig. 1) and the short distance in combination with the high hydraulic conductivity of layer 2. Moreover, this sub-catchment overlaps with the location of T-IP1 where EO and SRB were injected.

Conclusions

The good agreement of individual investigation results suggests that the relict rock glacier represents a heterogeneous aquifer system with a layered structure which exhibits similarities to the complex drainage behavior of karst aquifers. On one hand, a rather fast response to recharge events within a couple of hours and, on the other hand, a reasonably large storage component, allowing for relatively large base flow rates long after recharge events, can be observed. Although the silty and fine sand-dominated layer is not proven yet by geophysics, there is strong evidence from hydrograph analysis, residence times of isotopic data and from artificial tracer testing. This finding may have important implications for the hydrological modeling of alpine regions, as it may not be adequate to represent this type of aquifer by a single homogeneous model component. Ultimately, the storage capacity is a key factor for water resources management and helps to regulate the risk of natural hazards such as floods and debris flows in alpine catchments. In further consequence, this is essential for the assessment of the impact of climate change on natural hazards, on water ecology and the sustainability of economic water use in alpine regions. The results give a preliminary understanding of the drainage dynamics of a relict rock glacier. However, they are affected by uncertainties and limitations with regard to geometry and boundary condition of the aquifer as well as thermal conditions of the rock glacier sediments. Thus, further investigations related to the geometry and ground temperature of the relict rock glacier are subject to ongoing investigations. Moreover, the thermal behavior might exhibit helpful insights into the genesis and evolution of rock glaciers from active to relict phases related to the impact of climate change.

Acknowledgements This study was funded by the European Regional Development Fund (ERDF) and the Federal Government of Styria. The authors are grateful to the Hydrographic Service of Styria for providing the spring discharge data of the SRG spring (HZB No. 396762). The digital elevation models and the topographic maps were provided by the GIS Service of the federal government of Styria (GIS Steiermark). Water samples (dye tracer, stable isotopes) and charcoal samples (dye tracers) were analysed at JOANNEUM RESEARCH, Dept. of Water Resources and Environmental Analytics. The authors appreciate constructive comments from Victor Bense and an anonymous reviewer and Alan M. MacDonald the associate editor.

References

ANIP (Austrian Network of Isotopes in Precipitation) (2007) Österreichisches Netzwerk für Isotopen (^{18}O, ^{2}H, ^{3}H) in Niederschlägen und Oberflächengewässern [Austrian network for isotopes (^{18}O, ^{2}H, ^{3}H) in precipitation and surface waters]. Landesministerium, Ämter d. Landesregierung, ARC und Umweltbundesamt, Vienna. Available at http://www.umweltbundesamt.at. Accessed 02 Nov 2015

Azócar GF, Brenning A (2010) Hydrological and geomorphological significance of rock glaciers in the dry Andes, Chile. Permafrost Periglac 21(1):42–53

Baedke SJ, Krothe NC (2001) Derivation of effective hydraulic parameters of a karst aquifer from discharge hydrograph analysis. Water Resour Res 37(1):13–19

Ballantyne CK, Schnabel C, Xu S (2009) Exposure dating and reinterpretation of coarse debris accumulations ('rock glaciers') in the Cairngorm Mountains, Scotland. J Quat Sci 24:19–31

Banerjee B, Gupta SK (1975) The hidden layer problem in seismic refraction work. Geophys Prospect 23:642–652

Barnett TP, Adam JC, Lettenmaier DP (2005) Potential impacts of a warming climate on water availability in snow-dominated regions. Nature 438:303–309

Barsch D (1996) Rock glaciers: indicators for the present and former geoecology in high mountain environments. Springer Series in Physical Environment 16. Springer, Berlin

Bear J (1972) Dynamics of fluids in porous media. Elsevier, New York

Birk S, Hergarten S (2010) Early recession behaviour of spring hydrographs. J Hydrol 387(1–2):24–32. doi:10.1016/j.jhydrol.2010.03.026

Birk S, Liedl R, Sauter M (2004) Identification of localised recharge and conduit flow by combined analysis of hydraulic and physico–chemical spring responses (Urenbrunnen, SW-Germany). J Hydrol 286(1–4):179–193

Brenning A (2005) Geomorphological, hydrological and climatic significance of rock glaciers in the Andes of central Chile. Permafrost Periglac 16:231–240

Brutsaert W, Nieber JL (1977) Regionalized drought flow hydrographs from a mature glaciated plateau. Water Resour Res 13:637–643

Campbell DH, Clow DW, Ingersoll GP, Mast MA, Spahr NE, Turk JT (1995) Processes controlling the chemistry of two snowmelt-dominated streams in the Rocky Mountains. Water Resour Res 31(11):2811–2821

Clow DW, Schrott L, Wobb R, Campell DH, Torizzo A, Dornblaser M (2003) Ground water occurrence and contributions to streamflow in an alpine catchment, Colorado Front Range. Ground Water 41:937–950

Dewandel B, Lachassagne P, Bakalowicz M, Weng P, Al-Malki A (2003) Evaluation of aquifer thickness by analyzing recession hydrographs: application to the Oman ophiolite hard-rock aquifer. J Hydrol 274:248–269

Gödel S (1993) Geohydrologie der Blockgletscher im Hochreichhart-Gebiet (Seckauer Tauern, Steiermark) [Hydrogeology of rock glaciers in the Hochreichhart area (Seckauer Tauern Range, Styria)]. MSc Thesis, University of Vienna, Austria

Greenhalgh SA (1977) Comments on "The hidden layer problem in seismic refraction work". Geophys Prospect 25:179–181

Haeberli W, Beniston M (1998) Climate change and its impacts on glaciers and permafrost in the Alps. Ambio 27:258–265

Haeberli W, Hallet B, Arenson L, Elconin R, Humlum O, Kääb A, Kaufmann V, Ladanyi B, Matsuoka N, Springman S, Vonder Mühll D (2006) Permafrost creep and rock glacier dynamics. Permafrost Periglac 17(3):189–214

Harris SA, Pederson DE (1998) Thermal regimes beneath coarse blocky materials. Permafrost Periglac 9:107–120

Harrison S, Whalley B, Anderson E (2008) Relict rock glaciers and protalus lobes in the British Isles: implications for late Pleistocene mountain geomorphology and palaeoclimate. J Quat Sci 23:287–304

Hausmann H, Krainer K, Brückl E, Ullrich C (2012) Internal structure, ice content and dynamics of Ölgrube and Kaiserberg rock glaciers (Ötztal Alps, Austria) determined from geophysical surveys. Aust J Earth Sci 105(2):12–31

Hergarten S, Birk S (2007) A fractal approach to the recession of spring hydrographs. Geophys Res Lett 34:L11401. doi:10.1029/2007GL030097

Hergarten S, Winkler G, Birk S (2014) Transferring the concept of minimum energy dissipation from river networks to subsurface flow patterns. Hydrol Earth Syst Sci 18:4277–4288. doi:10.5194/hess-18-4277-2014

Hughes PD, Gibbard PL, Woodward JC (2003) Relict rock glaciers as indicators of Mediterranean palaeoclimate during the Last Glacial Maximum (Late Würmian) in northwest Greece. J Quart Sci 18(5):431–440

Jasper K, Calanca PL, Gyalistras D, Fuhrer J (2004) Differential impacts of climate change on the hydrology of two alpine river basins. Clim Res 26:113–129

Kasnavia T, Vu D, Sabatini DA (1999) Fluorescent dye and media properties affecting sorption and tracer selection. Ground Water 37(3):376–381

Kellerer-Pirklbauer A, Lieb KG, Kleinferchner H (2012) A new rock glacier inventory of the Eastern European Alps. Aust J Earth Sci 105(2):78–93

Kellerer-Pirklbauer A, Pauritsch M, Morawetz R, Kuehnast B, Schreilechner M, Winkler G (2014) Thickness and internal structure of relict rock glaciers: a challenge for geophysics—examples from two rock glaciers in the Eastern Alps. Geophys Res Abstr 16:EGU201–12581

Kellerer-Pirklbauer A, Pauritsch M, Winkler G (2015) Widespread occurrence of ephemeral funnel hoarfrost and related air ventilation in coarse-grained sediments of a relict rock glacier in the Seckauer Tauern Range. Austria Geog Ann A 97(3):453–471. doi:10.1111/geoa.12087

Klotz D (1982) Verhalten hydrologischer Tracer in ausgewählten Sanden und Kiesen [Characteristics of hydrological tracers in sand and gravel deposits]. GSF-Ber 290:17–29

Kovács A, Perrochet P, Király L, Jeannin P-Y (2005) A quantitative method for the characterisation of karst aquifers based on spring hydrograph analysis. J Hydrol 303:152–164

Krainer K, Mostler W (2002) Hydrology of active rock glaciers: examples from the Austrian Alps. Arc Antarct Alp Res 34:142–149

Krainer K, Ribis M (2012) A rock glacier inventory of the Tyrolean Alps (Austria). Aust J Earth Sci 105(2):32–47

Krainer K, Mostler W, Spoetl C (2007) Discharge from active rock glaciers, Austrian Alps: a stable isotope approach. Aust J Earth Sci 100:102–112

Krainer K, Bressan D, Dietre B, Haas JN, Hajdas I, Lang K, Mair V, Nickus U, Reidl D, Thies H, Tonidandel D (2014) A 10,300-year-old permafrost core from the active rock glacier Lazaun, southern Ötztal Alps (South Tyrol, northern Italy). Quat Res. doi:10.1016/j.yqres.2014.12.005

Kresic N (2007) Hydrogeology and groundwater modeling, 2nd edn. CRC, Boca Raton, FL

Kresic N, Bonacci O (2010) Spring discharge hydrograph. In: Kresic N, Stevanovic Z (eds) Groundwater hydrology of springs: engineering, theory, management, and sustainability. Elsevier, Amsterdam, pp 129–163

Langston G, Bentley LR, Hayashi M, McClymont AF, Pidlisecky A (2011) Internal structure and hydrological functions of an alpine proglacial moraine. Hydrol Process 25:2967–2982. doi:10.1002/hyp.8144

Liu FJ, Williams MW, Caine N (2004) Source waters and flow paths in an alpine catchment, Colorado Front Range, United States. Water Resour Res 40(9):W09401. doi:10.1029/2004WR003076

Maillet E (1905) Mécanique et physique du globe: essai d'hydraulique souterraine et fluviale [Mechanics and physiques of the world: an essay of subterranean and fluviatile hydraulics]. Hermann, Paris

Mair A (2002) Deformation und Ablagerungsraum der Rannachformation, Seckauer Alpen [Deformation and depositional environment of the Rannach formation, Seckauer Alps]. MSc Thesis, University of Graz, Austria

McGuire K, McDonnell J (2006) A review and evaluation of catchment transit time modelling. J Hydrol 330:543–563

Millar CI, Westfall RD (2008) Rock glaciers and related periglacial landforms in the Sierra Nevada, CA, USA: inventory, distribution and climatic relationship. Quat Int 188:90–104

Millar CI, Westfall RD, Delany DL (2013) Thermal and hydrologic attributes of rock glaciers and periglacial talus landforms: Sierra Nevada, California, USA. Quat Int 310:169–180

Morgenschweis G (2010) Hydrometrie [Hydrometry]. Springer, Heidelberg, Germany

Muir DL, Hayashi M, McClymont AF (2011) Hydrological storage and transmission characteristics of an alpine talus. Hydrol Process 25:2954–2966. doi:10.1002/hyp.8060

Nutbrown DA, Downing RA (1976) Normal-mode analysis of the structure of baseflow-recession curves. J Hydrol 30:327–340

Onaca AL, Urdea P, Ardelean AC (2013) Internal structure and permafrost characteristics of the rock glaciers of Southern Carpathians (Romania) assessed by geoelectric soundings and thermal monitoring. Geogr Ann A 95:249–266. doi:10.1111/geoa.12014

Paasche Ø, Dahl SO, Løvlie R, Nesje A (2007) Rockglacier activity during the last glacial–interglacial transition and Holocene spring snowmelting. Quat Sci Rev 26:793–807

Palmer D (1980) The generalized reciprocal method of seismic refraction interpretation. Society of Exploration Geophysicists, Tulsa, OK, 113 pp

Putnam AE, Putnam DE (2009) Inactive and relict rock glaciers of the Deboullie Lakes Ecological Reserve, northern Maine, USA. J Quat Sci 24:773–784

Rorabaugh MI (1964) Estimating changes in bank storage and groundwater contribution to streamflow. IAHS Publ 63:432–441

Roy JW, Hayashi M (2009) Multiple distinct groundwater flow systems of single moraine-talus feature in alpine watershed. J Hydrol 373:139–150

Sabatini DA (2000) Sorption and intraparticle diffusion of fluorescent dyes with consolidated aquifer media. Ground Water 38(5):651–656

Sahuquillo A, Gómez-Hernández JJ (2003) Comment on "Derivation of effective hydraulic parameters of a karst aquifer from discharge hydrograph analysis" by Baedke SJ and Krothe NC. Water Resour Res 39(6):1152. doi:10.1029/2002WR001472

Sauter M (1992) Quantification and forecasting of regional groundwater flow and transport in a karst aquifer (Gallusquelle, Malm, SW Germany). Tübinger Geowissenschaftliche Arbeiten, Reihe C, 13, Universitätsbibliothek, Tübingen, Germany

Scharbert S (1980) Die Bösensteingruppe und die Seckauer Tauern [The Bösenstein group and the Seckauer Tauern Range]. In: Oberhauser R, Bauer FK (eds) Der geologisch Aufbau Österreich [The geological structure of Austria]. Springer, Vienna, pp 368–370

Scharbert S (1981) Untersuchungen zum Alter des Seckauer Kristallins [Investigations about the age of the Seckauer crystalline]. Mitt Ges Geol Bergbaustud 27:163–188

Schmid SM, Fügenschuh B, Kissling E, Schuster R (2004) Tectonic map and overall architecture of the Alpine orogeny. Eclogae Geol Helv 97:93–117

Schmöller R (1978) Der Grundwasserleiter im Murboden des Fohnsdorfer Beckens als refraktionsseismisch überschossener Schicht [The aquifer in the "Murboden" of the Fohnsdorf Basin as a hidden layer in refraction seismic data]. Mitt Abt Geol Paläont Bergb Landesmus Joanneum 39:97–108

Schmöller R (1982) Some aspects of handling velocity inversion and hidden layer problems in seismic refraction work. Geophys Prospect 30:735–751

Schnegg PA (2002) An inexpensive field fluorometer for hydrogeological tracer tests with three tracers and turbidity measurement. In: Bovanegra E, Martinez D, Massone H (eds) XXXII IAH and ALHSUD Congress Groundwater and Human Development, Mar del Plata, Argentina, October 2002

Schön J (2011) Physical properties of rocks. Elsevier, Oxford

Schwartz F, Zhang H (2003) Fundamentals of groundwater. Wiley, New York

Stewart I, Cayan DR, Dettinger MD (2004) Changes in snowmelt runoff timing in western North America under a "business as usual" climate change scenario. Clim Change 6:217–232. doi:10.1023/B:CLIM.0000013702.22656.e8

Stichler W, Herrmann A (1983) Application of environmental isotope techniques in water balance studies of small basins. Proc. of the Hamburg Workshop "New Approaches in Water Balance Computations". IAHS Publ 148, IAHS, Wallingford, UK, pp 93–112

Tague C, Grant GE (2009) Groundwater dynamics mediate low-flow response to global warming in snow-dominated alpine regions. Water Resour Res 45:W07421. doi:10.1029/2008wr007179

Taucher W (2010) Climatic conditions of six selected sites in the Hohe and Niedere Tauern Range 1961–2006. MSc Thesis, University of Graz, Austria

Untersweg T, Proske H (1996) Untersuchungen an einem fossilen Blockgletscher im Hochreichhartgebiet (Niedere Tauern, Steiermark) [Investigations at a relict rock glacier in the Hochreichhart area (Niedere Tauern Range, Styria)]. Grazer Schriften Geogr Raumforschung 33:201–207

Untersweg T, Schwendt A (1995) Die Quellen der Blockgletscher in den Niederen Tauern [The rock glacier springs in the Niedere Tauern Range]. Bericht der wasserwirtschaftlichen Planung 78, Amt d. Steiermärkischen Landesregierung, Landesbaudirektion, Graz, Austria

Untersweg T, Schwendt A (1996) Blockgletscher und Quellen in den Niederen Tauern [Rock glacier in the Niedere Tauern Range]. Mitte Österr Geol Ges 87:47–55

Wels C, Cornett RJ, Lazarete BD (1991) Hydrograph separation: a comparison of geochemical and isotopic tracers. J Hydrol 122:253–274

Winkler G, Kellerer-Pirklbauer A, Pauritsch M (2012) Reliktische blockgletscher – grundwasserkörper in alpinen, kristallinen Einzugsgebieten [Relict rock glaciers: groundwater bodies in alpine, crystalline catchments]. Beitr Hydrogeo 59:119–137

Zurawek R (2002) Internal structure of a relict rock glacier, Sleza Massif, southwest Poland. Permafr Periglac Process 13:29–42

7.2. Publication II

Pauritsch M, Birk S, Wagner T, Hergarten S, Winkler G (2015) Analytical approximations of discharge recessions for steeply sloping aquifers in alpine catchments. Water Resources Research, 51, 8729–8740, doi: 10.1002/2015WR017749

AGU PUBLICATIONS

Water Resources Research

RESEARCH ARTICLE
10.1002/2015WR017749

Analytical approximations of discharge recessions for steeply sloping aquifers in alpine catchments

Marcus Pauritsch[1], Steffen Birk[1], Thomas Wagner[1], Stefan Hergarten[2], and Gerfried Winkler[1]

[1]Institute of Earth Sciences, NAWI Graz, University of Graz, Graz, Austria, [2]Institute of Earth and Environmental Sciences, University of Freiburg, Freiburg im Breisgau, Germany

Key Points:
- Analytical solutions are compared to a numerical model for sloping aquifers
- Estimated hydraulic properties for steep slopes are in a reasonable range
- No kinematic wave condition observable at steeply sloping relict rock glacier

Correspondence to:
G. Winkler,
gerfried.winkler@uni-graz.at

Citation:
Pauritsch, M., S. Birk, T. Wagner, S. Hergarten, and G. Winkler (2015), Analytical approximations of discharge recessions for steeply sloping aquifers in alpine catchments, *Water Resour. Res.*, *51*, doi:10.1002/2015WR017749.

Received 3 JUL 2015
Accepted 8 OCT 2015
Accepted article online 11 OCT 2015

Abstract The validity and applicability of various methods to infer hydraulic properties of sloping aquifers in alpine settings using the power law relationship between the discharge recession and its first time derivative is explored. For this purpose, a synthetic spring catchment implemented in the numerical groundwater flow model MODFLOW as well as the example of a relict rock glacier in an alpine setting is examined. The various approaches are found to differ particularly in the late time domain, whereas most of them agree fairly well in the early time domain and at the transition point between the two time domains. As the early recession may be affected by uncertainties from inappropriate initial conditions, it is proposed to use the transition point for estimating aquifer thickness and transmissivity. Using only prolonged winter recessions in the analysis of the field data from the relict rock glacier yields estimates of aquifer thickness and hydraulic conductivity consistent with results from a geophysical survey and tracer tests, respectively. In the other seasons, the recession is frequently interrupted by minor recharge events, and using the lower envelope of the entire data is found to yield estimates that are too high in the given case. It is thus recommended to focus on the winter recession in the analysis of hydrograph data from alpine settings.

1. Introduction

Discharge recession analyses of streams or springs are important and common tools for estimating effective hydraulic parameters of catchments or aquifers. *Brutsaert and Nieber* [1977] made a landmark contribution to discharge recession analyses by considering the first derivative of the discharge as a function of the discharge Q [L^3/T].

$$dQ/dt = aQ^b \tag{1}$$

With this formulation, the often difficult determination of initial times of recession events is being eliminated and the change of discharge in time can be described by a power law relationship of the discharge with a representing the aquifer properties and an exponent b. When Q is plotted against dQ/dt in a log-log plot, the recession curve is a straight line with slope b. There are several analytical solutions available for horizontal and sloping aquifers with b equal to 3 or 3/2 for the early time domain (hereinafter referred to as b_1) and 3/2, 1 or 0 for the late time domain (hereinafter referred to as b_2). The authors renounce to give a detailed review of these solutions, as this is already given in *Rupp and Selker* [2006a] and more recently in *Troch et al*. [2013].

The majority of investigations of nonhorizontal aquifer systems are considering entire catchment areas with mild to moderate slope angles, drained by a system of streams [e.g., *Rupp and Selker*, 2006a; *Rocha et al*., 2007]. The drained hillslopes are mostly considered to be relatively thin zones with thicknesses of a few meters. In contrast, investigations using spring data for recession analyses with analytical solutions based on equation (1) are rare [*Malvicini et al*., 2005]. *Malvicini et al*. [2005] used the early and late time domain solutions of *Brutsaert* [1994] and *Brutsaert and Lopez* [1998] to estimate hydraulic properties of sloping aquifers in the Philippines. They pointed out that due to the lower sensitivity to precipitation-related components and bank storage, spring hydrographs might even be more appropriate for this kind of investigations. The analytical solutions employed for parameter estimation were generally developed for very simplified, homogeneous aquifers. Yet *Szilagyi et al*. [1998] showed that increasing watershed complexity had minimal effect on the effective hydraulic parameters resulting from the recession flow analysis for synthetic catchments. *Troch et al*. [2002] developed a

hillslope-storage kinematic wave equation in which the three-dimensional aquifer is collapsed into a one-dimensional profile. This approach has been later adapted for the Boussinesq equation by *Troch et al.* [2003] and extended for nonhomogeneous slopes and exponential width functions [*Hilberts et al.*, 2004; *Troch et al.*, 2004]. These models have been compared to each other as well as to a three-dimensional Richards equation model to demonstrate their validity [*Paniconi et al.*, 2003]. Furthermore, the models allowed for investigating the effect of various profile and plan shapes. Their results revealed that the investigated hillslope types showed highly variable discharge behavior and that the applicability of the kinematic wave equation is dependent on both the slope angle and the shape of the aquifer. *Pauwels and Troch* [2010] used the rising limb of the hydrograph after the base flow recession to estimate aquifer parameters. They showed that their method is more accurate than the traditional base flow recession methods, as the rising limb is not affected by unrealistic initial conditions. However, the rising limb analysis requires accurate data for the recharge.

This paper focuses on three analytical approaches and their accuracies and limitations regarding the effect of slope angle rather than that of the shape of the aquifer. Due to the fact that the field example discussed later in the text and likely the majority of mountainous aquifers in general are especially related to rather steep slopes, this has been investigated in detail and expands on the understanding of these analytical approaches and their limitations. The first selected analytical solution was formulated by *Brutsaert* [1994] (hereinafter referred to as "Brutsaert solution") which encompasses the early and late time domain and is one of the most commonly used analytical solutions for discharge recession of sloping aquifers.

Parlange et al. [2001] developed a simple analytical approximation (hereinafter referred to as "Parlange approximation") based on dimensionless coordinates and variables to reduce the number of parameters. The translation of the dimensionless recession curve to observed data can be used for parameter estimation. *Mendoza et al.* [2003] used the Parlange approximation to estimate basin-wide hydraulic parameters of a semiarid mountainous catchment with data from gauging stations of subcatchments. They showed that even though they were using an analytical approximation for horizontal aquifers, reasonable estimates for hydraulic parameters were also achieved for these mountainous catchments. Additionally, they showed that this method can even be applied when data from the early time domain are scarce.

Following the approach of *Parlange et al.* [2001], *Hogarth et al.* [2014] developed a simple analytical approximation for sloping aquifers (hereinafter referred to as "Hogarth approximation"). They pointed out that as the water table in steep or thin aquifers still shows artifacts of the initial shape when running dry, the confident application of this approximation is limited to $0 < \varepsilon < 1$ with

$$\varepsilon = (L \tan i)/D \tag{2}$$

where L [L] is the length of the aquifer, i is the slope angle, and D [L] is the thickness of the initially saturated aquifer.

In alpine catchments, where slope angles can be steep (more than 15°) and ε is large, it is unclear if these analytical solutions are applicable for parameter estimation and if so, which is the best to be used in such environments. Note however that D is inversely proportional to ε and might be high (several tens of meters) in this type of environment (see equation (2)).

The Parlange and Hogarth approximations and the Brutsaert solution are compared to a numerical model, which serves as a reference. Using a simple hypothetical setting implemented in the numerical groundwater flow model MODFLOW [*McDonald and Harbaugh*, 1988], the deviations from the analytical solutions are analyzed as the slope angle increases. In addition to the synthetic data from the numerical models, discharge data from a relict rock glacier representing an aquifer system in an alpine environment are used to estimate the hydraulic properties of the aquifer (primarily transmissivity) using the three selected analytical methods. The results are then compared to a previous study in this investigation area [*Winkler et al.*, 2014] to put the range of parameters estimated by the analytical solutions into perspective and to draw conclusions about the applicability of these models for the purpose of parameter estimation in alpine environments.

2. Theory

Subsurface flow of an unconfined sloping aquifer resting on an impermeable layer can be described by

$$q = -kh(\partial h/\partial x \cos i + \sin i) \tag{3}$$

where q [L^2 / T] is the flow rate per unit width of the aquifer and k [L / T] is the hydraulic conductivity [*Boussinesq*, 1877]. q and k are given in x direction, parallel to the impermeable layer which has the slope angle i. The hydraulic head h [L] is measured perpendicular to the impermeable layer. Assuming an isotropic, homogeneous porous aquifer in absence of recharge or evapotranspiration, combining equation (3) with the continuity equation yields

$$\partial h/\partial t = k/f[\cos i \ \partial(h \ \partial h/\partial x)/\partial x + \sin i \ \partial h/\partial x] \tag{4}$$

where t [T] is time and f is the drainable porosity.

There is no generally applicable exact analytical solution to equation (4) because of its nonlinear form. However, there are exact solutions for particular cases available [e.g., *Boussinesq*, 1877] or approximate solutions with certain assumptions. Several authors have provided such solutions to these simplified approximations which are reviewed by *Rupp and Selker* [2006a] and *Troch et al.* [2013].

One analytical approximation of equation (4) is the linearized Brutsaert solution of an initially saturated aquifer, in which equation (3) is linearized in h as

$$-q = kpD \ \cos i \ \partial h/\partial x + kh \ \sin i \tag{5}$$

where p is introduced as a constant with $0 < p \leq 1$ to compensate for the approximation resulting from the linearization. p is regarded as a calibration constant. *Brutsaert* [1994] pointed out that previous studies suggested values of $p = 1/3$ or $p = 1/2$ by comparing a linearized approximation to an exact analytical solution of equation (4) by *Polubarinova-Kochina* [1962, p. 507] for an initially saturated horizontal aquifer [*Kraijenhoff van de Leur*, 1966, 1979; *Brutsaert and Nieber*, 1977] and the Dupuit formula for steady groundwater flow between two parallel open channels, respectively. As discussed in *Rupp and Selker* [2006a], the introduction of the calibration parameter p results in another unknown parameter, which is not desirable in cases where aquifer parameters such as k and f are to be estimated.

The Brutsaert solution gives the outflow rate of a hillslope as

$$q = 2DKf/L^3 \sum_{n=1,2,\ldots}^{\infty} \frac{z_n^2[(2e^{-aL}\cos z_n) - 1]\exp\left[-K\left(z_n^2/L^2 + U^2/4K^2\right)t\right]}{\left(z_n^2/L^2 + U^2/4K^2 + U/2KL\right)} \tag{6}$$

with $K = kpD \cos i/f$, $U = k \sin i/f$, and $a = -U/2K$. The parameter z_n is defined by the nonlinear equation $\tan z_n = z_n/(aL)$ and must be computed numerically in general. However, in the limiting cases of nearly horizontal flow or thick aquifers and a steep slope or a shallow aquifer, it can be approximated by $z_n = (2n-1)\pi/2$ and $z_n = n\pi$, respectively [*Brutsaert*, 1994].

Another possibility to simulate the discharge recession of a sloping aquifer is to use the Parlange approximation, which is designed as an analytical approximation for horizontal catchments but had also shown to work reasonably well under sloping conditions [*Mendoza et al.*, 2003]:

$$I^* = (5 - \sqrt{7}/2\sqrt{\pi})\sqrt{t^*}[1 - \exp(-1/t^*)] + 5/4 \ \mathrm{erfc}\left(1/\sqrt{t^*}\right) - 1/4\left[\mathrm{erfc}\left(1/\sqrt{t^*}\right)\right]^{\sqrt{7}} \tag{7}$$

where I^* is the dimensionless cumulative outflow and t^* is the dimensionless time:

$$t^* = Dkt/fB^2 \tag{8}$$

where B [L] is the total stream length. The first derivative of I^* gives the dimensionless discharge Q^* and the second derivative of I^* gives dQ^*/dt^*. When Q^* and dQ^*/dt^* are plotted in a logarithmic plot [*Brutsaert and Nieber*, 1977], a sharp transition point between the early and late time domain can be observed at $t^* = 0.5625$ [*Mendoza et al.*, 2003]. This theoretical curve can be translated to the measured field data by using

$$Q = HQ^* \tag{9}$$

$$dQ/dt = V \ dQ^*/dt^* \tag{10}$$

with

$$H = kAD^2/L^2 \tag{11}$$

$$V = Ak^2D^3/f\,L^4 \tag{12}$$

H [L^3/T] and V [L^3/T^2] represent the horizontal and vertical shift from the theoretical curve and can be used for parameter estimation. A [L^2] is the catchment area for both sides of the draining channel, given by $A = 2BL$. With known aquifer dimensions (A and L) and an assumed value of the drainable porosity f, the transmissivity T [L^2/T] and the aquifer thickness D can be estimated [*Parlange et al.*, 2001; *Mendoza et al.*, 2003]:

$$T = VfL^2/H \tag{13}$$

$$D = H^2/(VfA) \tag{14}$$

There is an ongoing discussion how to determine the transition point in measured data [*Mendoza et al.*, 2003; *Wang*, 2011]. *Mendoza et al.* [2003] used the transition points of the lower envelope, linear regression and upper envelope to give a range for the hydraulic properties of the watersheds. The resulting range of the estimated T was within an order of magnitude, which is reasonable for practical applications.

Hogarth et al. [2014] expanded equation (7) to include sloping aquifers by estimating the interaction between diffusion and gravity controlled flow and formulated:

$$I^* = I_0(1-t^*/t_D) + (t^*/t_D)[a+(1-a)I_0/I_{0D}]^{tD} \tag{15}$$

with

$$a = (\varepsilon t_D)^{1/t_D} \tag{16}$$

$$\varepsilon t_D = 1 + [(1+e)/2\varepsilon]\ \ln[1+4\varepsilon/(1+e)] \tag{17}$$

where I_0 is the dimensionless cumulative outflow of a horizontal aquifer (see equation (7)) and t_D is the drying time of the aquifer.

The Hogarth approximation shows a linear discharge recession of the late time domain ($b_2 = 0$), as suggested by *Bogaart et al.* [2013], whereas the Parlange approximation and the Brutsaert solution have an exponential discharge recession ($b_2 = 1$). Although $b_2 = 1$ can often be observed for field data of sloping aquifers, *Stagnitti et al.* [2004] showed that the exponential discharge recession of the late time domain is actually an artifact of the linearization of the Boussinesq equation which prevents a drying front in the aquifer and therefore leads to an infinite recession [*Bogaart et al.*, 2013].

3. Methods

Three analytical solutions that encompass both, the early and late time domains are selected and compared to a numerical reference model. The first is the well-known and widely examined Brutsaert solution (see equation (6)). The second is the Parlange approximation for horizontal aquifers (see equation (7)), as it was shown by *Mendoza et al.* [2003] that this approximation can yield reasonable ranges of aquifer parameters for sloping aquifers although it is strictly valid for horizontal aquifers only. The third and the most recent analytical solution (Hogarth approximation) will be used to examine how much the estimation of hydraulic properties will be affected when the aquifer properties (e.g., i and D) exceed the given restriction of $\varepsilon = 1$ [*Hogarth et al.*, 2014].

These analytical solutions are compared to a suite of numerical simulations of simple rectangular and homogeneous aquifers for a wide range of slopes i (0°, 5°, 10°, 15°, 20°, and 25°). The numerical model is implemented in MODFLOW [*McDonald and Harbaugh*, 1988], using the Newton-formulation NWT solver which is a robust approach for simulating the falling dry and rewetting of cells [*Niswonger et al.*, 2011; *Hunt and Feinstein*, 2012]. The model simulates one-dimensional groundwater flow with a uniform cell discretization of 10 m in flow direction and a single cell perpendicular to the flow direction. The sides and the upper end of the aquifer have no-flow boundary conditions and the outlet is represented by a constant head of 0.005 m. The initial condition of the numerical model is a completely saturated aquifer, except for the constant head cell which represents the outlet. Although this type of outlet differs from the initial conditions of

the analytical models (fully saturated aquifer also at $x = 0$), at the given cell sizes, the differences between the numerical and the analytical models can only be observed at the very first time steps which can be neglected for the scope of this investigation.

As an example of a sloping aquifer in an alpine catchment, data from the relict Schöneben Rock Glacier (hereinafter referred to as "SRG") are being used. The slope angle of the SRG is estimated to be identical to the average surface slope of about 15°. A more detailed description of the investigation area is given by *Winkler et al*. [2012, 2014]. The chosen aquifer configuration of the numerical and analytical models is $L = 700$ m, $B = 300$ m, and $D = 30$ m with $k = 10^{-5}$ m/s and $f = 0.2$, comparable to the characteristics of the SRG. Applying the three analytical approximations described above, mean daily discharge data of the SRG spring (HZB-number 396762) from 8 November 2008 to 7 March 2014, measured at an official gaging station of the Hydrographic Service of Styria, located about 20 m downstream of the actual spring, are used to estimate the hydraulic conductivity of the rock glacier. The noise in the discharge data has been reduced according to the method proposed by *Rupp and Selker* [2006b] by scaling dt for each observation in time to the observed decrease in discharge dQ rather than keeping dt constant. For this noise reduction, the measurement error of the stage is 1 mm and the coefficient C in *Rupp and Selker* [2006b, equation (15)] was set to 2.

4. Results

In the beginning of the early time domain, a small deviation between the numerical model and the analytical solutions can be seen (Figure 1), which can be explained by the slight differences of the boundary condition representing the spring. This deviation can be further minimized by choosing a smaller cell and time discretization in the numerical model but as it is not the aim of this investigation to produce a perfect fit of the numerical model, this short-term initial deviation is neglected further on.

As can be seen in Figure 1a, the transition point between the early and the late time domain is more or less identical for the different methods in the case of a horizontal aquifer. The slope of the early time domain is consistently at a value of $b_1 = 3$. For the late time domain, the recession curves of the Parlange and Hogarth approximations as well as that of the numerical model have $b_2 = 3/2$ for horizontal aquifers, while the linearized Brutsaert solution differs from the others with $b_2 = 1$. For mildly sloping aquifers (Figure 1b), the numerical model and the Hogarth approximation both show an intermediate recession of $b_{im} = 1$. This is followed by a late recession of $b_2 = 1/3$ for the numerical model and $b_2 = 0$ for the Hogarth approximation. The intermediate recession ($b_{im} = 1$) disappears with increasing slope angles (Figures 1c–1f). Note that after the period with $b_2 = 1/3$, the recession behavior of the numerical model changes back to $b_2 = 1$ (break in slope left of t6 in Figure 2a). However, by the time the discharge recession of the numerical model changes from $b_2 = 1/3$ to $b_2 = 1$, the aquifer is almost completely dry (Figure 2b).

In addition, the recession curves of the Brutsaert solution and the numerical model show a kinematic wave condition [*Henderson and Wooding*, 1964; *Beven*, 1982] with the characteristic drop of dQ/dt at the transition point which is getting more amplified as the slope angle increases. This effect can be observed at the numerical model for slope angles of 10° and larger (Figures 1c–1f), whereas in the recession curves of the Brutsaert solution this condition can already be seen at slope angles of 5° (Figure 1b). As the kinematic wave condition simulated by the Brutsaert solution is appearing more pronounced compared to the numerical model, a lower dQ/dt value can be observed at this point. This offset results mainly in an underestimation of the aquifer length L when this method is used for parameter estimation. To fit the transition point of the Brutsaert solution to the transition point of the numerical model with the given aquifer properties ($L = 700$ m, $B = 300$ m, $D = 30$ m, $k = 10^{-5}$ m/s, and $f = 0.2$), dependent on the slope angle, an aquifer length of 450–500 m is needed. Note that the Brutsaert solution shows an ambiguity as the vertical offset of the transition points could also be reduced by adjusting the other parameters. Then however, unreasonable values would have to be considered in order to achieve an exact fit. Moreover, adjusting these parameters may also affect other parts of the recession curve leading to an overall poor fit.

With increasing slope angles, the position of the kinematic wave condition within the Q–dQ/dt plot is shifted to the right. Therefore, b_1 increases and deviates from the original value of 3. Because of the shifted transition point of the numerical model, there is an increasing deviation to the transition point of the Parlange approximation with increasing slope angles. As a result, when this method is applied, an additional

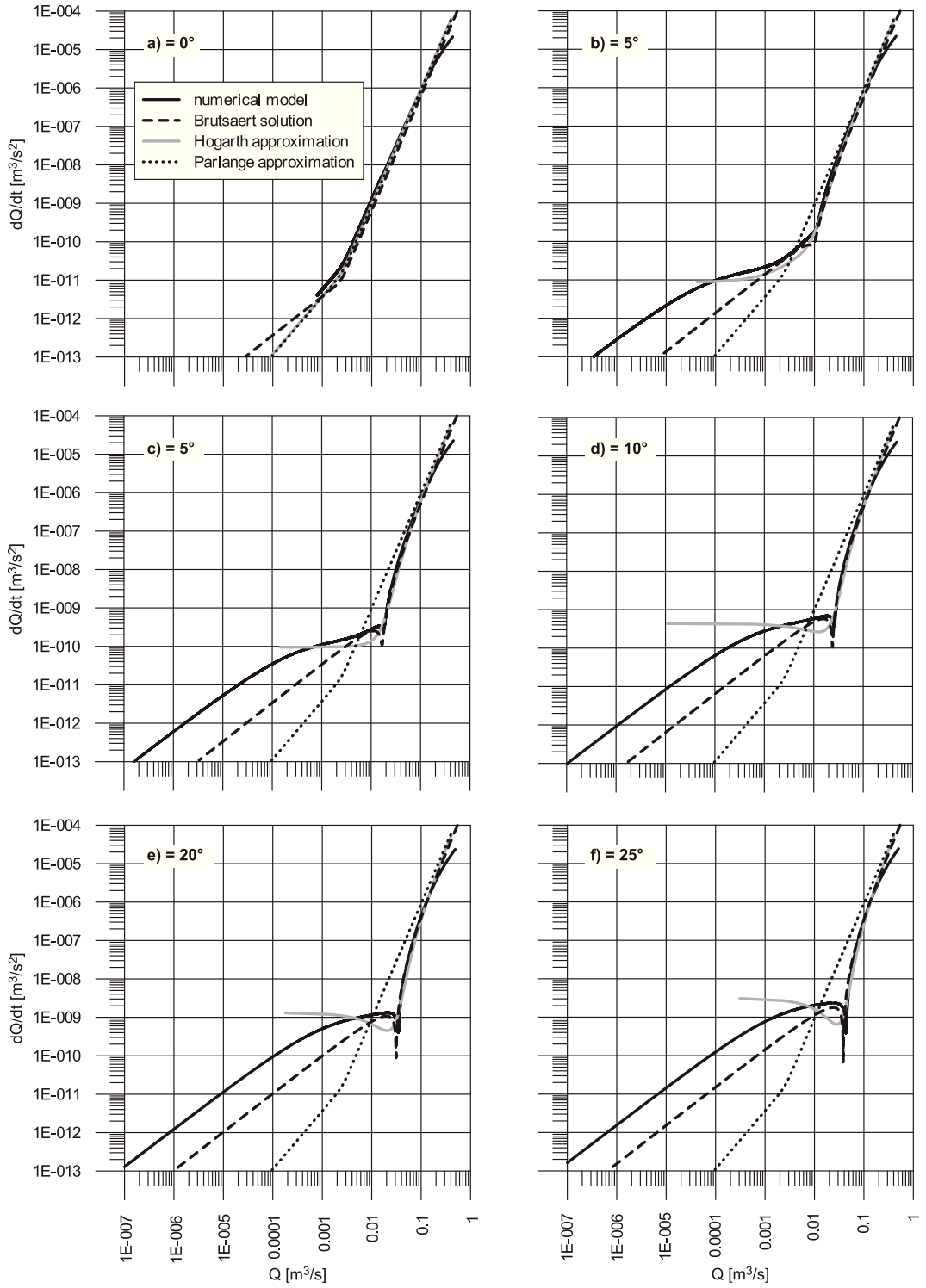

Figure 1. Recession flow curves of the numerical and analytical models for slope angles of (a) 0°, (b) 5°, (c) 10°, (d) 15°, (e) 20°, and (f) 25° shown as Q versus dQ/dt in a log-log plot.

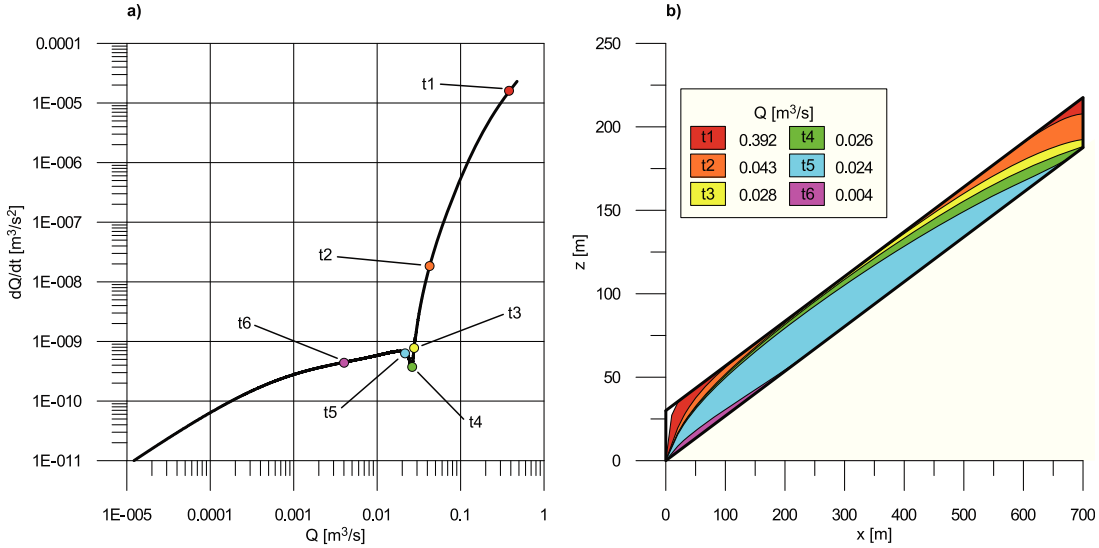

Figure 2. (a) Recession flow curve of the numerical model for a slope angle of 15° with colored points, indicating the positions of the according hydraulic heads presented in Figure 2b in a Q versus dQ/dt plot. (b) A longitudinal cross section of a sloping aquifer with the hydraulic heads and the discharge Q (m^3/s) at selected time steps (t1–t6). Note the kinematic wave condition at t4 where the upper end of the aquifer is falling dry.

shift in H and V is needed which consequently introduces an error of the estimated parameters. With the given aquifer properties ($L = 700$ m, $B = 300$ m, $D = 30$ m, $k = 10^{-5}$ m/s, and $f = 0.2$), the estimate of the hydraulic conductivity from the Parlange approximation is 3×10^{-5}, 5×10^{-5}, 7×10^{-5}, 8×10^{-5}, and 1×10^{-4} m/s for a slope angle of 5°, 10°, 15°, 20°, and 25°, respectively.

The recession curve of the Hogarth approximation is forming a soft bend rather than a discrete transition and therefore it is challenging to mark the exact position of the transition point. When taking the inflection point of the recession curve (where b_1 starts to decrease again) as transition point for mildly sloping aquifers (0°–10°, see Figures 1a–1c), the offset of the transition points between the Hogarth approximation and the numerical model is negligible. For steeply sloping aquifers (15°–25°, see Figures 1d–1f), taking the transition point where dQ/dt is at its minimum, results in a higher dQ/dt and lower Q compared to the numerical model and a correction of this offset induces unreasonable aquifer parameters and therefore questions its applicability for aquifer parameter estimation.

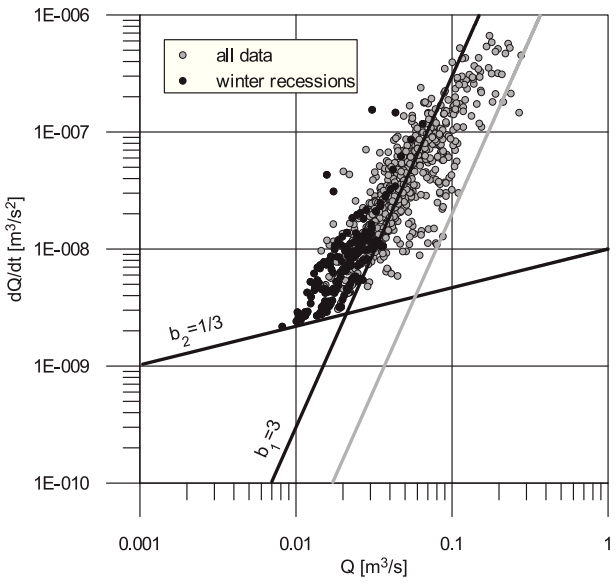

Figure 3. Recession data of the SRG for all available data and only the winter recessions data with the recession slope curves as lower envelopes with $b_1 = 3$ and $b_2 = 1/3$.

Examining the SRG data (Figure 3) reveals that most of the data points can be assigned to b_1. Even though discharge measurements of long recharge free time periods are available during snow-covered winter periods lasting more than 100 days, data from the late time domain are scarce. Nevertheless, *Hogarth et al.* [2014] used a comparable data set and *Mendoza et al.* [2003] had shown that for the opposite case (e.g., scarce data for b_1) aquifer properties still can be estimated. As can be seen in Figure 3, a transition point can be

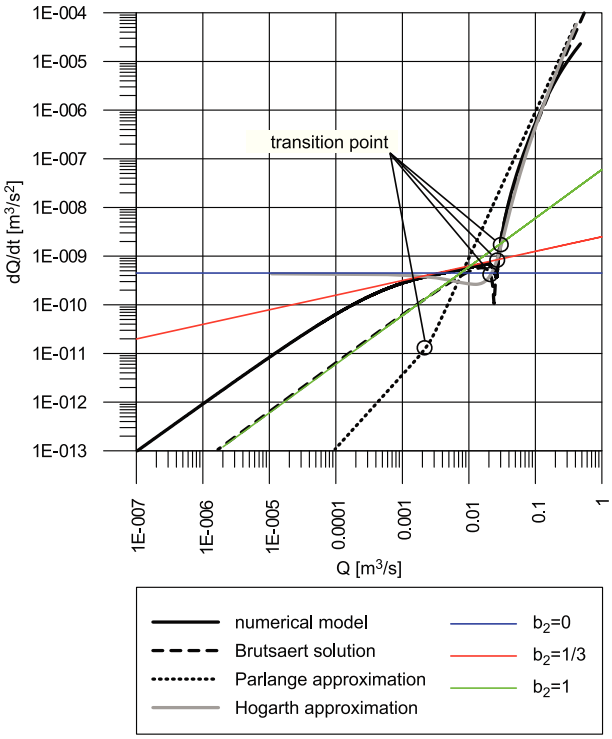

Figure 4. Recession flow curves of the numerical and analytical models for a slope angle of 15° with extrapolated b_2 and the suggested transition points.

determined at $Q = 0.06$ m^3/s and dQ/d$t = 4 \times 10^{-9}$ m^3/s^2 by fitting the lower envelopes of the discharge data to the data with recession slopes of $b_1 = 3$ and $b_2 = 1/3$. At high values of Q, a deviation of the data points from $b_1 = 3$ can be observed. It was discussed in *Pauwels and Troch* [2010] that such a deviation could be explained by the unrealistic initial condition of an initially saturated aquifer. However, also the heterogeneity of the aquifer or an overlapping effect of subareas within the aquifer with various slope angles can be seen as a potential cause for this. The latter could also explain the differences in the theoretical and actual b_2 [*Rupp and Selker*, 2006a]. When the discharge data are limited to the recession during winter time, the risk of small recharge events (i.e., recharge events that only slow down the recession but do not cause an increase in discharge) distorting b is minimized. In this case, b_1 can be clearly set to 3 while b_2 stays the same and the transition point is located at $Q = 0.02$ m^3/s and dQ/d$t = 3 \times 10^{-9}$ m^3/s^2 (Figure 3).

As there is no evidence of a kinematic wave condition observable in the measured data of the SRG, three options can be considered. The first possibility is that the slope angle and/or the aquifer length is overestimated, as a distinctive kinematic wave condition requires a preferably long aquifer length and high slope angle. It can be seen in Figure 1 that the effect of a kinematic wave behavior only appears with the given aquifer dimensions at a slope angle greater than 5°–10°. Geophysical investigations indicate that the slope of the SRG is inhomogeneous and some parts of it can have mild slope angles [*Winkler et al.*, 2012, 2014]. Thus, an effective aquifer with smaller dimensions and/or smaller slope angle can be considered. Second, the plan shape of the effective aquifer might not be rectangular but convergent so that the flow domain decreases toward the spring which reduces the outflow and inhibits a kinematic wave condition in a homogeneous aquifer [*Troch et al.*, 2003; *Paniconi et al.*, 2003; *Hilberts et al.*, 2004]. The third option is that data belonging to the kinematic wave of the SRG are not recorded properly because of measurement uncertainties. When this part of the recession curve is missing, it is reasonable to estimate the transition point by the intersection of b_1 with the extrapolated straight line of b_2 (Figure 4). In Figure 2, it can be seen that close to the kinematic wave condition (t3–t5), only minor changes of the hydraulic head occur.

With the earlier described aquifer dimensions and a slope angle taken as the average surface slope of 15°, using the lower envelope of all available data, translating the transition points from the dimensionless form (equations (1–14)) yields an aquifer thickness of $D = 60$ m for the Parlange approximation and $D = 25$ m for the Hogarth approximation. Using the Brutsaert solution yields to an aquifer thickness of $D = 45$ m. As can be seen in Table 1, when only the winter recession is considered, an aquifer thickness of $D = 10$–15 m is found to be sufficient. Indeed, a recently completed geophysical survey suggests that the maximum thickness of the saturated zone is approximately within the latter range [*Winkler et al.*, 2014]. The transmissivity T is very similar using either the Brutsaert solution or the Hogarth approximation but in contrast, the Parlange approximation results in a transmissivity that is about 1 order of magnitude larger, reflecting the incorrect assumption of a horizontal aquifer. Using only the winter recessions reduces the transmissivity obtained from the Brutsaert solution and Hogarth approximation but increases the transmissivity from the

Table 1. Estimated Hydraulic Properties of SRG[a]

Analytical Model	D (m)	T (m^2/s)	k (m/s)
All Data			
Parlange approximation	60	3.6×10^{-3}	6.0×10^{-5}
Brutsaert solution	45	5.6×10^{-4}	1.3×10^{-5}
Hogarth approximation	25	6.0×10^{-4}	2.4×10^{-5}
Winter Recessions			
Parlange approximation	10	7.0×10^{-3}	7.0×10^{-4}
Brutsaert solution	15	2.1×10^{-4}	1.4×10^{-5}
Hogarth approximation	12	2.0×10^{-4}	1.7×10^{-5}

[a]Slope angle for Parlange approximation: 0°; slope angle for Brutsaert solution and Hogarth approximation: 15°.

Parlange approximation. Assuming the aforementioned range of the aquifer thicknesses, the corresponding hydraulic conductivity ranges between 1.3 $\times$ 10^{-5} and 6 $\times$ 10^{-5} m/s when the complete data set is used and between 1.4 $\times$ 10^{-5} and 7.0 $\times$ 10^{-4} m/s when only the winter recessions are considered. This range is generally reasonable in the given type of setting and found to be consistent with estimates based on tracer velocities observed at the SRG [*Winkler et al*., 2014]. Using only the Brutsaert solution and Hogarth approximation, this range can be further narrowed to 1.4 $\times$ 10^{-5} and 1.7 $\times$ 10^{-5} m/s. As explained above, however, the aquifer might have an irregular slope obscuring the kinematic wave condition. Furthermore, the slope angle of 15° might be an overestimate, which is also indicated by the aforementioned geophysical survey at least in some parts of the aquifer close to the spring. Therefore, and for the sake of completeness of the investigation, the transmissivity of the SRG was additionally estimated with the previously used set of slope angles. The results in Table 2 show that at a slope angle of 0°, the transmissivity using the Hogarth approximation is 11 and 46 times, and using the Brutsaert solution 16 and 64 times higher than at 25° when using the complete data set or only the winter recessions, respectively.

5. Discussion

It is clearly visible in Figure 1 that the analytical methods have a highly variable b_2 for all investigated slope angles and except for the Parlange and Hogarth approximations at 0°, none of the analytical models was able to exactly reproduce the results of the numerical model, which might have its own limitations. However, the NWT solver used in the numerical model improves the handling of drying cells and allows simulating a drying front proceeding toward the outlet [*Niswonger et al*., 2011; *Hunt and Feinstein*, 2012]. When the late time domain recession of $b_2 = 1/3$ changes to $b_2 = 1$, the aquifer is almost completely dry (see t6 in Figure 2) and the water level reaches the lowest point of the numerical model. At this point, the advantages of the NWT solver cease and the following recession with $b_2 = 1$ is representing an infinite discharge recession [*Bogaart et al*., 2013]. This effect is not observed in nature as among other things, at this point the discharge of a natural aquifer would result in drainage of the unsaturated zone which is not included in the numerical model and the Boussinesq equation. As this part of the recession curve can therefore be considered as an artifact of the numerical solution, it has no physical relevance and can be neglected for the purpose of parameter estimation.

Considering mildly sloping aquifers, the Hogarth approximation gives a close fit to the numerical model but at higher slope angles the deviation increases. *Hogarth et al*. [2014] point out that their approximation can be applied with confidence for aquifers with $\varepsilon \leq 1$ (see equation (1)) because their results show that aquifers with $\varepsilon \geq 1$ still show artifacts of the initial condition at the time of the transition point (when the hydraulic head reaches the aquifer bottom at the upper end of the aquifer). With the earlier described aquifer dimensions, ε already exceeds one at a slope angle of 5°. As can be seen in Figure 2b at the time step t4, artifacts of the initial condition cannot be observed in our results, even though $\varepsilon = 6.25$ at a slope of 15° in this example. Therefore, this suggests that the Hogarth approximation can still be applied even when $\varepsilon > 1$.

Table 2. Estimated Transmissivity (m^2/s) of SRG

Analytical Model	$i = 0°$	$i = 5°$	$i = 10°$	$i = 15°$	$i = 20°$	$i = 25°$
All Data						
Parlange approximation	3.6×10^{-3}					
Brutsaert solution	5.7×10^{-3}	1.5×10^{-3}	8.8×10^{-4}	5.6×10^{-4}	4.5×10^{-4}	3.5×10^{-4}
Hogarth approximation	3.9×10^{-3}	2.1×10^{-3}	1.2×10^{-3}	6.0×10^{-4}	5.1×10^{-4}	3.6×10^{-4}
Winter Recessions						
Parlange approximation	7.0×10^{-3}					
Brutsaert solution	9.0×10^{-3}	6.0×10^{-4}	1.0×10^{-4}	2.1×10^{-4}	1.8×10^{-4}	1.4×10^{-4}
Hogarth approximation	6.0×10^{-3}	6.0×10^{-4}	3.0×10^{-4}	2.0×10^{-4}	1.5×10^{-4}	1.3×10^{-4}

However, note that the offset of the transition point for slopes $>10°$ ($\varepsilon = 4.11$) requires unreasonable aquifer parameters and therefore seems to indicate an upper limit of the Hogarth approximation in this setting. Further investigations are necessary to clarify this.

Although the Brutsaert solution fails to reproduce $b_2 = 1/3$ because of the linearization of the Boussinesq equation [*Stagnitti et al*., 2004; *Bogaart et al*., 2013], it seems more convenient to use the Brutsaert solution at slope angles greater than 10° because the transition from b_1 to b_2 of the numerical model can be reproduced more closely compared to the other analytical models. Note however that using b_2 of the Brutsaert solution as a lower envelope of measured data will lead to a slight overestimation of the transmissivity T. Additionally to the general mathematical uncertainties of the analytical approaches for calculating b_2, a high quality of the discharge data is required, as dQ/dt is getting smaller and might be within the measurement uncertainty of discharge at very low stages. Thus, aquifer parameters related to b_2 are afflicted with a high uncertainty. b_1 on the other hand can be reproduced very accurately by the analytical solutions. The downside of this early time domain is that the initial conditions still have a major impact on the recession behavior and a completely saturated aquifer, as assumed in the analytical models, will not be realistic in most cases. As a consequence, following previous authors [*Mendoza et al*., 2003], the transition point between the early and late time domain is taken into account for shifting the dimensionless recession curves of the Parlange and Hogarth approximations toward the measured data. However, this is complicated by the occurrence of kinematic wave conditions at slope angles greater than 5°. For cases with kinematic wave condition, the exact position of the transition point (the time when the hydraulic head at the end of the aquifer reaches the aquifer bottom) might not be detected because of the chosen measurement interval and measurement errors. Therefore, especially the vertical position of the transition point is challenging to determine. However, because of the minor changes in hydraulic head right before the kinematic wave condition (see Figure 2b, t3), a rough estimation of the vertical position of the transition point is sufficient when this method is used for parameter estimations and it is convenient to specify the transition point at the intersection of the extended b_2 with b_1 (Figure 4).

The illustrating example of the SRG data shows that even though the recession dynamics are not exactly represented by any of the analytical methods, reasonable aquifer parameters are still estimated by shifting the transition point. As a kinematic wave condition can only be observed in the numerical model and the Brutsaert solution at a slope angle greater than 10° and/or a long aquifer length, the absence of a kinematic wave condition in the data of the SRG might suggest that the slope angle and/or the aquifer length is overestimated. It is also possible that the geometry of the effective aquifer resembles a convergent shape rather than the simplified aquifer with parallel sides, as the investigations of *Troch et al*. [2003], *Paniconi et al*. [2003], and *Hilberts et al*. [2004] have shown that the plan shape of the aquifer is also crucial for the discharge behavior and the validity of a kinematic wave assumption. However, as discussed in *Pauwels and Troch* [2010] and *Bogaart et al*. [2013], there are many other factors in natural aquifers that can alter the observed values of b as for example initial conditions, evaporation, interactions with the vadose zone and spatial heterogeneity. In the case of the SRG, in particular, the complex aquifer geometry involving a mixture of multiple slope angles and a presumed heterogeneity of the aquifer might have a strong influence whereas a convergent aquifer shape is not detectable based on geophysical observations [*Winkler et al*., 2014]. Nevertheless, assuming the aforementioned aquifer dimensions and using the analytical models for parameter estimation, the resulting values of transmissivity and aquifer thickness are in a rather narrow range, especially when only the analytical models for sloping aquifers are considered (Brutsaert solution and Hogarth approximation). This range is further minimized when only the winter recession data are considered, as this is less affected by recharge events than the recession periods in other seasons. The resulting parameter estimates are in good agreement with the findings of previous investigations in this area [*Winkler et al*., 2014].

6. Conclusions

Three analytical solutions describing the discharge recession of sloping aquifers are selected to analyze their limitations and accuracies for parameter estimation in alpine settings where high slope angles are common. The application of the selected analytical solutions reveals deviations between the various approaches. The methods mainly differ in the values of b_2, i.e., in the discharge recession after the transition

point, whereas the values of b_1 and the location of the transition point are found to be nearly identical in the Brutsaert solution, the Hogarth approximation, and the numerical model. In contrast, the Parlange approximation exhibits an increasing deviation from the other methods with increasing slope angle. As the recession curve of the Hogarth approximation leads to the closest fit to the numerical model at low slope angles, it is suggested to use this method for mildly sloping aquifers with $i \leq 5°$. The Brutsaert solution is suggested for steeper slope angles ($i > 5°$) because of its ability to simulate a kinematic wave condition that can (potentially) be observed at such slope angles.

As the early recession behavior represented by b_1 may be influenced by the initial condition, differences from the idealized assumption of a fully saturated layer are likely and the location of the transition point between b_1 and b_2 is proposed as the most appropriate approach for inferring the aquifer thickness and hydraulic conductivity. The application of the method is illustrated using spring hydrograph data from a relict rock glacier. Based on the given example, it is recommended to use only the data of the winter recession, as this period is less influenced by minor discharge events compared to the other seasons. The aquifer thickness estimated based on winter recessions is found to be consistent with independent estimates from a geophysical survey, while the estimate obtained by using the lower envelope of all data yields relatively high values.

The numerical model and the Brutsaert solution suggest the occurrence of kinematic wave conditions at the transition point if the slope angle exceeds approximately 5°–10°. This, however, is not evident in hydrograph data analyzed here, although the average surface slope of the relict rock glacier is approximately 15°. As there are many other factors that are influencing the discharge behavior of (sloping) aquifers, this example points out the challenges that can occur during an interpretation when strongly simplified models are applied to complex and heterogeneous aquifer systems. Nevertheless, the estimated effective hydraulic properties are in good agreement to previous investigations.

In summary, it can be concluded that using analytical models with the proposed approach based on the evaluation of the transition point in the recession data is found to be suitable for inferring hydraulic properties even for steeply sloping aquifers. The relict rock glacier examined herein is a typical example of a complex and heterogeneous aquifer in an alpine setting where the application of an analytical solution is rather challenging. Despite these complexities, the approach of focusing on the winter recessions proposed here and using more than one method (multimethod approach) is found to provide reasonable ranges of aquifer properties.

Acknowledgments
The authors are grateful to the Hydrographic Service of Styria for providing the spring discharge data. The data of SRG spring (HZB-number 396762) in Figure 3 are available via the e-mail address wasserhaushalt@bmlfuw.gv.at or the homepage http://ehyd.gv.at/. We appreciate the constructive suggestions of three anonymous reviewers which helped to improve the paper. This study was funded by the European Regional Development Fund (ERDF) and the Federal Government of Styria.

References

Beven, K. (1982), On subsurface stormflow: Predictions with simple kinematic theory for saturated and unsaturated flows, *Water Resour. Res.*, *18*, 1627–1633.

Bogaart, P. W., D. E. Rupp, J. S. Selker, and Y. van der Velde (2013), Late-time drainage from a sloping Boussinesq aquifer, *Water Resour. Res.*, *49*, 7498–7507, doi:10.1002/2013WR013780.

Boussinesq, J. (1877), Essai sur la théorie des eaux courantes, *Mem. Acad. Sci. Inst. Fr.*, *23*, 252–260.

Brutsaert, W. (1994), The unit response of groundwater outflow from a hillslope, *Water Resour. Res.*, *30*, 2759–2763.

Brutsaert, W., and J. P. Lopez (1998), Basin-scale geohydrologic drought flow features of riparian aquifers in the southern Great Plains, *Water Resour. Res.*, *34*, 233–240.

Brutsaert, W., and J. L. Nieber (1977), Regionalized drought flow hydrographs from a mature glaciated plateau, *Water Resour. Res.*, *13*, 637–643.

Henderson, F. M., and R. A. Wooding (1964), Overland flow and groundwater flow from a steady rainfall of finite duration, *J. Geophys. Res.*, *69*, 1531–1540.

Hilberts, A. G. J., E. E. van Loon, P. A. Troch, and C. Paniconi (2004), The hillslope-storage Boussinesq model for non-constant bedrock slope, *J. Hydrol.*, *291*, 160–173, doi:10.1016/j.jhydrol.2003.12.043.

Hogarth, W. L., L. Li, D. A. Lockington, F. Stagnitti, M. B. Parlange, D. A. Barry, T. S. Steenhuis, and J. Y. Parlange (2014), Analytical approximation for the recession of a sloping aquifer, *Water Resour. Res.*, *50*, 8564–8570, doi:10.1002/2014WR016084.

Hunt, R. J., and Feinstein, D. T. (2012), MODFLOW-NWT: Robust handling of dry cells using a Newton formulation of MODFLOW-2005, *Ground Water*, *50*, 659–663, doi:10.1111/j.1745-6584.2012.00976.x.

Kraijenhoff van de Leur, D. A. (1966), Runoff models with linear elements, in *Recent Trends in Hydrograph Synthesis, Versl. en Meded. 13, Tech. Meet. 21*, pp. 31–64, Comm. Hydrol. Onderzoek T.N.O., Netherlands.

Kraijenhoff van de Leur, D. A. (1979), *Rainfall-runoff relations and computational methods, Publ. 16*, pp. 245–320, Int. Inst. For Land Reclam. And Impr., Wageningen, Netherlands.

Malvicini, C. F., T. S. Steenhuis, M. T. Walter, J. Parlange, and M. F. Walter (2005), Evaluation of spring flow in the Uplands of Matalom, Leyte, Philippines, *Adv. Water Resour.*, *28*(10), 1083–1090.

McDonald, M. G., and A. W. Harbaugh (1988), A modular three-dimensional finite-difference ground-water flow model, *U.S. Geol. Surv. Tech. Water Resour. Invest., Book 6, Chap. A1*, 586 pp.

Mendoza, G. F., T. S. Steenhuis, M. T. Walter and J. Y. Parlange (2003), Estimating basin-wide hydraulic parameters of a semi-arid mountainous watershed by recession-flow analysis, *J. Hydrol.*, *279*(1–4), 57–69.

Niswonger, R. G., S. Pandai, and M. Ibaraki (2011), MODFLOW-NWT, a Newton formulation for MODFLOW-2005, *U.S. Geol. Surv. Tech. Methods*, *Book 6*, *Chap. A37*, 44 pp.

Paniconi, C., P. A. Troch, E. E. van Loon, and A. G. J. Hilberts (2003), Hillslope-storage Boussinesq model for subsurface flow and variable source areas along complex hillslopes: 2. Intercomparison with a three-dimensional Richards equation model, *Water Resour. Res.*, *39*(11), 1317, doi:10.1029/2002WR001730.

Parlange, J. Y., M. B. Parlange, T. S. Steenhuis, W. L. Hogarth, D. A. Barry, L. Li, F. Stagnitti, A. Heilig, and J. Szilagyi (2001), Sudden drawdown and drainage of a horizontal aquifer, *Water Resour. Res.*, *37*, 2097–2101.

Pauwels, V. R. N., and P. A. Troch (2010), Estimation of deep aquifer hydraulic conductivity values through baseflow hydrograph rising limb analysis, *Water Resour. Res.*, *46*, W03501, doi:10.1029/2009WR008255.

Polubarinova-Kochina, P. Ya. (1962), *Theory of Groundwater Movement*, translated from Russian, edited by R. J. M. De Wiest, 613 pp., Princeton Univ. Press, Princeton, N. J.

Rocha, D., J. Feyen, and A. Dassargues (2007), Comparative analysis between analytical approximations and numerical solutions describing recession flow in unconfined hillslope aquifers, *Hydrogeol. J.*, *15*, 1077–1091.

Rupp, D. E., and J. S. Selker (2006a), On the use of the Boussinesq equation for interpreting recession hydrographs from sloping aquifers, *Water Resour. Res.*, *42*, W12421, doi:10.1029/2006WR005080.

Rupp, D. E., and J. S. Selker (2006b), Information, artifacts, and noise in dQ/dtQ recession analysis, *Adv. Water Resour.*, *29*(2), 154–160.

Stagnitti, F., L. Li, J. Y. Parlange, W. Brutsaert, D. A. Lockington, T. S. Steenhuis, M. B. Parlange, D. A. Barry, and W. L. Hogarth (2004), Drying front in a sloping aquifer: Nonlinear effects, *Water Resour. Res.*, *40*, W04601, doi:10.1029/2003WR002255.

Szilagyi, J., M. B. Parlange, and J. D. Albertson (1998), Recession flow analysis for aquifer parameter determination, *Water Resour. Res.*, *34*(7), 1851–1857.

Troch, P., E. van Loon, and A. Hilberts (2002), Analytical solutions to a hillslope-storage kinematic wave equation for subsurface flow, *Adv. Water Resour.*, *25*, 637–649, doi:10.1016/S0309-1708(02)00017-9.

Troch, P. A., C. Paniconi, and E. E. van Loon (2003), Hillslope-storage Boussinesq model for subsurface flow and variable source areas along complex hillslopes: 1. Formulation and characteristic response, *Water Resour. Res.*, *39*(11), 1316, doi:10.1029/2002WR001728.

Troch, P. A., A. H. van Loon, and A. G. J. Hilberts (2004), Analytical solution of the linearized hillslope-storage Boussinesq equation for exponential hillslope width functions, *Water Resour. Res.*, *40*, W08601, doi:10.1029/2003WR002850.

Troch, P. A., et al. (2013), The importance of hydraulic groundwater theory in catchment hydrology: The legacy of Wilfried Brutsaert and Jean-Yves Parlange, *Water Resour. Res.*, *49*, 5099–5116, doi:10.1002/wrcr.20407.

Wang, D. (2011), On the base flow recession at the Panola Mountain Research Watershed, Georgia, United States, *Water Resour. Res.*, *47*, W03527, doi:10.1029/2010WR009910.

Winkler, G., A. Kellerer-Pirklbauer, and M. Pauritsch (2012), Reliktische Blockgletscher—Grundwasserkörper in alpinen, kristallinen Einzugsgebieten, *Beitr. Hydrogeol.*, *59*, 119–137.

Winkler, G., M. Pauritsch, T. Wagner, A. Kellerer-Pirkelbauer, M. Avian, and S. Hergarten (2014), *EFRD-Project—Groundwater storage and discharge dynamics of relict rock glaciers*, Univ. of Graz, Graz, Austria. [English translation.]

7.3. Publication III

Pauritsch M, Wagner T, Winkler G, Birk S (accepted) Investigating groundwater flow components in an Alpine relict rock glacier (Austria) using a numerical model. Hydrogeology Journal, doi: 10.1007/s10040-016-1484-x.

Investigating groundwater flow components in an Alpine relict rock glacier (Austria) using a numerical model

Marcus Pauritsch[1]*, Thomas Wagner[2], Gerfried Winkler[2], Steffen Birk[2]

[1] Tannhofweg 14/8, 8044 Graz, Austria;

[2] Institute of Earth Sciences, NAWI Graz Geocenter, University of Graz, Heinrichstrasse 26, 8010 Graz, Austria; marcus.pauritsch@edu.uni-graz.at, thomas.wagner@uni-graz.at, gerfried.winkler@uni-graz.at, steffen.birk@uni-graz.at

*Corresponding author: marcus.pauritsch@edu.uni-graz.at; phone +43 69915018727

Abstract

Relict rock glaciers are complex hydrogeological systems that might act as relevant groundwater storages. Therefore, the discharge behavior of these alpine landforms needs to be better understood. Hydrogeological and geophysical investigations at a relict rock glacier in the Niedere Tauern Range (Austria) reveal a slow and fast flow component that appear to be related to the heterogeneous structure of the aquifer. A numerical groundwater flow model was used to indicate the influence of important internal structures such as layering, preferential flow paths and aquifer-base topography. Discharge dynamics can be reproduced reasonably by both introducing layers of strongly different hydraulic conductivities or by a network of highly conductive channels within a low-conductivity zone. Moreover, the topography of the aquifer base influences the discharge dynamics, which can be observed particularly in simply structured aquifers. Hydraulic conductivity differences of three orders of magnitude are required to account for the observed discharge behavior: a highly conductive layer and/or channel network controlling the fast and flashy spring responses to recharge events, as opposed to less conductive sediment accumulations sustaining the long-term base flow. The results show that the hydraulic behavior of this relict rock glacier and likely that of others can be adequately represented by two aquifer components. However, the attempt to characterize the two components by inverse modeling results in ambiguity of internal structures when solely discharge data are available.

Keywords: relict rock glacier; Austria; groundwater flow; hydraulic properties; numerical modeling

1. Introduction

Mountainous and, in particular, alpine groundwater is contributing significantly to the stream flow of rivers in valleys and consequently in the foreland (e.g., Campbell et al. 1995; Clow et al. 2003; Tague and Grant 2009; Muir et al. 2011; Welch et al. 2012). With increasing population and propagation of tourist industries and recreational activities in mountainous areas, knowledge of the hydraulic behavior and storage capacities of mountainous aquifers is getting more important for sustainable water resources management as well as for predicting natural hazards as for example flash floods and debris flows (e.g. Lauber et al. 2014).

Especially in alpine catchments of crystalline regions, a major portion of the groundwater contributing to the streamflow originates from debris accumulations such as moraines and rock glaciers (e.g., Hood and Hayashi 2015, Wagner et al., 2016). While the hydrogeology of moraines, talus and hillslope aquifers is subject of intensive investigations (e.g., Clow et al. 2003; Roy and Hayashi 2009; Muir et al. 2011), knowledge about the hydraulic behavior and storage capacities of rock glaciers is sparse (Krainer and Mostler 2002; Krainer et al. 2007; Millar et al. 2013; Winkler et al. 2016a). Nevertheless, rock glaciers are common landforms all around the globe in mountainous areas and at high latitudes. For instance, in the Austrian Alps, Kellerer-Pirklbauer et al. (2012) and Krainer and Ribis (2012) have identified a total of 4792 rock glaciers covering an area of about 286 km². Bollmann et al. (2012) identified 1697 rock glaciers in the South Tyrolean Alps in Italy and Schmid et al. (2015) used Google Earth to map 702 rock glaciers in selected areas of the Hindu Kush Himalayan region. Therefore, rock glaciers have a high potential to influence the discharge behavior of rivers downstream of their catchments (Wagner et al. 2016).

Rock glaciers in general are scree masses that are supersaturated with ice and gravitationally move downslope with velocities of a few centimeters up to several meters per year (e.g., Barsch 1996; Haeberli et al. 2006). The size and shape of rock glaciers depends on climatic conditions, cirque geometry and debris supply of the comprising headwalls (Degenhardt 2009). Therefore, the range in size is highly variable (e.g., Kellerer-Pirklbauer et al. 2012; Krainer and Ribis 2012). The thickness of rock glaciers depends among other things on the topography of the underlying bedrock/base and is a priori difficult to estimate. However, previous investigations reported thicknesses in the order of several tens of meters (e.g., Krainer et al. 2015; Monnier and Kinnard 2015, Winkler et al. 2016a). Rock glaciers can be classified into active (currently moving), inactive (no movement, but ice is present) and relict forms (no ice mass and no movement). Active and inactive rock glaciers can also be summarized to intact rock glaciers, as both types contain ice in contrast to relict rock glaciers,

where ice has melted and morphological structures such as ridges and furrows might become more obvious.

Investigations of rock glaciers mainly focus on the distribution, movement and the inner structure of intact rock glaciers (e.g., Haeberli et al. 2006; Jansen and Hergarten 2006; Leopold et al. 2011; Monnier et al. 2011). Monnier and Kinnard (2015) investigated the internal structure of an active rock glacier in the Dry Andes with ground penetrating radar. Their results suggest a heterogeneous structure with an upper and lower ice-rich layer and an intermediate zone with a high fraction of liquid water. Additionally, their results show inner structures in the form of upward-dipping reflectors caused by the movement of the rock glacier. Krainer et al. (2015) investigated an active rock glacier in the Italian Alps. They also identified a layered structure at two drill core sites on the rock glacier. Relict rock glaciers are often used as an indicator of previous permafrost conditions for climate studies (e.g., Hughes et al. 2003; Matthews et al. 2015), but their inner structure and hydraulic properties are largely unknown. Recently, Winkler et al. (2016a) performed hydrogeological investigations at the relict Schöneben rock glacier located in the Austrian Eastern Alps (hereinafter referred to as SRG), describing its storage and flow components by using data of the spring hydrograph as well as natural and artificial tracers and geophysical surveys. They suggest that the rock glacier is a heterogeneous aquifer with a layered internal structure. Their investigation further suggests that there is a rather thin (approximately 10 m) layer at the base of the relict rock glacier, which consists of silty or fine sand material providing a considerable storage capacity controlling the base flow observed at the rock glacier spring (see Fig. 9 in Winkler et al., 2016a). This layer is supposed to represent glacial sediment deposits (probably morainic sediments), which would be in agreement with the findings at an active rock glacier, where moraine deposits have been encountered in two drill cores at its base (Krainer et al. 2015). The hydraulic properties of the layer at the base of the Schöneben rock glacier were additionally estimated by Pauritsch et al. (2015) using analytical models of sloping aquifers by focusing on winter base flow data. The derived hydraulic conductivity in the order of 10^{-5} m/s is consistent with findings of Winkler et al. (2016a). The upper layers of the relict rock glacier likely consist of coarser material with a higher permeability that may explain the rapid response of the spring to recharge events. They can be activated when the lower layer is saturated or simply due to the differences of hydraulic conductivity (Winkler et al. 2016a). Another explanation might be the existence of preferential flow paths. Preferential flow paths related to cracks in the soil and roots of plants have been observed at hillslopes (e.g., Graham et al. 2010). Similarly, rapid localized flow through solution conduits is well known from karst aquifers (e.g., Worthington 2009). In this paper the term „preferential flow paths" refers to channel flow (and not layer-controlled flow). In rock glaciers preferential flow might be possible through washed-out

channels within an otherwise fine-grained layer. The existence of such channels is suggested by excavations at a relict rock glacier nearby the SRG (Untersweg and Proske 1996).

At present, a large portion of the rock glaciers are relict forms, and considering climate change (global warming) it can be assumed that today's intact rock glaciers will in future become relict ones, too. Therefore, knowledge about the hydrogeological properties of relict rock glaciers is essential for predicting future changes in the discharge behavior of rivers in alpine catchments which currently contain intact rock glaciers.

Simple lumped-parameter models are able to satisfyingly simulate the discharge behavior of complex aquifers and even of this particular relict rock glacier (Wagner et al., 2016). But they cannot be used to investigate and distinguish between different types of heterogeneity related to the internal structure (e.g., layered structure or preferential flow paths). To resolve such a task, a distributed numerical model is preferable. Numerical models have been extensively used during the last decades and represent a helpful tool for estimating aquifer parameters (Carrera et al. 2005) and also help to improve the conceptual understanding of a hydrogeological setting (e.g., Eisenlohr et al. 1997a,b; Mansour et al. 2012). Thus, in this paper the current conceptual understanding regarding the drainage processes within the relict Schöneben rock glacier (Winkler et al. 2016a) is tested using a three-dimensional numerical groundwater flow model. The main purpose of this paper is to indicate the major features of the internal structure (layering, draining channels, topography) controlling the discharge behavior of the relict rock glacier and to compare them with the current conceptual understanding. To this end, several model runs with increasing complexity are provided. As there are no boreholes or other information about groundwater heads, only the discharge of the draining spring is used for calibration. Due to these limitations, the attention is turned towards reproducing the discharge dynamics in general rather than the observed discharge exactly.

2. Field site and data set

The investigation area in this research is the relict Schöneben rock glacier (SRG) located in the Niedere Tauern Range in Austria at E14°40'25'' and N47°22'39'' (see inlet of Fig. 1). The SRG is situated in a northeast-facing alpine cirque which also represents the hydrological catchment of the SRG, covering an area of 0.67 km² with a maximum elevation of 2295 m a.s.l. The elevation of the tongue-shaped SRG ranges from 1715 m a.s.l. to 1912 m a.s.l., it has a length of about 750 m, a maximum width of about 250 m, and covers an area of 0.11 km² (Fig. 1). The surface of the SRG is covered by coarse-grained, blocky material consisting of gneissic rocks ranging from cubic decimeters

to a few cubic meters. The characteristic morphology with distinct collapse structures (i.e., caused by the melting of the ice and the resulting loss in volume), the partial vegetation cover (mainly grasses and dwarf pines) and the low slope gradient of the rock glacier front indicate that the SRG can be assumed to be a relict rock glacier. This is supported by an average water temperature above 2.2 °C at the spring emerging at the front of the rock glacier (Kellerer-Pirklbauer et al. 2015; Winkler et al. 2016a).

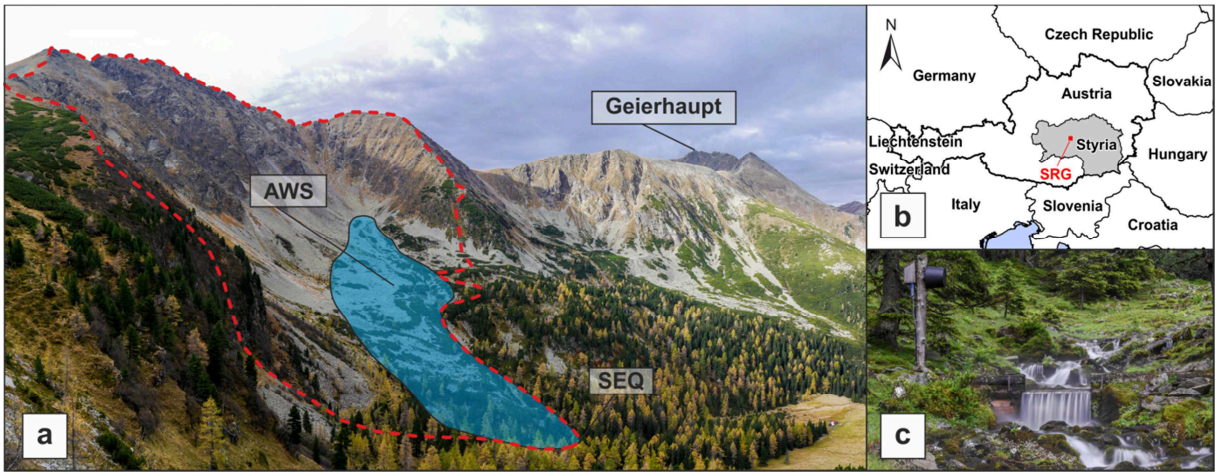

Fig.1: Field site impression of the Schöneben Rock Glacier (SRG) catchment. (a) Overview of the investigation area with the SRG highlighted in blue and the hydrological catchment delineated with a red dashed line; *AWS* = automatic weather station; *SEQ* = rock glacier spring; *Geierhaupt* = highest peak in the surroundings (2417 m a.s.l.); (b) location of SRG within Austria and Styria; (c) rectangular notch weir situated about 40 m downstream of *SEQ*.

Steep rock faces surround the rock glacier in the eastern, southern and western area with talus slopes situated between the rock faces and the SRG itself (Fig. 1a). The catchment is drained by one large spring (hereinafter referred to as SEQ) located directly at the front of the SRG (Fig. 1).

The SEQ is a spring belonging to the official spring network of the Hydrographic Service of Styria (HZB-number 396762). The stage is continuously monitored at a rectangular notch weir situated about 40 m downstream of the spring. Stage data are available since July 2002 and are recorded in hourly intervals. Individual discharge measurements (using the salt dilution method) are used to relate the monitored stage to the actual discharge. Precipitation is continuously monitored at an automatic weather station located directly at the SRG at 1822 m a.s.l. (AWS, see Fig. 1a). Precipitation data are available since November 2011, recorded in hourly time steps.

3. Model setup

The groundwater model is implemented in MODFLOW (McDonald and Harbough 1988) using the NWT solver (Niswonger et al. 2011; Hunt and Feinstein 2012), which employs a Newton-Raphson solution with improved handling of dry cells. This is an important feature as the topography of the investigation area is showing a high relief, frequently causing the upper cells to fall dry. The application of other solvers, for example the PCG2 solver combined with a rewetting package, may result in an unstable model that often fails to converge.

The model domain covers an area of 225,300 m² and is set up with uniform cell sizes of 10 m x 10 m in 66 columns and 80 rows. As there is no actual boundary between the SRG and the talus slopes but rather a smooth transition, the SRG and the talus slopes are assumed to form one merged aquifer system (z1 in Fig. 2). The boundaries of the numerical model are therefore chosen to be beyond the actual boundaries of the SRG to include the adjacent talus slopes to the east and south. The boundary conditions (except for the spring and the top of the active cells) are set to no-flow boundaries as the groundwater flow through the bedrock is assumed to be negligible. Surface elevation data are adopted from a downsampled digital elevation model (DEM) with a resolution of 10 m (based on the chosen MODFLOW cell sizes) based on airborne laser scan data (ALS) with a resolution of 1 m provided by the GIS Service of the government of the federal state of Styria (GIS Steiermark). Elevation data of the underlying bedrock are based on a digital elevation model resulting from geophysical surveys on the SRG (Fig. 2a) comprising seismic refraction investigations along three profiles (Winkler et al. 2016a) and ground penetrating radar (GPR) investigations along eight profiles (two additionally available profiles are not used herein as one of them lies outside the model area and the other is discarded due to poor data quality; see Winkler et al. 2016b). Interestingly, the results of the geophysical surveys show that the thickness of the SRG is increasing towards the southeast at the transition to the talus slopes. As the geophysical investigations did not capture the full extent of the aquifer in this part, the aquifer thickness in this area is subject to a high degree of uncertainty. Therefore, two approaches were applied to determine the geometry of the aquifer base. In a first approach the slopes of the rock faces located above the talus slopes are extrapolated below the surface and intersected with the elevation of the bedrock at the last point of the geophysical investigation profile. Including these extended profiles, the depth of the bedrock is interpolated using kriging with the software Surfer (Fig. 2b). The alternative approach uses a linear extrapolation of the geophysical profiles, i.e. the depth is assumed to decrease linearly from the last point of the profile towards the upper end of the debris slope (Fig. 2c).

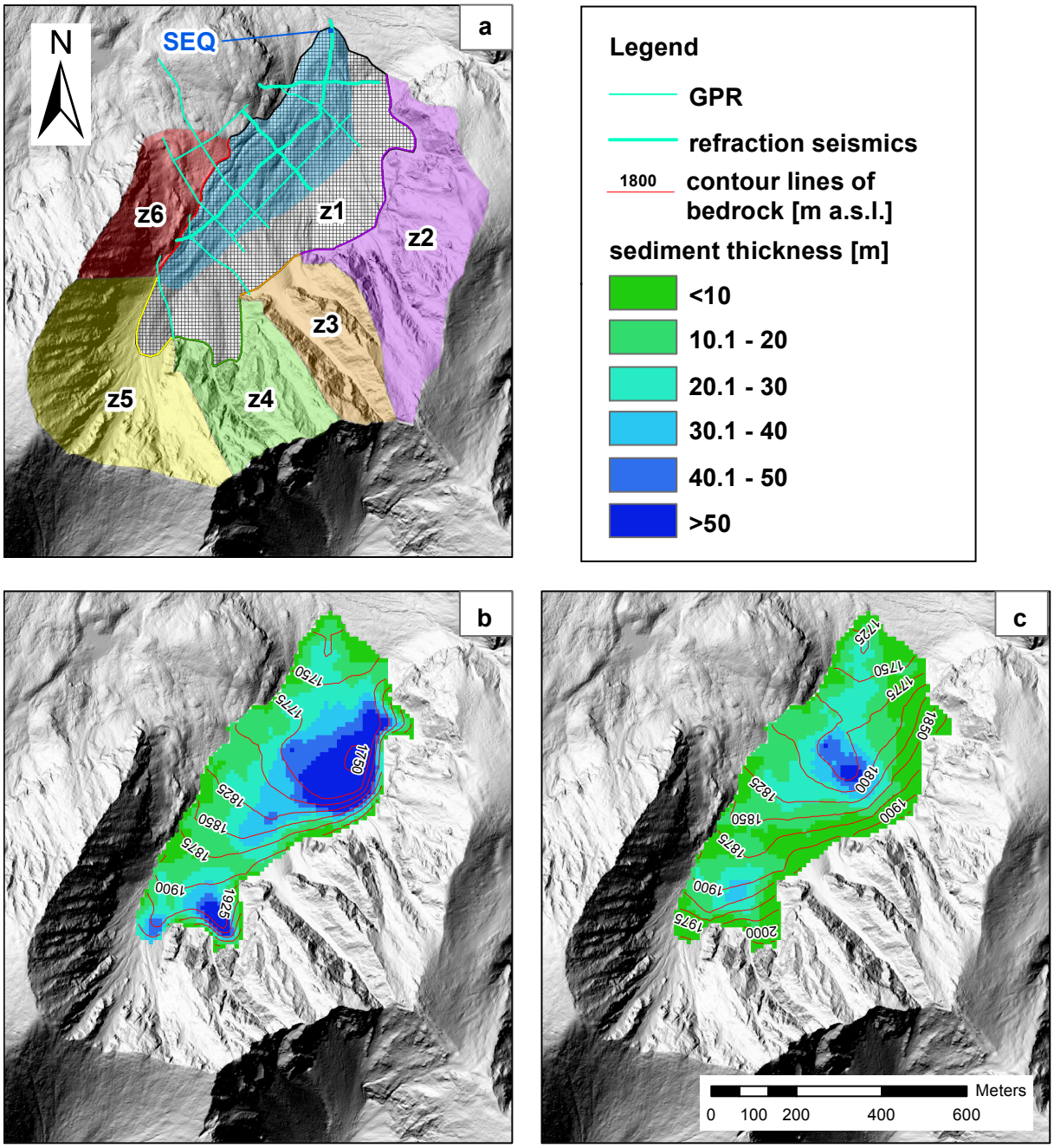

Fig. 2: SRG catchment with model area. (a) *Cell grid* and recharge zones (*z1-z6*) with corresponding input cells (*color-coded*); delineation of the actual SRG within the model area highlighted as *blue polygon* (see Fig. 1); profiles of geophysical investigations and constant-head cell at the spring (*SEQ*); (b) *Color-coded* sediment thickness; *contour lines* indicate the aquifer base topography based on geophysical data and extrapolated rock faces; (c) *Color-coded* sediment thickness; *contour lines* indicate an alternative aquifer base topography based on geophysical data and linearly decreasing depth towards the boundary.

It is assumed that there is no significant groundwater flow between the SRG catchment and its adjacent catchments because of the compact gneissic geology and the steep relief. Moreover, groundwater storage is assumed to occur only where unconsolidated rocks are present (scree and, especially, in the relict rock glacier itself). Bare rocks and steep cliffs are assumed to have negligible storage capacities. Also, the potential storage in the bedrock is assumed to be of minor importance as no considerable weathering zone is observable.

The recharge to the rock glacier aquifer is determined based on precipitation data from the automatic weather station located on the SRG (AWS in Fig. 1a) and an estimated evapotranspiration. The actual evapotranspiration is computed using an estimate of potential evapotranspiration based on Thornthwaite (1948) as input for a soil water balance model at a daily time step as described, e.g., by Peters et al. (2005). A relatively low value of 20 mm is used for the soil moisture storage at field capacity because the surface of the investigation area is mostly covered by coarse rock debris. Moreover, the application of a simple lumped-parameter model indicated a minor role of the soil moisture accounting store (Wagner et al. 2016). The actual evapotranspiration is assumed to be equal to potential evapotranspiration if the soil moisture storage amounts at least to 70 % (14 mm) of the field capacity; below this value actual evapotranspiration is linearly decreased towards zero. Recharge occurs if the net inflow (precipitation minus actual evapotranspiration) to the soil moisture storage causes an exceedance of field capacity (time series is shown in Fig. 3).

The resulting direct recharge (i.e., precipitation falling directly onto the surface of z1 (Fig. 2a), 31 % of the total catchment area) is distributed homogeneously across the model. The recharge from the surrounding rock faces of the hydrological catchment primarily consists of surface runoff and is added to the recharge of the peripheral cells, proportional to the area percentage of the respective subcatchment (Fig. 2a). The areal percentages are 19 %, 10 %, 11 %, 20 % and 9 % for the recharge zones z2, z3, z4, z5, and z6, respectively.

The parameter estimation software PEST (Doherty 2013) is employed for automatic calibration of the groundwater models. The hydraulic conductivity and the specific yield of specified groups of cells are treated as calibration parameters. According to the assumed plausibility of the parameter values and (in the case of the upper limit of hydraulic conductivity) to avoid model instabilities, parameter ranges between $1x10^{-2}$ and $1x10^{-7}$ m/s as well as 0.1 and 0.3 were defined for hydraulic conductivity and specific yield, respectively. The specific storage is defined as a constant value of $1x10^{-4}$ 1/m. As there are no boreholes or other information about groundwater levels, the model has to be calibrated solely to the discharge of the spring (SEQ). During calibration the discharge is weighted inversely proportional to the observed values (Doherty 2013) in order to compensate for the high

variability of discharge (Winkler et al. 2016a). The simulation is restricted to time periods when melting snow can be neglected in order to avoid the uncertainties involved in modeling the snow melt. Therefore the model is calibrated using the hydrograph of the SEQ in the time period from 25 June 2013 to 14 March 2014 (263 days; see Fig. 3a). This year is chosen because it has three distinct recharge events following a long dry period, whereas the hydrograph recession of most other years is interrupted by several smaller recharge events which complicate the interpretation. The transient simulation comprises 151 stress periods and a total of 8321 time steps with a steady-state water table as initial condition. The stationary boundary conditions are defined as constant recharge (distributed on the six recharge zones (z1-z6); Fig. 2). The total recharge rate is thereby specified to be equal to the measured discharge at the beginning of the simulation period. In the time period from days 127 to 150, minor snowfall events occurred according to observations from an automatic digital camera monitoring the area. Because the precipitation was stored temporarily in the snow cover, the recharge occurred delayed (compared to the precipitation records at the automatic weather station) when the snow melted in the following days. As this delay is not considered in the recharge model, this time period is given only 10 % weight in the calibration. Moreover, the first 45 days of the simulation are regarded as a warm-up period (potentially affected by the initial condition) and the discharge data during that time are not used at all for calibration. Special attention is given to the accurate simulation of the winter base flow, as this time period remains unaffected by recharge events, and therefore groundwater flow components other than the base flow can be neglected. Thus, the weight in the calibration during this time period is multiplied by a factor of 10. The goodness-of-fit of the model results is analyzed using the root-mean-square error (RMSE), the weighted root-mean-square error (RMSEw) (see table 1) and visual inspection of the simulated versus the observed discharge time series (neglecting the warm-up period). The model is verified by simulating the time period of 21 July 2012 to 15 April 2013 (269 days; see Fig. 3b). This time period also exhibits a winter base flow without intermediate recharge events (see Winkler et al. 2016a), and pictures of the automatic digital camera are available to identify snowfall events (Wagner et al., 2016).

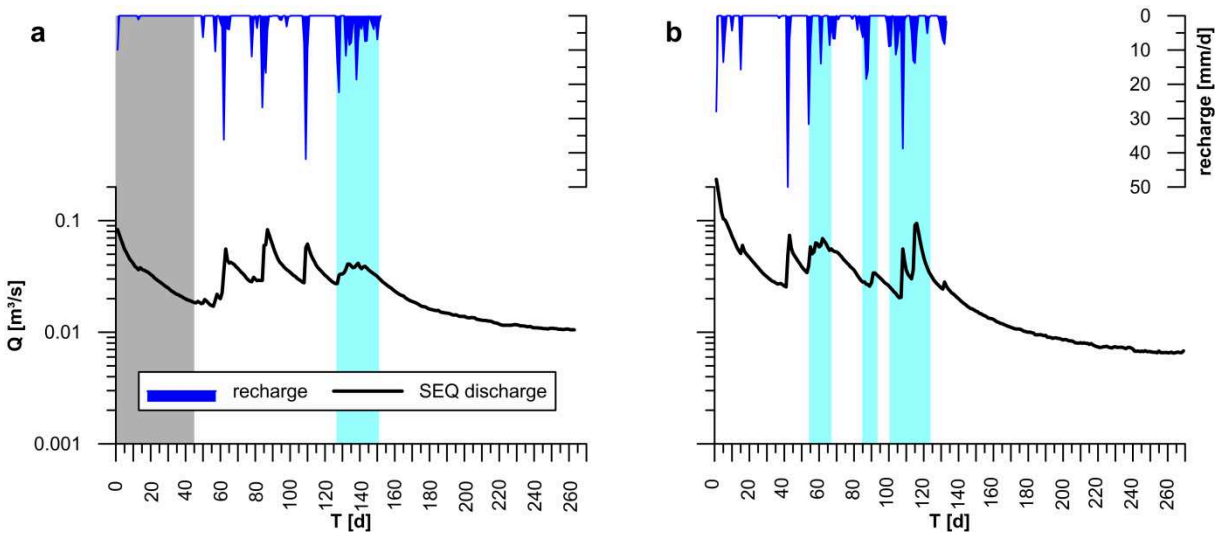

Fig. 3: *Recharge* and *discharge* (*Q*) time series of (a) the calibration period and (b) the verification period. The *grey area* marks the warm-up period. The *light blue areas* mark time periods with snow influence. *T* = Time

In order to investigate the effects of different kinds of internal structures of the SRG and, moreover, to verify the current conceptual understanding of groundwater flow processes in relict rock glaciers, several scenarios (i-viii) with increasing complexity are simulated and compared to each other. For these eight scenarios the aquifer base topography with extrapolated rock faces (Fig. 2b) is applied. The model setups of the investigated scenarios in this research can be grouped in laterally homogeneous (i – iv) and heterogeneous (v - viii) models which are presented in Fig. 4. The laterally homogeneous scenarios contain models with one (i), two (ii and iii) or three (iv) layers with different hydraulic parameters for each layer. The thickness of the lower layer in (ii) and (iii) covers 20 % and 80 % of the total aquifer thickness at each cell, respectively. In scenario (iv) the layered structure of the SRG is further refined by subdividing the lower layer of (ii) into two layers, each covering 10 % of the total aquifer thickness. A thin lower layer is in accordance with the current conceptual understanding of the relict SRG (Winkler et al. 2016a). Note that the upper two layers presented in Fig. 9 of Winkler et al. (2016a) are not further distinguished in the numerical models as these two layers are, compared to the lower layer, rather similar and highly conductive. Results of seismic refraction surveys showed a maximum total thickness of the rock glacier of more than 50 m (Fig. 2). However, the saturated zone was not detectable because a “blind zone” with a thickness of 19 m is possible with the applied setup of the geophysical survey, meaning that a saturated layer with a thickness of up to 19 m could have been missed in the survey (Winkler et al. 2016a and b).

In the laterally heterogeneous scenarios a zone with higher hydraulic conductivity is introduced to models with one (v, vi) or two layers (vii, viii). This represents a washed-out channel (according to field observations/excavations from a nearby relict rock glacier; Untersweg and Proske 1996) or channel network which is lacking fine-grained material and is embedded in a less permeable (fine-grained) matrix. The orientation of the channels is defined to follow the topography of the model base and to connect the spring with one (v, vii) and five (vi, viii) dominant gullies from outside the model area (see Fig. 2). In the two-layered scenarios (vii, viii), the channel and channel network are introduced to the lower layer (model runs with channels in both layers did not change the results). During calibration, the channel network is treated as one zone in order to minimize the number of adjustable parameters. A test run of model (vi) where the hydraulic parameters of the channels were individually calibrated has shown to have a nearly identical discharge behavior as one where channels were calibrated as a single zone due to a narrow range of calibrated hydraulic conductivity in the individual channels (not shown here).

Furthermore, three models (ii-a), (vi-a) and (viii-a) are presented with setups equivalent to models (ii), (vi) and (viii), but with an alternatively shaped aquifer base topography (Fig. 2c). These models are aimed to investigate to what degree the discharge behavior of the spring is affected by the morphology of the base both without and with a draining channel network.

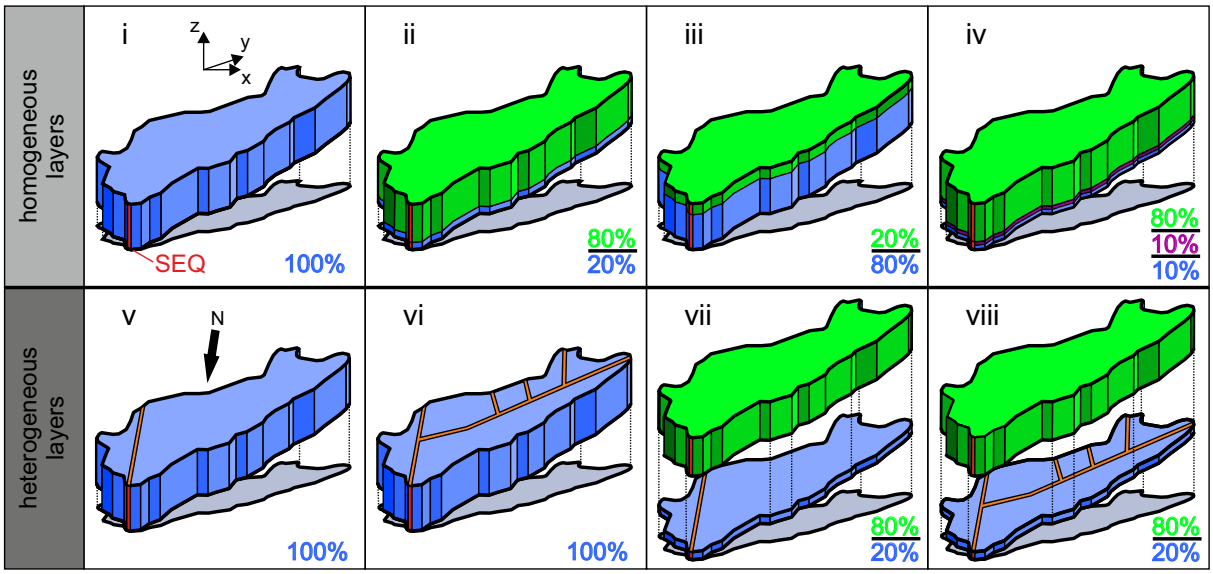

Fig. 4: Three-dimensional sketches of the investigated internal structures of the model. *Colors* indicate zones with uniform hydraulic parameters within one scenario. *Percentages* indicate the thickness of layers. *Red bars* indicate the outflow cell (*SEQ*). Note that the actual surface and aquifer base topography is not represented here for more clarity of the sketch; color codings (e.g., *blue colors* in (i) and (v)) do not necessarily represent similar hydraulic parameters.

4. Results

The comparisons of the simulated to the measured discharge of the SEQ in the calibration and verification periods are presented in Figs. 5 and 6. The estimated aquifer parameters and the goodness-of-fit measures RMSE and RMSEw are presented in table 1. Some deviation between simulated and observed discharge is expected in the time period from days 127 to 150 that was less weighted in the calibration, as the recharge was affected by snow fall and snow melt processes that are not considered by the model. As a consequence, the observed discharge dynamics are not well reproduced within this period, and therefore are not further discussed. Nevertheless, the following winter base flow recession appears to be largely unaffected by these short-term effects. Likewise, several snowfall and melting events occurred during the time period used for verification between days 50 and 120 (Figs. 5 and 6), resulting in delayed responses of SEQ and/or overestimated recharge as precipitation at least was partially stored in the snow cover.

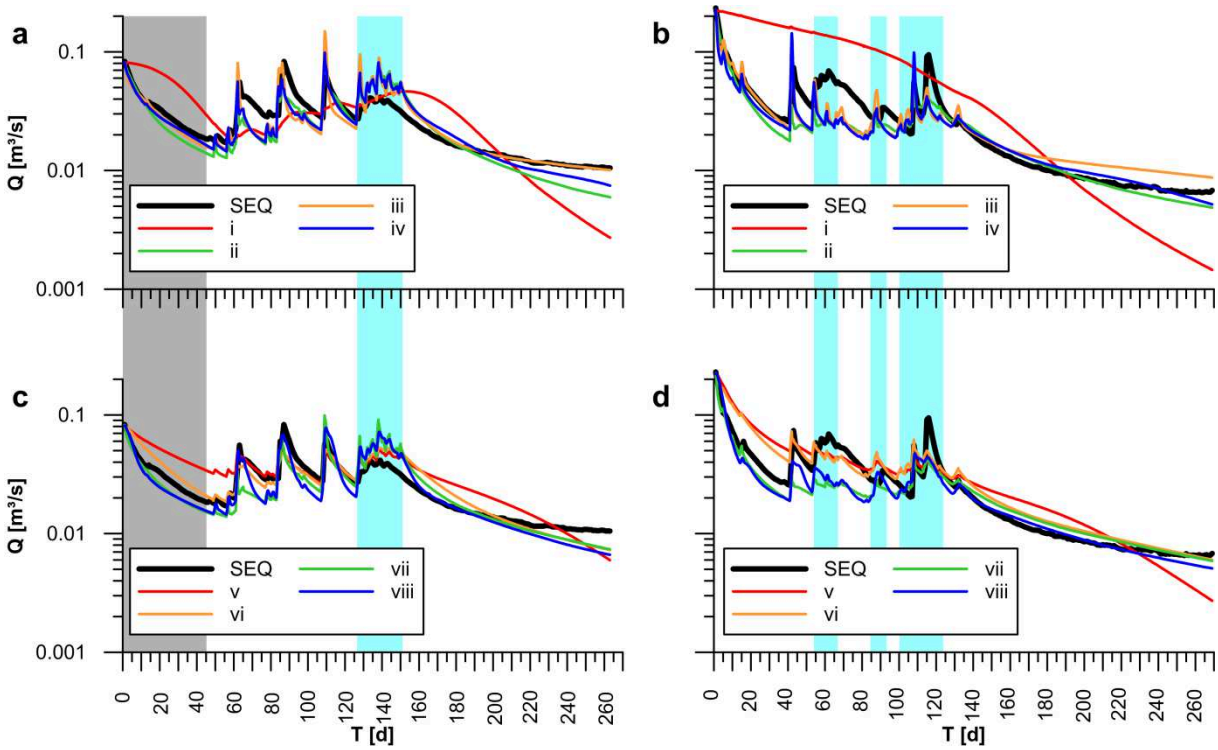

Fig. 5: Hydrographs of the investigated model scenarios compared to the observed data of *SEQ*. The *grey area* marks the warm-up period. The *light blue areas* mark time periods with snow influence. (a) and (b) show the scenarios with homogeneous layers (models i-iv in Fig. 4) for the calibration (25 June 2013 to 14 March 2014) and verification (21 July 2012 to 15 April 2013) time period, respectively. (c) and (d) show the scenarios with heterogeneous layers for the calibration and verification time period, respectively (models v-viii in Fig. 4).

Using the aquifer base topography of Fig. 2b, the results of the laterally homogeneous scenarios (Fig. 5a and b) show that the single-layered scenario (i) visually has a very poor fit. This is supported by the goodness-of-fit measures presented in table 1. This scenario obviously fails to reproduce the discharge behavior of the SEQ, which is characterized by sharp peaks after recharge events and a slowly decreasing base flow. The introduction of a second homogeneous layer in the scenarios (ii) and (iii) greatly improves the model fit. Nevertheless, it can be seen that in (ii) the short-term recessions after recharge events as well as the winter base flow recessions are too fast and that the absolute value of discharge is too low between the recharge events and during the winter base flow. Scenario (iii) shows that with a thick lower layer the absolute value of discharge between the recharge events is closer to the observed values. The thick lower layer also leads to higher hydraulic heads and an improved fit of the winter base flow recession in the calibration (Fig. 5a, RMSEw in Table 1) but overestimates the base flow in the verification time period (Fig. 5b). The introduction of

a third layer in (iv) leads to similar discharge dynamics compared to (ii), with similar discharge peaks but a slightly slower base flow recession. In general, the estimated aquifer parameters show a high hydraulic conductivity for the upper layer and a lower hydraulic conductivity in the lower layer (table 1) with the single-layered scenario (i) showing intermediate values. Interestingly, calibration of (iv) results in a very low conductivity middle layer that acts as a barrier between the higher conductivity upper and lower layers.

Table 1: Estimated hydraulic parameters of the investigated scenarios and goodness-of-fit measures for the calibration period. *HC*=hydraulic conductivity; *SY*=specific yield; subscripts: *u*=upper-, *m*=middle-, *l*=lower layer, *c*=channel; *RMSE*=unweighted root-mean-square error; *RMSEw*=weighted root-mean-square error.

Scenario	HC_u [m/s]	HC_m [m/s]	HC_l [m/s]	HC_c [m/s]	SY_u [-]	SY_m [-]	SY_l [-]	SY_c [-]	RMSE [m³/s]	RMSEw [m³/s]
i	$3.67x10^{-4}$	-	-	-	0.30	-	-	-	$1.41x10^{-2}$	$8.70x10^{-3}$
ii	$5.33x10^{-3}$	-	$4.93x10^{-5}$	-	0.10	-	0.30	-	$1.40x10^{-2}$	$4.01x10^{-3}$
iii	$1.00x10^{-2}$	-	$1.22x10^{-5}$	-	0.21	-	0.10	-	$1.78x10^{-2}$	$2.46x10^{-3}$
iv	$8.00x10^{-3}$	$8.00x10^{-7}$	$1.70x10^{-4}$	-	0.10	0.30	0.30	-	$1.38x10^{-2}$	$3.17x10^{-3}$
v	$2.72x10^{-5}$	-	-	$1.00x10^{-2}$	0.10	-	-	0.10	$9.32x10^{-3}$	$5.53x10^{-3}$
vi	$9.67x10^{-5}$	-	-	$1.00x10^{-2}$	0.17	-	-	0.10	$8.78x10^{-3}$	$3.87x10^{-3}$
vii	$8.61x10^{-3}$	-	$3.54x10^{-5}$	$2.13x10^{-3}$	0.10	-	0.30	0.19	$1.44x10^{-2}$	$3.08x10^{-3}$
viii	$2.61x10^{-3}$	-	$2.60x10^{-6}$	$2.01x10^{-3}$	0.22	-	0.30	0.30	$1.14x10^{-2}$	$3.08x10^{-3}$
ii-a	$2.02x10^{-3}$	-	$7.27x10^{-6}$	-	0.30	-	0.30	-	$1.33x10^{-2}$	$4.49x10^{-3}$
vi-a	$7.18x10^{-7}$	-	-	$1.00x10^{-2}$	0.17	-	-	0.10	$1.14x10^{-2}$	$2.66x10^{-3}$
viii-a	$3.97x10^{-3}$	-	$7.29x10^{-6}$	$1.59x10^{-3}$	0.30	-	0.30	0.30	$1.30x10^{-2}$	$4.00x10^{-3}$

It can be seen in Figs. 5c and 5d that the introduction of a draining channel to a single-layered model in (v) is not sufficient to represent the fast flow component of the SRG (see also Table 1). The discharge recession is generally too slow, resulting in overestimated discharge during base flow. Interestingly, the discharge recession during the winter base flow shows a further decrease after approximately 200 days. At that time the upper part of the aquifer has fallen dry and the drying front has advanced to the area where a relatively flat basin is present in the east (see Fig. 2b). The model

fit improves by extending the channel to a channel network in scenario (vi). However, the simulated discharge also shows deviations to the measured discharge of the SEQ. While the peaks of the major recharge events in the calibration period are close to the observed data, the discharge response to small recharge events appears too sharp and overestimated. Furthermore, similar to most of the aforementioned scenarios, the long-term winter base flow is underestimated, i.e., the simulated discharge recession is too fast. In the verification period the simulated winter base flow is close to that of the SEQ, but the discharge dynamics of the preceding time period are not well matched. The scenarios (vii) and (viii) represent two-layered versions of (v) and (vi), respectively, in which the channel and the channel network is only present in the lower layer (see Fig. 4). The hydrograph of (vii) is similar to that of (ii), indicating that the upper layer is dominating the quick flow component rather than the channel. The channel network of (viii) obviously has a larger influence than the single channel in (vii) and results in a quickly responding hydrograph but with broad peaks (resulting in a slightly better RMSE, but identical RMSEw, Table 1). Moreover, the base flow between the recharge events and the winter base flow recession are similar to the layered scenarios (ii, iii and vii).

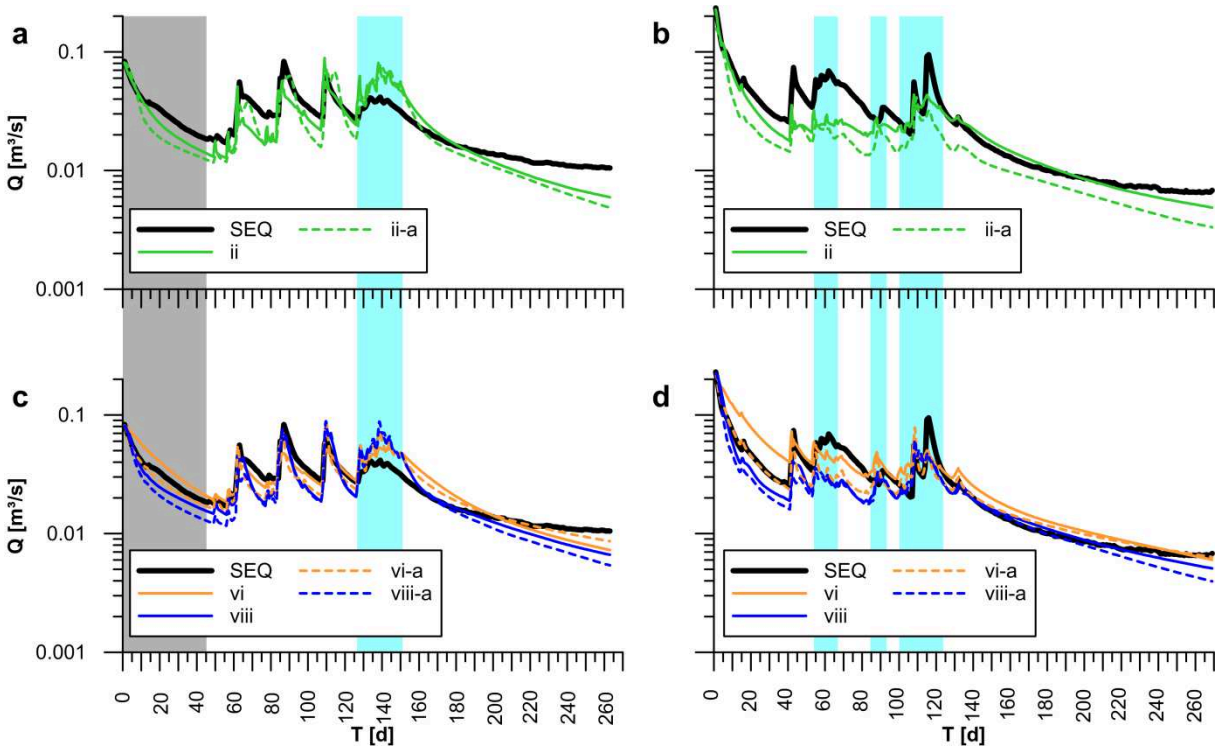

Fig. 6: Hydrographs of the investigated model scenarios compared to the observed data of *SEQ*. The *grey area* marks the warm-up period. The *light blue areas* mark time periods with snow influence. (a) and (b) show a comparison of laterally homogeneous layered scenarios with differently shaped topography of the model base for the calibration (25 June 2013 to 14 March 2014) and verification (21 July 2012 to 15 April 2013) time period, respectively (*solid line*=extrapolated rock faces (see Fig. 2b); *dashed line*=linearly decreasing depth towards boundary (see Fig. 2c). (c) and (d) show a comparison of two laterally heterogeneous layered scenarios with differently shaped topography of the model base for the calibration and verification time period, respectively (*solid lines*=extrapolated rock faces (see Fig. 2b); *dashed lines*=linearly decreasing depth towards boundary (see Fig. 2c).

Examining the results of the scenarios using the alternatively shaped model base (Fig. 2c) shows that the topography of the base has some influence on the discharge behavior of the homogeneous layered model. As it can be seen during the calibration (Fig. 6a), (ii-a) shows double peaks at the major recharge events. In the verification time series (Fig. 6b) the double peaks cannot be observed and the discharge dynamics of (ii-a) appear more realistic than (ii), although the absolute discharge is underestimated. Using the alternatively shaped base (Fig. 2c) results in a winter recession approximately following an exponential decrease (Fig. 6a,b). The heterogeneous layered scenarios

(vi-a) and (viii-a) visually only slightly differ from (vi) and (viii), respectively (Fig. 6c,d), but yield higher RMSE values (indicating an inferior fit) and different parameter estimates (table 1). While the matrix of (vi-a) has a lower hydraulic conductivity compared to (vi), the matrix of the lower layer of (viii-a) has a higher hydraulic conductivity and specific yield compared to (viii).

5. Discussion

The model results indicate that this aquifer has at least two domains with different aquifer properties. This finding is in good agreement with the outcomes of Winkler et al. (2016a), who used spring data as well as natural and artificial tracers to show that the relict Schöneben rock glacier is a heterogeneous aquifer with an assumed layered structure. Importantly, this investigation indicates that both scenarios, one with a layered internal structure and the other with an internal structure with draining channels, can simulate the fast and slow groundwater flow components that were shown to exist in the previous studies (Wagner et al. 2016; Winkler et al. 2016a). Moreover, the numerical modeling exercise supports the existence of a rather thin lower layer with low hydraulic conductivity, which might include channels with a high hydraulic conductivity. However, the findings cannot give a clear preference to one of the investigated internal structures.

If both a layered structure and channels exist, the discharge behavior is dependent on the extent of the channel network. With a single channel (vii) the discharge is dominated by the layered structure, and the channel only plays a subordinate role (Fig. 5c,d). With a network of channels in the lower layer (viii) the influence of the channels increases. Scenarios (vii) and (viii) (Fig. 4) illustrate that both types of heterogeneity influence the discharge behavior in a different way. The different extent of the draining channels mainly affects the fit of the discharge peaks and the short-term runoff after recharge events. In contrast, the base flow between the recharge events and the winter base flow is similar in both scenarios and also similar to the corresponding scenario without channels. Therefore, the base flow is dominated by the layered structure rather than by the draining channels.

According to the conceptual model of the relict rock glacier of Winkler et al. (2016a) and drill core observations of Krainer et al. (2015), the basal layer might represent morainic remnants. As this layer was not detectable in the geophysical investigations at the SRG, there is no information about the lateral distribution and extension of this layer. Excavations at the neighboring Hochreichart Rock Glacier showed that there is a washed-out zone in the proximity of the spring that is lacking fine-grained material (Untersweg and Proske 1996) and therefore has a high hydraulic conductivity. Thus, it might be reasonable to assume that this layer is not homogeneously distributed across the aquifer.

Assuming slow development processes of a talus-derived rock glacier, preexisting water flow paths or newly evolving ones will probably prevent sedimentation of fine-grained sediments or wash them out, therefore leaving a channel network of unknown extent between patchily distributed sediment accumulations of lower hydraulic conductivity. Graham et al. (2010) showed at excavations of a hillslope watershed that a network of preferential flow paths occurred at the soil-bedrock boundary, which was controlled by the bedrock topography. Scenario (vi) shows that with such a channel network even a single-layered model can reproduce the discharge dynamics of SEQ reasonably well, and the fit of the simulated hydrograph could be even further optimized by adjusting the number and extent of the channels. Yet, this would suggest a matrix hydraulic conductivity of about 10^{-4} to 10^{-5} m/s, which is in discrepancy with the geophysical investigations suggesting coarse-grained sediments based on seismic velocities. Moreover, fine-grained sediments, for instance from the development, evolution, and movement of the rock glacier itself, are likely to exist as a potential source of low conductive zones (e.g., Zurawek 2002; Hausmann et al. 2012).

As a saturated zone needs to exist within the rock glacier to provide groundwater (especially base flow) for the spring, the thickness of the saturated zone is estimated to be around 10-15 m based on recession analysis but seems to be limited to a maximum thickness of 19 m based on seismic refraction results (see Fig. 9 in Winkler et al. 2016a). However, as can be seen in Fig. 5a, model setups containing thin lower layers lead to an underestimation of the base flow between the major recharge events as well as during the winter base flow recession in the calibration period. Keeping in mind that the specific yield of the thin lower layers is always calibrated to 0.3, which was specified as the upper limit of realistic values (see table 1), this result indicates that the storage of a thin lower layer is not sufficient to reproduce the observed discharge during base flow conditions. This might be related to the simplified aquifer base topography of the model.

The comparison of the scenarios with differently shaped aquifer bases in Fig. 6 shows that even though a large part of the aquifer is identical (see Fig. 2), the different aquifer base topographies and the resulting differences in aquifer thickness cause changes of the discharge dynamics or the estimated aquifer parameters. Because of the higher sediment thickness, scenario (ii) shows a slower recession and higher base flow relative to (ii-a) (Fig. 6a,b). Similarly, the lower thickness of the lower layer of (vi-a) compared to (vi) (Fig. 2) results in a slightly faster recession between the major recharge events. However, due to the higher number of adjustable parameters in the more complex scenarios ((viii) and (viii-a)) the effect of the different sediment thickness can be compensated by changes of the hydraulic parameters. Hence, the role of the base topography appears to be more important in the less complex scenarios.

According to these results, for the SRG the modeled aquifer base topography based on the extrapolated rock faces in the eastern part of the model area seems more likely, because the higher thicknesses result in a higher storage capacity, which is preferable to simulate the observed base flow. The estimated hydraulic conductivity of the SRG (table 1) is in good agreement with findings of Pauritsch et al. (2015) and Winkler et al. (2016a). Nevertheless, the winter base flow cannot be reproduced correctly in the calibration period with either of the applied aquifer bases. Remarkably, the base flow recession in the verification period is better matched by the scenarios containing the thin base layer, but even here the models tend to underestimate base flow at the late stage. The observed winter base flow clearly deviates from a single exponential recession. In fact, from ten days onward the recession is found to follow a power law (Winkler et al. 2016a). The simulated recession curves also deviate from an exponential recession (which would be a straight line in the semi-log plots shown in Figs. 5 and 6), but not as much as the observed discharge. Conceptually, a fractal size distribution of storage elements has been proposed to explain the power-law recession of spring hydrographs (Hergarten and Birk 2007). This suggests that the assumption of homogeneous layers might be oversimplified and discontinuities should be considered. In particular, the assumption of heterogeneous layers with spatially varying thickness could provide a larger storage compared with the model setups considered here and still be consistent with the results from the geophysical investigations that covered only parts of the aquifer.

Another explanation for the discrepancies of the simulated and observed base flow might be the influence of the vadose zone, which was not considered in the models. However, because of the coarse blocky debris and its low retention capabilities, precipitation can instantaneously infiltrate through the top layer of the rock glacier. Precipitation is therefore assumed to quickly pass through the unsaturated zone to become groundwater recharge. This is supported by the findings of the tracer test conducted in 2012 (Winkler et al., 2016a), where the tracer, injected at a distance of 350 m from the spring at the surface of the rock glacier, was detected after 2-3 hours at the spring. In addition, Wagner et al. (2016) showed that parameters of a simple lumped-parameter model indicate a rather fast transfer of seepage water towards the saturated zone (time parameter x_4 in Wagner et al, 2016). Furthermore, it was assumed in the model that the contribution of the mountain block recharge, i.e., groundwater flow out of the bedrock of the contributing catchment into the rock glacier (e.g., Welch et al. 2012), is negligible in such a crystalline catchment with an insignificant weathering zone. Assuming an additional constant inflow from the bedrock (mountain block recharge), a slightly better model fit to the winter base flow is conceivable. However, as this would have little effect on the discharge dynamics and as there is no data or field evidence of such a flow component, such a more complex model was not considered herein.

More plausible explanations for the discrepancies of the simulated and measured discharge might be unrealistic initial conditions and/or underestimated recharge. The influence of the initial condition could be further reduced by extending the simulation to perennial time periods, but this would require the introduction of a snow model, thus leading to more adjustable parameters. An underestimation of the recharge might result from the general uncertainties in the measurement of precipitation in alpine terrains. Wagner et al. (2016) demonstrated that a lumped-parameter model is able to simulate the perennial discharge behavior of the SRG reasonably well, but only when additional water is considered (water exchange coefficient x_2 in Wagner et al. 2016) to compensate for water balance deficits. In the numerical groundwater model, such water balance deficits were not compensated and thus are likely to account at least partly for the deviation of the simulated from the observed discharge. As a consequence, the most complex model structures considered here do not perform much better than the less complex models (apart from the most simple single-layer scenario). A simple lumped-parameter model as employed by Wagner et al. (2016) therefore might be an appropriate choice for predictive hydrological modeling. In this study, however, the modeling is aimed at supporting the aquifer characterization, which requires a process-based groundwater model.

In the absence of spatial information about hydraulic heads, the calibration of the groundwater model solely relies on spring discharge and therefore leads to ambiguous results, in particular with regard to the distribution of fine-grained sediments and preferential flow paths. Nevertheless, the results of the present modeling study are helpful for the design of future investigation and monitoring campaigns. As the installation of piezometers is technically difficult and expensive, the use of additional geophysics seems more beneficial. Based on the outcome of the modeling scenarios, more precise information about the distribution and thickness of the fine-grained sediments, which are assumed to exist as a thin (< 19 m) layer at the base of the aquifer, is paramount. For this task, additional seismic refraction investigations with adjusted setups (narrower geophone distance) seem to be particularly promising. In addition, an extension of the previously conducted investigation towards southeast would be of great help, as this area appears to provide the highest thickness of the sediments and, thus, potentially high storage that may account for the observed recession base flow.

There are several other methods that could be envisaged for future investigations, but each of them has some drawbacks that need to be considered as well. Additional ground-penetrating radar measurements (GPR) can be applied considering varying frequencies (especially lower ones) to improve the existing data. Similar results related to challenging GPR data were shown by Merz et al. (2015) who addressed the high level of noise (especially in areas with low ice contents) to

interferences caused by the boulders of the surface layer and shallow heterogeneities. However, they have shown that airborne ground-penetrating radar (antenna mounted on a helicopter) greatly improves the quality of the data. Also other airborne geophysical methods such as frequency-domain or time-domain electromagnetics might help to gain further insights. Nevertheless, all airborne methods prefer constant elevation above ground (de Barros Camara and Guimaraes 2016), which can be challenging in alpine terrain. Electrical resistivity tomography might be a cost-effective solution, but the coarse blocky material at the surface of relict rock glaciers results in a weak electrode coupling to the ground. Furthermore, the extended, air filled voids, and the lack of mineral soils or ice lead to weak electrical contacts between the individual blocks which makes the application of this method rather challenging (Hillbich et al., 2009; Kellerer-Pirklbauer et al., 2014). However, capacitively coupled resistivity methods, which use an alternating current across a transmitter-earth capacitor, can be used as an alternative to overcome these (Hauck, 2013).

Thus, characterizing the hydrogeological properties and functioning of rock glaciers remains a challenging but important task. Rock glaciers represent significant aquifers in alpine catchments and are the source of many important water basins (e.g., Wagner et al. 2016). Furthermore, high heavy metal concentrations within the melt water of an active rock glacier recently reported by Krainer et al. (2015) illustrate the vulnerability of these aquifers to contamination. In addition, rock glaciers are potentially affected by impacts of the future global warming. Assessing groundwater flow and transport processes in a changing environment is particularly challenging. While purely empirical models are considered inadequate for accomplishing this task (e.g., Rehrl and Birk 2010), further progress in the hydrogeological characterization of rock glaciers is needed to reduce the ambiguity of the calibration of process-based distributed models. The above-mentioned findings provide a guideline towards the further investigation of the rock glacier considered here that can likely be transferred to similar settings elsewhere.

6. Conclusions

A number of model scenarios representing the relict SRG have been elaborated using a numerical groundwater flow model. Several scenarios differing in the internal structure and the topography of the aquifer base were considered to indicate the major features that control the discharge behavior of the rock glacier spring. The results of this modeling study converge to a consistent conceptual understanding of the hydrological functioning of the rock glacier. Two aquifer components are found to be needed to account for the observed discharge behavior: a highly conductive layer and/or channel network controlling the fast and flashy spring responses to recharge event, as opposed to

less conductive sediment accumulations sustaining the long-term base flow. Despite the ambiguity of the specific implementation, the parameter estimates obtained from the model calibration provide order-of-magnitude estimates of the hydraulic properties of these two components. The hydraulic conductivity of the highly conductive component is found to be in the order of 10^{-2}-10^{-3} m/s, whereas the hydraulic conductivity of the low-conductivity elements is about three orders-of-magnitude less. The specific yield of the high-conductivity elements varied between the different model setups. Assuming a low-conductivity layer at the aquifer base covering 20 % of the total thickness, the specific yield of this layer is consistently 0.3, which corresponds to the upper limit assumed to be plausible. As the long-term base flow is underestimated by most of the model scenarios, the specific yield or the thickness of this layer might be even larger than assumed here.

The topography of the aquifer base is found to have an impact on the discharge behavior particularly when a simple internal structure is considered. If more complex aquifer structures with a high number of adjustable parameters are employed, changes in the topography can be compensated by the adjustment of other parameters. This ambiguity can only be resolved if additional data are included as constraint on the aquifer properties and internal structure (especially further geophysical investigations) or as additional calibration target (e.g., hydraulic heads).

The Schöneben Rock Glacier in the Niedere Tauern Range, Austria, is one example of a relict rock glacier and its hydrological functioning might be representative for other relict rock glaciers as well. Thus, the insights obtained herein will have implications for intact rock glaciers in the course of climate warming and future investigations of contaminant transport in rock glaciers. As such, studying the discharge behavior of relict rock glaciers (and other alpine debris accumulations) contributes largely to a better understanding of the complex hydrological processes in alpine regions and of their contribution to the fragile ecological systems in such environments.

Acknowledgments

This study was funded by the European Regional Development Fund (ERDF) and the Federal Government of Styria. The authors are grateful to the Hydrographic Service of Styria for providing the discharge data. The digital elevation models and the topographic maps were provided by the GIS Service of the Federal Government of Styria (GIS Steiermark). We acknowledge the constructive suggestions by Majdi Mansour, an anonymous reviewer and the associate editor Alan MacDonald, which greatly improved the paper.

References

Barsch D (1996) Rockglaciers: Indicators for the present and former geoecology in high mountain environments. Springer Series in Physical Environment 16. Springer

Bollmann E, Rieg L, Spross M, Sailer R, Bucher K, Maukisch M, Monreal M, Zischg A, Mair V, Lang K, Stötter, J (2012) Blockgletscherkataster Südtirol – Erstellung und Analyse [Rock glacier registry Southern Tyrol – creation and analysis], Innsbrucker Geographische Studien 39, Permafrost in Südtirol: 147-171

Campbell DH, Clow DW, Ingersoll GP, Mast MA, Spahr NE, Turk JT (1995) Processes Controlling the Chemistry of Two Snowmelt-Dominated Streams in the Rocky Mountains, Water Resour Res 31(11):2811-2821, doi:10.1029/95WR02037

Carrera J, Alcolea A, Medina A, Hidalgo J, Slooten LJ(2005) Inverse problem in hydrogeology, Hydrogeol J 13(1):206-222, doi:10.1007/s10040-004-0404-7

Clow DW, Schrott L, Webb R, Campbell DH, Torizzo A, Dornblaser M (2003) Ground Water Occurrence and Contributions to Streamflow in an Alpine Catchment, Colorado Front Range, Ground Water 41: 937-950, doi:10.1111/j.1745-6584.2003.tb02436.x

De Barros Camara E, Guimaraes SNP (2016) Magnetic airborne survey – geophysical flight, Geosci Instrum Method Data Syst 5: 181-192, doi:10.5194/gi-5-181-2016

Degenhardt JJ (2009) Development of tongue-shaped and multilobate rock glaciers in alpine environments – Interpretations from round penetrating radar surveys, Geomorphology 109(3-4):94–107, doi:10.1016/j.geomorph.2009.02.020

Doherty J (2013) PEST: Model-independent parameter estimation, user manual, Watermark Numerical Computing. http://www.pesthomepage.org/downloads.php

Eisenlohr L, Bouzelboudjen M, Király L, Rossier Y (1997a) Numerical versus statistical modelling of natural response of a karst hydrogeological system, J Hydrol 202(1-4):244-262, doi:10.1016/S0022-1694(97)00069-3

Eisenlohr L, Király L, Bouzelboudjen M, Rossier Y (1997b) Numerical simulation as a tool for checking the interpretation of karst spring hydrographs, J Hydrol 193(1-4):306-315, doi:10.1016/S0022-1694(96)03140-X

Graham CB, Woods RA, McDonnell JJ (2010) Hillslope threshold response to rainfall: (1) A field based forensic approach, J Hydrol 393(1–2):65–76, doi:10.1016/j.jhydrol.2009.12.015

Haeberli W, Hallet B, Arenson L, Elconin R, Humlum O, Kääb A, Kaufmann V, Ladanyi B, Matsuoka N, Springman S, Mühll DV (2006) Permafrost creep and rock glacier dynamics, Permafr Periglac Process 17:189–214, doi:10.1002/ppp.561

Hauck C (2013) New Concepts in Geophysical Surveying and Data Interpretation for Permafrost Terrain, Permafr Periglac. Process 24:131–137, doi: 10.1002/ppp.1774

Hausmann H, Krainer K, Brückl E, Ulrich C (2012) Internal structure, ice content and dynamics of Ölgrube and Kaiserberg rock glaciers (Ötztal Alps, Austria) determined from geophysical surveys, Aust J Earth Sci 105(2):12-31

Hergarten S, Birk S (2007) A fractal approach to the recession of spring hydrographs. Geophys Res Lett 34: L11401, doi:10.1029/2007GL030097

Hilbich C, Marescot L, Hauck C, Loke MH, Mäusbacher R (2009) Applicability of Electrical Resistivity Tomography Monitoring to Coarse Blocky and Ice-rich Permafrost Landforms, Permafr Periglac. Process 20: 269–284, doi: 10.1002/ppp.652

Hood JL, Hayashi M (2015) Characterization of snowmelt flux and groundwater storage in an alpine headwater basin, J Hydrol 521:482-497, doi:10.1016/j.jhydrol.2014.12.041

Hughes PD, Gibbard PL, Ehlers J (2013) Timing of glaciation during the last glacial cycle: evaluating the concept of a global 'Last Glacial Maximum' (LGM), Earth Sci Rev 125:171-198, doi:10.1016/j.earscirev.2013.07.003

Hunt RJ, Feinstein DT (2012) MODFLOW-NWT: Robust Handling of Dry Cells Using a Newton Formulation of MODFLOW-2005, Ground Water50:659–663, doi:10.1111/j.1745-6584.2012.00976.x

Jansen F, Hergarten S (2006) Rock glacier dynamics: stick-slip motion coupled with hydrology, Geophys Res Lett 33:L10502, doi:10.1029/2006gl026134

Kellerer-Pirklbauer A, Lieb KG, Kleinferchner H (2012) A new rock glacier inventory of the Eastern European Alps, Aust J Earth Sci 105(2):78-93

Kellerer-Pirklbauer A, Pauritsch M, Morawetz R, Kuehnast B, Schreilechner M, Winkler G (2014) Thickness and internal structure of relict rock glaciers: a challenge for geophysics—examples from two rock glaciers in the Eastern Alps, Geophys Res Abstr 16:EGU2014–12581

Kellerer-Pirklbauer A, Pauritsch M, Winkler G (2015) Widespread occurrence of ephemeral funnel hoarfrost and related air ventilation in coarse-grained sediments of a relict rock glacier in the Seckauer Tauern Range, Austria. Geogr Ann A 97(3):453-471, doi:10.1111/geoa.12087

Krainer K, Mostler W (2002) Hydrology of active rock glaciers: examples from the Austrian Alps, Arc Antarc Alp Res 34:142-149, doi:10.2307/1552465

Krainer K, Ribis M (2012) A rock glacier inventory of the Tyrolean Alps (Austria), Aust J Earth Sci 105(2):32-47

Krainer K, Mostler W, Spoetl C (2007) Discharge from active rock glaciers, Austrian Alps: a stable isotope approach, Aust J Earth Sci 100:102-112

Krainer K, Bressan D, Dietre B, Haas JN, Hajdas I, Lang K, Mair V, Nickus U, Reidl D, Thies H, Tonidandel D (2015) A 10,300-year-old permafrost core from the active rock glacier Lazaun, southern Ötztal Alps (South Tyrol, northern Italy), Quat Res 83(2):324-335, doi:10.1016/j.yqres.2014.12.005

Lauber U, Kotyla P, Morche D, Goldscheider N (2014) Hydrogeology of an Alpine rockfall aquifer system and its role in flood attenuation and maintaining baseflow, Hydrol Earth Syst Sci 18:4437-4452, doi:10.5194/hess-18-4437-2014

Leopold M, Williams MW, Caine N, Völkel J, Dethier D (2011) Internal structure of the Green Lake 5 rock glacier, Colorado Front Range, USA, Permafrost Periglac 22:107–119, doi:10.1002/ppp.706

Mansour MM, Hughes AG, Robins NS, Ball D, Okoronkwo, C (2012) The role of numerical modelling in understanding groundwater flow in Scottish alluvial aquifers. In: Shepley, M.G., (ed.) Groundwater resources modelling: a case study from the UK. Geological Society, London, Special Publications 364:85-98

Matthews JA, Wilson P (2015) Improved Schmidt-hammer exposure ages for active and relict pronival ramparts in southern Norway, and their palaeoenvironmental implications. Geomorphology 246:7-21, doi:10.1016/j.geomorph.2015.06.002

McDonald MG, Harbaugh AW (1988) A modular three-dimensional finite-difference ground-water flow model. In: U.S. Geological Survey Techniques of Water-Resources Investigations, Book 6, A1, 586 p

Merz K, Maurer H, Buchli T, Horstmeyer H, Green AG and Springman SM (2015) Evaluation of Ground-Based and Helicopter Ground-Penetrating Radar Data Acquired Across an Alpine Rock Glacier, Permafrost Periglac 26:13–27, doi:10.1002/ppp.1836

Millar CI, Westfall RD, Delany DL (2013) Thermal and hydrologic attributes of rock glaciers and periglacial talus landforms: Sierra Nevada, California, USA, Quat Int 310:169-180, doi:10.1016/j.quaint.2012.07.019

Monnier S, Camerlunck C, Rejiba F, Kinnard C, Feuillet T, Dhemaied A (2011) Structure and genesis of the Thabor rock glacier (Northern French Alps) determined from morphological and ground-penetrating radar surveys, Geomorphology 134:269-279, doi:10.1016/j.geomorph.2011.07.004

Monnier S, Kinnard C (2015) Internal Structure and Composition of a Rock Glacier in the Dry Andes, Inferred from Ground-penetrating Radar Data and its Artefacts, Permafrost Periglac 26(4):335-346, doi:10.1002/ppp.1846

Muir DL, Hayashi M, McClymont AF (2011) Hydrological storage and transmission characteristics of an alpine talus. Hydrol Process 25:2954-2966, doi:10.1002/hyp.8060

Niswonger RG, Pandai S, Ibaraki M (2011) MODFLOW-NWT, A Newton formulation for MODFLOW-2005. In: U.S. Geological Survey Techniques and Methods 6, A37, 44 p

Pauritsch M, Birk S, Wagner T, Hergarten S, Winkler G (2015) Analytical approximations of discharge recessions for steeply sloping aquifers in alpine catchments, Water Resour Res 51:8729-8740, doi:10.1002/2015WR017749

Peters E, Van Lanen HAJ, Torfs PJJF, Bier G (2005) Drought in groundwater - Drought distribution and performance indicators, J Hydrol 306 (1-4):302-317, doi:10.1016/j.jhydrol.2004.09.014

Rehrl C, Birk S (2010) Hydrogeological characterisation and modelling of spring catchments in a changing environment, Aust J Earth Sci 103 (2):106-117

Roy JW, Hayashi M (2009) Multiple distinct groundwater flow systems of single moraine-talus feature in alpine watershed, J Hydrol 373:139-150, doi:10.1016/j.jhydrol.2009.04.018

Schmid MO, Baral P, Gruber S, Shahi S, Shrestha T, Stumm D, Wester P (2015) Assessment of permafrost distribution maps in the Hindu Kush Himalayan region using rock glaciers mapped in Google Earth, The Cryosphere 9:2089-2099, doi:10.5194/tc-9-2089-2015

Tague C, Grant GE (2009) Groundwater dynamics mediate low-flow response to global warming in snow-dominated alpine regions, Water Resour Res 45, W07421, doi:10.1029/2008wr007179

Thornthwaite CW (1948) An approach towards a rational classification of climate, Geogr Rev 38:55-94, doi:10.1097/00010694-194807000-00007

Untersweg T, Proske H (1996) Untersuchungen an einem fossilen Blockgletscher im Hochreichhartgebiet (Niedere Tauern, Steiermark) [Investigations at a relict rock glacier in the Hochreichhart area „Niedere Tauern Range, Styria]“, Grazer Schriften der Geographie und Raumforschung 33:201–207

Wagner T, Pauritsch M, Winkler G (2016) Impact of relict rock glaciers on spring and stream flow of alpine watersheds: Examples of the Niedere Tauern Range, Eastern Alps (Austria), Aust J Earth Sci 109, doi:10.17738/ajes.2016.0006

Welch LA, Allen DM, van Meerveld HJ (2012) Deep groundwater contributions to mountain headwater streams and sensitivity to available recharge, Can Water Resour J 37, doi:10.4296/cwrj3703907

Winkler G, Wagner T, Pauritsch M, Birk S, Kellerer-Pirkelbauer A, Benischke R, Leis A, Morawetz R, Schreilechner MG, Hergarten S (2016a) Identification and assessment of flow and storage components of the relict Schöneben Rock Glacier, Niedere Tauern Range, Eastern Alps (Austria), Hydrogeol J 24:937-953, doi:10.1007/s10040-015-1348-9

Winkler G, Pauritsch M, Wagner T, Kellerer-Pirklbauer A (2016b) Reliktische Blockgletscher als Grundwasserspeicher in alpinen Einzugsgebieten der Niederen Tauern (Relict rock glaciers as groundwater storages in alpine catchment areas in the Niedere Tauern Range), Berichte zur wasserwirtschaftlichen Planung Steiermark, Bd. 87. Graz, p. 134. http://www.wasserwirtschaft.steiermark.at/cms/dokumente/11913323_102332494/6885027d/87.pdf [Accessed 12 September 2016]

Worthington SRH (2009) Diagnostic hydrogeologic characteristics of a karst aquifer (Kentucky, USA). Hydrogeol J 17:1665-1678, doi:10.1007/s10040-009-0489-0

Zurawek R (2002) Internal Structure of a relict rock glacier, Ślęża Massif, Southwest Poland, Permafr Periglac Process 13:29–42, doi:10.1002/ppp.403

7.4. Publication IV

Wagner T, Pauritsch M, Winkler G (2016) Impact of relict rock glaciers on spring and stream flow of alpine watersheds: Examples of the Niedere Tauern Range, Eastern Alps (Austria). Austrian Journal of Earth Sciences, 109, doi: 10.17738/ajes.2016.0006.

Austrian Journal of Earth Sciences | Vienna | 2016 | Volume 109/1 | xxx - xxx | DOI: 10.17738/ajes.2016.0006

Impact of relict rock glaciers on spring and stream flow of alpine watersheds: Examples of the Niedere Tauern Range, Eastern Alps (Austria)

Thomas WAGNER[1) *], Marcus PAURITSCH[1)] & Gerfried WINKLER[1)]

Institute of Earth Sciences, NAWI Graz Geocenter, University of Graz, Heinrichstrasse 26, 8010 Graz, Austria;

[*)] Corresponding author, thomas.wagner@uni-graz.at

KEYWORDS Niedere Tauern Range; relict rock glacier; storage capacity; streamflow; alpine catchment; rainfall-runoff model

Abstract

In crystalline mountain regions, relict rock glaciers are apparent sediment accumulations that likely influence the runoff in alpine watersheds as a result of their discharge behavior. However, little is known about their impact on the streamflow further downstream. More than 560 mostly relict rock glacier-related landforms have been identified in the Styrian part of the Niedere Tauern Range (Austria). The catchment of a single relict rock glacier (Schöneben Rock Glacier, SRG), and two catchments with relict rock glaciers in their headwaters were investigated with a simple lumped-parameter rainfall-runoff model. The model parameters of the SRG catchment are in agreement with the existing conceptual understanding of the discharge dynamics and provide the parameter configuration to simulate the runoff of ungauged relict rock glacier catchments in the area. In addition, a semi-distributed approach was applied to quantify the impact of relict rock glacier-influenced headwaters on the downstream runoff. The results suggest that the contribution ranges from about a quarter to more than four times its areal share. The highest impact is observed during the late snow melt period and in the late summer. This highlights the relevance of these sediment accumulations in relation to water management issues, in particular concerning altering meteorological conditions due to climate change.

Reliktische Blockgletscher sind augenscheinliche Sedimentanhäufungen in kristallinen Gebirgsregionen, die aufgrund ihrer Abflussdynamik die Entwässerung alpiner Einzugsgebiete beeinflussen. Jedoch ist ihre Auswirkung auf unterstromige Gerinne weitgehend unbekannt. Mehr als 560 meist reliktische Blockgletscher sind im Steirischen Anteil der Niederen Tauern (Österreich) ausgewiesen. Ein über einen reliktischen Blockgletscher (Schöneben Blockgletscher, SRG) entwässerndes Einzugsgebiet und zwei Einzugsgebiete, die ihrerseits reliktische Blockgletscher in ihren hoch gelegenen Anteilen beinhalten, wurden mit Hilfe eines einfachen, räumlich nicht aufgelösten (lumped Parameter) Niederschlags-Abflussmodells untersucht. Die Modellparameter des SRG-Einzugsgebiets stimmen mit dem vorliegenden konzeptionellen Modell überein und dienen als Grundlage der Parameterkonfiguration zur Abflusssimulation anderer Blockgletschereinzugsgebiete in der Region, für die keine Abflussdaten zur Verfügung stehen. Zusätzlich wurde ein semi-distributiver Ansatz angewendet, um den Einfluss von Blockgletscher beeinflussten Einzugsgebieten auf die unterstromigen Gerinne zu quantifizieren. Die Ergebnisse zeigen, dass der Abflussanteil unterstromig von einem Viertel bis zu mehr als dem Vierfachen des Flächenanteils der übergeordneten Einzugsgebiete beträgt. Die höchsten Anteile können gegen Ende der Schneeschmelze und im Spätsommer beobachtet werden. Dies unterstreicht die wasserwirtschaftliche Bedeutung dieser Schuttakkumulationen in alpinen Einzugsgebieten, vor allem unter der Berücksichtigung der sich ändernden meteorologischen Bedingungen im Zuge des Klimawandels.

1. Introduction

Runoff in alpine catchments is strongly affected by water stored in the form of snow and groundwater in the soil and sediment accumulations within the catchment. The influence of snow accumulation and melt is of obvious importance during winter base flows and the subsequent snow melt period, during which large increases in runoff are observable (e.g. López-Moreno and García-Ruiz, 2004). However, their role shifts as climate change progresses; air temperature might increase, periods of solid precipitation are reduced, and snow melt periods will begin earlier in the year (e.g. Barnett et al., 2005; Wagner et al., 2012). The impact of the soil on headwater runoff is usually low in alpine catchments, especially where bare rocks and scree slopes are predominant. Due to this, and the generally lower temperatures compared to valleys and forelands, evapotranspiration rates are reduced. The hydrological importance of sediment accumulations, such as talus deposits, moraines or rock glaciers, was recently documented (Clow et al., 2003; Millar et al., 2013; Hood and Hayashi, 2015; Winkler et al., 2016b). The storage capacity of these sediments becomes especially noticeable during the summer and autumn months, during which, on the one hand, groundwater is stored during dry periods, and, on the other hand, a water buffer is provided for flood propagation triggered by local storm events. Numerous field observations during summer and autumn showed that springs at the base of relict rock glaciers still provide runoff when other springs have already fallen dry. This is important for the sensitive ecosystem in high alpine catchments. However, the actual observations have not

yet been quantified; especially not on a regional scale. Such an understanding is important for the sustainable use of water for human consumption and for small hydroelectric power plants.

Rock glaciers in general are common morphological features in the Alps (e.g. more than 4790 in the Austrian Alps, Kellerer-Pirklbauer et al., 2012; Krainer and Ribis, 2012) and thus also of great hydrological importance. Recently, knowledge on rock glaciers increased strongly, especially in the Austrian Alps. A state-of-the-art review of recent research related to permafrost in Austria is given in a special issue edited by Krainer et al. (2012). Rock glaciers in general are typical landforms indicating mountain permafrost conditions during their genesis and evolution and can be classified as intact (active and inactive) and relict ones. Active rock glaciers are frozen debris bodies with interstitial ice or ice lenses, gravitationally moving down-slope or down-valley, usually in the order of decimeters to a few meters per year (e.g. Barsch, 1996; Haeberli et al., 2006). Rock glaciers become inactive (but still intact) when movement comes to an end but ice is still present within the rock glacier. Rock glaciers are frequently characterized by distinct flow structures with ridges and furrows at the surface with some similarity to the surface of pahoehoe lava flows. The evolution of first intact, including active and inactive, and later relict rock glaciers is strongly affected by a shift of the lower limit of mountain permafrost and the subsequent disappearance of permafrost ice within the rock glaciers. Relict rock glaciers have a similar shape as intact ones but additionally show clear collapse structures because of the melted ice and the resulting loss of volume. Rock glaciers usually have a thickness in the order of several tens of meters. Monnier et al. (2011) and Monnier and Kinnard (2015) used ground penetrating radar to investigate two active rock glaciers in the French Alps and Chilean Andes. Their results suggest a heterogeneous, layered inner structure of the rock glacier which is in good agreement with the findings of Hausmann et al. (2012) at intact rock glaciers in the Austrian Alps based on surface geophysical investigation methods. Recently Krainer et al. (2015) investigated two drill cores of an active rock glacier in the Italian Alps which showed sequences of ice rich and unfrozen layers and also indicating a layering due to grain size variations. Recent investigations at a relict rock glacier (SRG, the rock glacier studied herein) in the Austrian Alps (Winkler et al., 2016b) also indicate a layered structure with coarse grained upper layer(s) and a fine grained bottom layer confirming first observations at a relict rock glacier in Poland (Zurawek, 2002, 2003). As such, the main feature of the internal structure of a rock glacier seems to be its layering differentiating relict rock glaciers from talus and moraines.

However, still relatively little is known on the hydrological behavior of rock glaciers and areas affected by alpine permafrost in general. Here, the focus is on the hydrology of relict rock glaciers, which are abundant in the Austrian Alps (more than 3000, Kellerer-Pirklbauer et al., 2012; Krainer and Ribis, 2012). To study the hydrology of relict rock glaciers is particularly important as it can be assumed that permafrost ice of intact rock glaciers is increasingly melting due to the climate change (global warming). A change from intact to relict rock glaciers might lead to a change in the hydraulic properties and drainage behavior of these landforms.

Therefore, the aim of this work is to investigate the impact of relict rock glaciers on the downstream flow using a simple lumped-parameter rainfall-runoff model. Model parameters are interpreted in terms of catchment characteristics; more specifically this study investigates if the sub-catchments containing larger areas of relict rock glaciers yield larger values of model parameters representing storage capacities. This may imply that sediment accumulations represent potential groundwater stores. Moreover, the use of the rainfall-runoff model in a simple semi-distributed manner explicitly accounts for the effects of sub-catchments influenced by rock glaciers and therefore permits separating their contribution from the total streamflow further downstream. This will help to understand the effects of such sediment accumulations for water management issues as well as flood risk assessment.

2. Study area

2.1 Geography and geology

The Styrian part of the Niedere Tauern Range (2440 km^2) in the Eastern Alps (Austria) is the regional focus of this investigation (Figure 1a, b). Its subunits, from west to east, are the Schladminger Tauern, the Wölzer Tauern, the Rottenmanner Tauern, and the Seckauer Tauern Ranges (Figure 1a). The boundaries are formed by the Enns valley in the north, the Palten-Liesing valley in the east, the Mur valley in the south, and the upper Mur valley and the border to Salzburg in the west. About half of the area is above 1500 m a.s.l. and 11 % are above 2000 m a.s.l. (Figure 1a). The highest mountain is the Hochgolling with 2862 m a.s.l., in the Schladminger Tauern Range. Geologically, the Styrian part of the Niedere Tauern Range belongs to the Silvretta-Seckau and Koralpe-Wölz nappe system of the Upper Austroalpine subunit and its permo-mesozoic cover sequences. The Niedere Tauern Range mainly consits of various types of gneisses and mica schists (Schmid et al., 2004; Gasser et al., 2009). In the north, the upper rock unit is part of the Greywacke zone.

The data base for the identification of the rock glaciers was an inventory which is described in detail by Kellerer-Pirklbauer et al. (2012). The former inventory was based on a 10 m resolution digital elevation model (DEM), DEM-derived maps such as slope maps, orthophoto analysis and in many cases mapping campaigns. This inventory was modified manually by applying a 1 m resolution DEM based on air borne laser-scan data (ALS; provided by the GIS Service of the Federal Government of Styria; GIS Steiermark). The rock glaciers were identified by morphological features such as flow structures with ridges and furrows, rock glacier fronts and in the case of relict rock glaciers the occurrence of collapse structures (Winkler et al., 2016a).

A total of 561 rock glacier-related landforms are distinguished in the area (Winkler et al., 2016a), of which only seven are likely to be still intact rock glaciers (all in the western part of the Niedere Tauern Range), while the remaining ones are relict. Approximately 12 % of the area above 1500 m a.s.l. and 27 % above 2000 m a.sl. are drained through rock glaciers. These percentages increase for the Seckauer Tauern Range (eastern-most subunit of the Niedere Tauern Range) to 22 % and 51 %, respectively (Winkler et al., 2016a). The glaciation of the last glacial maximum has affected the investigation area quite differently from west to east. This is also reflected in the distribution, size, and condition of the rock glaciers (Winkler et al., 2016a). In the west (the Schladminger Tauern Range) there are many smaller rock glaciers, including some presumably intact rock glaciers at high elevations (mean surface area: 0.43 km²; mean elevation: 2013 m). In the east (the Seckauer Tauern Range) rather large relict rock glaciers are dominant and extend down to lower elevations (mean surface area: 0.96 km²; mean elevation: 1832 m). In general, the Niedere Tauern Range is situated in the south of the Northern Calcareous Alps with annual precipitation between 1500-2000 mm/year. The primary weather influence (prevailing winds) is from the west and northwest. Additionally, low-pressure systems from the south can be significant. The prevailing mountain climate is characterized by snow accumulation in winter and a snow melt period in spring. In summer and autumn, thunder storms might produce strong precipitation events.

In this paper, we focus on the Unterwald/Liesing catchment (UWcatch) in the Seckauer Tauern Range including the two sub-catchments of Finsterliesing (FLcatch) and Schöneben (SRGcatch) (Figure 1c).

The rock glacier catchments have been delineated using the rock glacier boundaries, and based on a 1 m DEM (ALS data set) the contributing catchment has been extracted using standard ArcGIS hydrology tools. The investigated (sub-) catchments (UWcatch, FLcatch, SRGcatch) are influenced by relict rock glacier catchments to various degrees. Based on the areal coverage of the relict rock glacier catchments in relation to the whole catchment, the influence of these subcatchments can be quantified by its proportion ranging from 12 % (UWcatch) to 100 % (SRGcatch). In the particular case of the SRGcatch, the catchment is drained completely via the rock glacier (its spring SEQ) and therefor the influence is 100 %. Flow dynamic and storage capacity of the SRGcatch are investigated in detail. The relict rock glacier itself covers about 16.5 % (~0.11 km²) of the catchment with a size of 0.67 km² (Table 1); 56.7 % of the catchment is made up of bare rocks and the remaining 26.8 % are covered by other debris accumulations with sparse vegetation (Figure 2).

SEQ basically shows a fast flow component reacting to precipitation/recharge events within a couple of hours (based on hydrograph analysis and natural tracer data). Additionally it shows a substantial slow flow component with a reaction time in the order of a few months (based on hydrograph analysis and artificial tracer tests) that provides the base flow in the winter months and during longer periods of no precipitation/recharge (Winkler et al., 2016b). A two-component separation of discharge based on electrical conductivity and isotope measrements, triggered by precipitation events, indicates an event water contribution in the order of 20 % in relation to older, longer stored water coming from the aquifer itself (Winkler et al., 2016b). These rather high contributions of pre-event water are in good agreement with observations in other low-order watersheds (e.g. Buttle, 1994; Kirchner, 2003). All this indicates potential buffer capabilities of this relict rock glacier that might be relevant for stream flow further downstream.

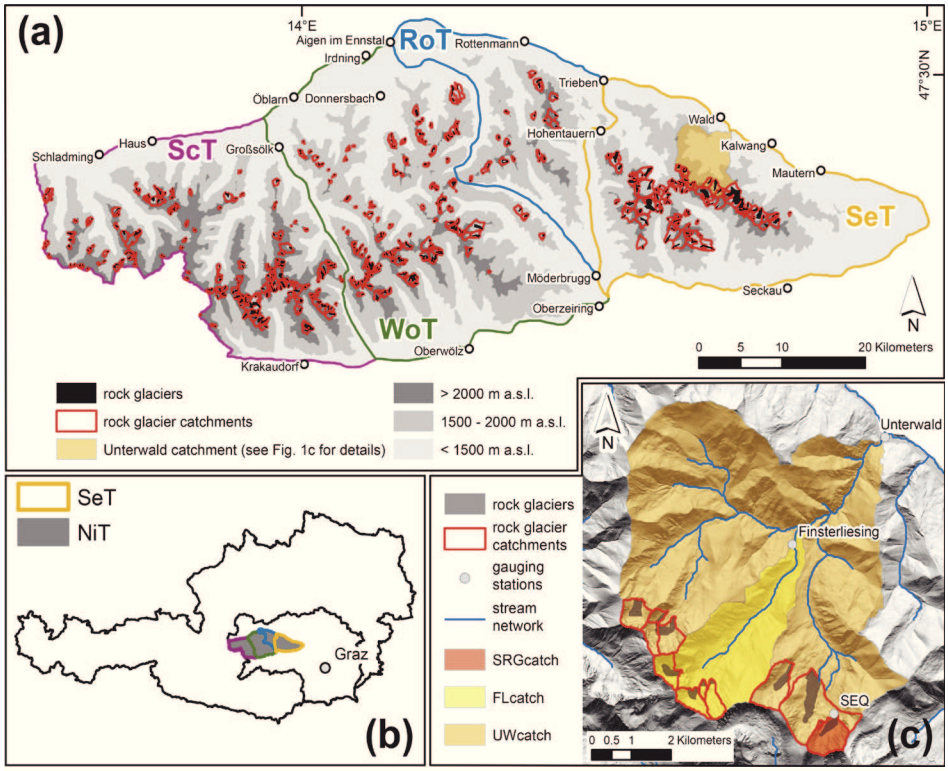

Figure 1: Investigation area, (a) overview of the Niedere Tauern Range (NiT) including its subunits, all identified rock glaciers, the related rock glacier catchments and the Unterwald catchment (UWcatch); ScT = Schladminger Tauern Range, WoT = Wölzer Tauern Range, RoT = Rottenmanner Tauern Range and SeT = Seckauer Tauern Range; (b) shows the study area within the Austrian and Styrian boundaries; Graz = capital of Styria; (c) details of the Unterwald (UWcatch), Finsterliesing (FLcatch) and Schöneben (SRGcatch) catchments including the areal extend of relict rock glaciers and their catchments.

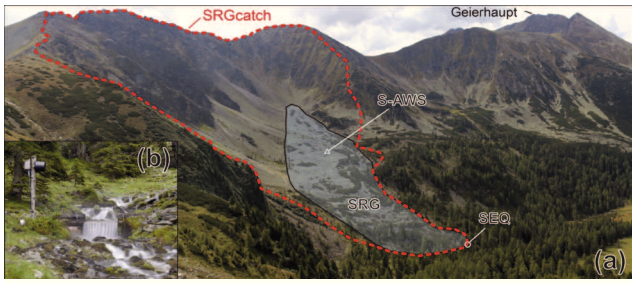

Figure 2: The relict Schöneben Rock Glacier (SRG) and its catchment (SRGcatch). The spring (SEQ) and the weather station (S-AWS) are indicated. The highest mountain of the SeT, Geierhaupt (2417 m a.s.l.), is visible in the background; in the neighboring cirque, another relict rock glacier is recognizable. Viewpoint in a south-western direction from a nearby mountain where an automatic remote digital camera (S-RDC) is installed to take daily pictures of the snow cover of the area. The gauging station of SEQ a few meters downstream of the actual spring is shown in (modified after Winkler et al., 2016b).

2.1 Meteorological and hydrological data

The hydrological significance in the area is shown by displaying the long-term mean annual runoff from relict rock glacier-influenced catchments on the downstream stream network (Figure 3). A simple approach would take into account the areal ratio of the relict rock glacier catchments related to the whole catchments at a specific point along the stream network. However, as precipitation and temperature have certain altitudinal dependencies, computing relative runoff from relict rock glacier-influenced sub-catchments allows a more accurate consideration of headwaters and emphasizes their importance. Here, these effects are taken into account in the following way. The discharge (Q) based on the water balance neglecting storage changes was computed (Q = precipitation (P) – evapotranspiration (ETa)). This was estimated from the long-term precipitation and temperature data (1971-2000) obtained from the Climate Atlas Styria (Prettenthaler et al., 2010) on a 50 x 50 m grid provided by the federal state of Styria. The data set has been compiled from all available weather stations in Styria (including an elevation-correlation to consider altitudinal differences and wind-correction for precipitation). The simple temperature based empirical formula of Turc (Gray, 1970) to compute ETa and the formula of Oudin et al. (2005) used later in the rainfall-runoff model to compute potential evapotranspiration were applied herein. Both are designed to cope with limited data availability as is often the case in high alpine catchments. Simplicity in evapotranspiration formulas have been shown to be beneficial for efficient rainfall-runoff modelling (Oudin et al., 2005) and simple temperature based formulas outperformed more data demanding, complex approaches.

For example, the hydrological significance of relict rock glacier catchments on the total long-term runoff is displayed, when considering long-term average runoffs at the outflow of the Ingering creek towards the Mur valley. 24 % of the runoff consists of water draining relict rock glacier bodies (Figure 3). For the Liesing creek, 14 % of the long-term averaged runoff passes through relict rock glaciers; one of them being the SRG. Values from the Hagen and Gaal creek are even higher. A large influence from the relative area of the rock glacier catchments on these values is obvious. Considering only the relative area, values of 21 % for the Ingering creek and 12 % for the Liesing creek are computed. Although these numbers are not very different, taking the altitudinal effect of precipitation and temperature into account, allows to more accurately consider the alpine headwaters (where relict rock glaciers are to be found). As this first analysis is only a long-term annual average, it is to be expected that seasonal or short term (daily) contributions might show considerable variations.

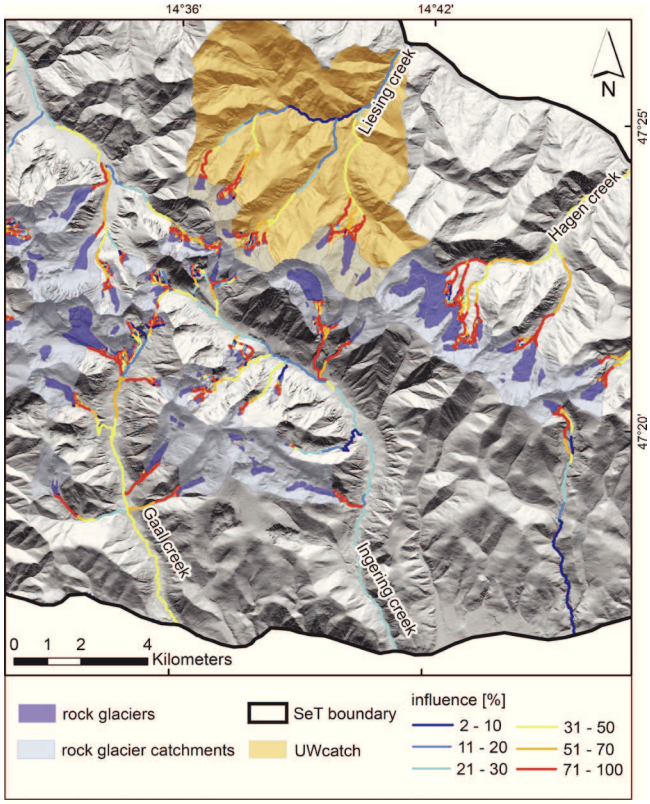

Figure 3: Runoff contribution map of the area: considering long-term runoff estimates based on a simple water balance (discharge (Q) = precipitation (P) – evapotranspiration (ETa)); the proportion (in %) of water draining relict rock glacier bodies are displayed along the downstream stream network approaching the main valleys. The Unterwald catchment (UWcatch) is highlighted in orange.

To be able to provide an analysis of higher temporal resolution, daily data has been investigated. On a daily time scale, the Schöner-ZAMG data set (Schöner and Dos Santos Cardoso, 2004) provides air temperature and precipitation data at a 1km horizontal resolution. It is based on all available meteorological stations of Austria and was used as consistent data input for the various catchments covering a time frame from 1948 to 2007. Moreover, the meteorological data of the weather station S-AWS, which was installed in 2011 directly in the SRGcatch (Figure 2; Winkler et al., 2016a,b), is used as the forcing input for simulating the Schöneben spring (SEQ) discharge. As these two data sets unfortunately do not over-

lap, a direct comparison is not possible. However, using both data sets as input to model the SRGcatch, similar resulting model parameter sets would indicate that both input data sets are consistent. It should be noted that microclimatic effects in mountainous catchments, such as local downpours and short temperature-induced snowmelt or accumulation periods, are not necessarily reflected in both data sets. The undercatch of precipitation measurements under windy conditions and solid precipitation leads to underestimation of precipitation (e.g. Sevruk et al., 2009; Wolff et al., 2015). However, visual snow cover data is available from an automatic remote digital camera (S-RDC) installed in 2011 at the opposite mountain ridge of the SRG, some 500 meters to the northeast at an elevation of 1960 m a.s.l. This information is used to check the physical relevance of the snow module used in the rainfall-runoff model.

The gauging station Schöneben spring (SEQ) belongs to the official spring network of the Hydrographic Service of Styria (HZB number 396762). Unterwald (UW) is also a current official station of the Hydrographic Service of Styria (HZB number 211821), whereas Finsterliesing (FL) is a former official station of the Hydrographic Service of Styria (HZB number HD 2600) that was abandoned in 2008 (Table 1). It should be noted that all three gauging stations are in an alpine setting where data acquisition is difficult and the limitations/errors of discharge measurements (relationship of water level measured at the weir and the discharge) should be kept in mind (e.g. Weijs et al., 2013).

3. Methods

A global, lumped-parameter conceptual rainfall-runoff model (Figure 4) is applied to the SRGcatch using the discharge time series of the spring and meteorological input data from the local weather station S-AWS and alternatively, from a gridded dataset with a 1 km resolution (Schöner-ZAMG data set; Schöner and Dos Santos Cardoso, 2004). A uniform spatial distribution of precipitation is assumed due to the relatively small size of the catchment. The main reason for applying this type of rainfall-runoff model is that data availability in alpine catchments is usually sparse, and temperature and precipitation are the only forcing input parameters available for the area of interest. The simple models for snow accumulation and melt, as well as potential evapotranspiration, have their own limitations (e.g. Andréassian et al., 2004). None the less, this approach allows applying a consistent data set to a number of catchments of different sizes and locations. Moreover, ungauged (sub-) catchments with characteristics comparable to one for which discharge data are available can be analyzed using the parameter set of the calibrated and validated model for the gauged catchment (i.e. regionalization based on physical similarity; e.g. Oudin et al. 2008).

The calibrated and validated rainfall-runoff model is used to aid in aquifer and catchment characterization and further determine storage capabilities/components of the relict rock glacier and its adjacent debris accumulations. The remaining part of the catchment is of little interest for groundwater storage due to its steep slopes composed of bare rock with no obvious weathering zone and scarce vegetation (Figure 2).

After a detailed local study of the SRGcatch for which much additional data is available (Winkler et al., 2016b), a more regional approach is followed where the limits of data availability in alpine catchments is more of a concern. The rainfall-runoff model is applied to the FLcatch and the UWcatch where streamflow is influenced only to some extent by relict rock glaciers in the headwaters (see Figure 1c). The storage parameters of the rainfall-runoff model are then related to catchment characteristics and especially the importance of relict rock glaciers is investigated. Moreover, the model parameter set of the SRGcatch can be applied to the relict rock glacier-influenced parts of the catchments FLcatch and UWcatch in a simple semi-distributed approach. On the one hand, this allows comparing the parameter sets of the lumped approach to the one with the semi-distributed. On the other hand, the direct influence of the relict rock glacier catchments on the downstream sections (at the gauging stations) can be analyzed. As such, the percentage of runoff can be analyzed in more detail as compared to the long-term annual average of the runoff contribution map (Figure 3). In addition to the mean influence of runoff from rock glacier-influenced subcatchments, the daily and seasonal impacts can be identified.

gauging station	stream	HZB number	area	avg height	relief factor	area RG		area RGcatch		available Q time series
			[km²]	[m]	[m]	[km²]	[%]	[km²]	[%]	
SEQ	Schöneben creek	396762	0.67	2005.8	580.0	0.11	16.56	0.67	100.00	07/2002 – 08/2014
FL	Finsterliesing	- (HD 2600)	7.26	1715.0	1277.2	0.17	2.36	1.07	14.78	01/1998 – 04/2008
UW	Liesing creek	211821	44.10	1521.1	1598.4	1.02	2.31	5.31	12.05	01/1989 – 12/2009

Table 1: Gauging stations Unterwald (UW), Finsterliesing (FL) and Schöneben Rock Glacier spring (SEQ), their related catchment characteristics and the available discharge (Q) time series. Area = total catchment area; avg height = the average elevation of the total catchment; relief factor = difference between maximum and minimum elevation of the catchment; area RG = areal extent of relict rock glaciers within the catchment; area RGcatch = areal extend of the catchments that are drained through rock glaciers (extracted using standard ArcGIS hydrology tools).

Thus, and due to existing data limitations, such simple rainfall-runoff models are important hydrological modelling tools.

3.1 Lumped-parameter rainfall-runoff model

The simple rainfall-runoff model GR4J of Perrin et al. (2003) with a daily time step was applied and extended using a snow module based on Majone et al. (2010) and the computation of potential evapotranspiration proposed by Oudin et al. (2005). In the study of Perrin et al. (2003), 429 catchments were simulated for developing the GR4J model. These catchments show a great range of climatic conditions from semi-arid via temperate to tropically humid extending over flat as well as mountainous regions. However, no high alpine catchments were analyzed. Catchment areas range from 0.1 to 9890 km², and mean annual precipitation ranges from 300 to 2300 mm. The model has 4 parameters that are free to be calibrated (the symbols are kept as introduced by Perrin et al. (2003) for comparability): x_1 (the maximum capacity of the production or soil moisture accounting store in mm); x_2 (a water exchange coefficient in units of mm that can be positive if water enters the catchment, negative if water exits the catchment unobserved, or zero if there is no water exchange); x_3 (the maximum capacity of the routing store in mm) and x_4 (a time parameter expressed in units of days). The time parameter x_4 is applied for the unit hydrographs UH1 and UH2 that are used to simulate the time lag between a rainfall event and the resulting stream flow. For UH1 the water is distributed over a number of days (smallest integer exceeding x_4) with its maximum at the last day of the hydrograph. For UH2 the water is distributed over a time period about twice the number of days of UH1 (smallest integer exceeding $2^* x_4$). The peak outflow is reached at a similar time as the peak for UH1, then the water outflow decreases to zero at the end. The remaining parameters of the model have been found to be of minor importance on the model performance and have been kept constant in the GR4J by Perrin et al. (2003). For example the time lag for the direct runoff unit hydrograph (UH2) has been fixed to be twice the time lag of the unit hydrograph supplying the routing store (UH1).This is understandable, as it causes both unit hydrographs to have their peaks at (nearly) identical times. Moreover, a fixed 1:9 split of a direct and a slower flow component that passes the routing store has been introduced by Perrin et al. (2003). To support the findings of these authors, the influence of the latter on the model performance was investigated by incorporating this ratio as a free parameter. As a result, the approach of Perrin et al. (2003) was followed and analogous to them the parameters were kept constant here as well. Although solid precipitation is observed in some of the 429 catchments, no snow accumulation and melt was explicitly considered in the GR4J. However, as solid precipitation plays an obvious role in alpine catchments, a snow module was added using the simple degree-day snow module proposed by Majone et al. (2010) where only air temperature is required (adding three free parameters, T_s = temperature at which snow starts to fall; T_m = temperature at which snow starts to melt; C_m = melt factor that allows a certain amount of snow melt per degree temperature increase). In addition the GR4J requires potential evapotranspiration as model input which was determined by using a simple temperature dependent approach proposed by Oudin et al. (2005). This approach was already successfully applied in a modified monthly based version of the GR4J by Wagner et al. (2013) for a complex karst catchment in an alpine region. They could show that changes in the discharge characteristics after a flood event were only reproducible if parameters of the model were adapted. As such, the changes in storage capabilities of the rainfall-runoff model could be related to changes in the functionality of the karst system. It is noteworthy that e.g. Perrin et al. (2003), Mouelhi et al. (2006) and Wagner et al. (2013) pointed out that parameters in such simple models have physical relevance although their values are not comparable to field measurements (e.g. soil thickness).

In the following, we will call the model with its extensions GR4J+. Here, the impact of relict rock glaciers should become noticeable through applying GR4J+ to the catchments of the Seckauer Tauern Range if these landforms represent effective buffers/storage components within alpine watersheds. Moreover, a simple semi-distributed model approach is also applied. The discharge from all the rock glacier-influenced headwaters within the catchments FLcatch and UWcatch is computed separately with the GR4J+ using the modeled parameter set of the SRGcatch. The simulated runoff is then added as an external input (after the production store; Figure 4) to the remaining catchments FLcatch and UWcatch (without the rock glacier sub-catchments). In the following, this approach will be called GR4J+sd. As such, the remaining part of the catchment can be calibrated and validated without considering the relict rock glacier-influenced headwaters.

The model basically solves a water balance equation and common problems related thereto are to be expected (e.g. Uhlenbrook, 2006). Calibration and validation of the model is done by a split sample test (Klemes, 1986) using a combination of the classic Nash-Sutcliffe efficiency criterion (Nash and Sutcliffe, 1970) and the modified Nash-Sutcliffe criteria based on log-transformed and square root-transformed discharges (see Wagner et al., 2013). The classic Nash-Sutcliffe criteria places weight on high flows; the Nash-Sutcliffe efficiency criterion based on square root transformed streamflow places weight on low flow simulations and the third places weight on the intermediate flow (Perrin et al., 2003). All three criteria are computed separately, summed up and divided by 3 to remain within the criteria range (-infinity to 100 %) of the classical Nash-Sutcliffe criteria. We will call this combination $\overline{\text{NSE}}$. To assure that the model is not "right for the wrong reason" (Kirchner, 2006), the model is calibrated/validated and the results of the SRGcatch (the values of the parameter sets) are compared to supplementary information from field work (soil and vegetation cover; geomorphological mapping, surface geophysics, tracer tests, etc.) at the SRGcatch (e.g. Winkler et al., 2016a,b). Although model parameters cannot be estima-

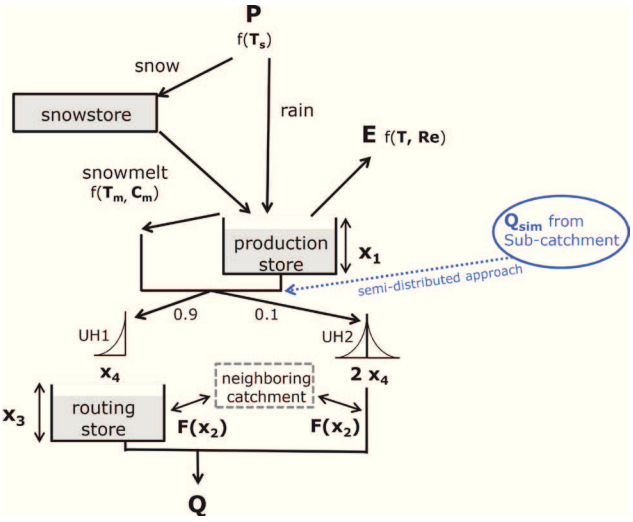

Figure 4: Model structure of the applied lumped-parameter rainfall-runoff model: GR4J+ = GR4J (Perrin et al., 2003) + snow module based on Majone et al. (2010) + potential evapotranspiration computation using the formula suggested by Oudin et al. (2005). Note the location where the simulated runoff from a sub-catchment (or sub-catchments) is added to the model if a simple semi-distributed approach is applied (GR4J+sd). P = precipitation; T = air temperature; T_s = temperature at which snow starts to fall; T_m = temperature at which snow starts to melt; C_m = melt factor that allows a certain amount of snow melt per degree temperature increase; Re = extraterrestrial solar radiation; x_1 = maximum capacity of the production store; F = groundwater exchange term acting on the fast and slow flow components; x_2 = water exchange coefficient; x_3 = maximum capacity of the routing store; x_4 = time parameter; UH1 and UH2 = unit hydrographs to account for the time lag between rainfall and resulting streamflow that depend on the time parameter x_4; Q_{sim} from sub-catchment = external input of runoff from a separately modelled sub-catchment; Q = runoff simulated by the rainfall-runoff model.

ted by field measurements directly (e.g. Mouelhi et al., 2006; Wagner et al., 2013), they do in fact have a physical relevance and a rational interpretation of the model output compared to field data is advised. If for example a catchment is composed of mainly bare rocks (like the SRGcatch) and the model would suggest a large value of x_1, which can be interpreted as the maximum capacity of a soil moisture accounting store (Perrin et al., 2003), the field data would simply question the model output/plausibility.

Rainfall and/or snowmelt (from the snow store) reach the production store (or soil moisture accounting store) with a maximum capacity x_1. A small amount of water percolates from this reservoir depending on the maximum capacity and the actual water level in the reservoir. This percolation is mainly interesting for low flow simulations. The actual evapotranspiration is computed based on the water content in the store relative to the maximum capacity x_1 and the potential evapotranspiration based on Oudin et al. (2005). If the maximum capacity of the store is reached, an outflow is generated. This is followed by a fixed separation of 1:9 where 10 % of the water goes to a unit hydrograph with a certain time lag (twice x_4 as fixed in the GR4J model of Perrin et al., 2003) representing direct runoff. The remaining 90 % of the water are distributed via a unit hydrograph with a time lag of x_4 that finally passes through a non-linear routing store of maximum capacity x_3. The routing store is draining according to the maximum capacity and the water level in the reservoir at each time step (Figure 4). As mentioned before, the fixed split of 1:9 is an outcome of the GR4J model development (see Perrin et al., 2003 and references therein). Nevertheless, various other fixed splits have been tested (e.g. 2:8, 3:7 and 0:10). Moreover, this split has been introduced as an additional free to be calibrated parameter. These results support the findings of Perrin et al. (2003), as this fixed split of 1:9 yielded the best model fit. Model runs including the split as an additional free parameter resulted in splits close to 1:9 (e.g. 0.7:9.3 or 1.1:8.9). However the model fit did not improve substantially to justify this additional parameter (as reported in Perrin et al., 2003). Importantly, the calibration of this split gave similar x_1 and x_3 compared to the fixed split of 1:9. If other fixed splits are used (2:8 and 3:7), x_1 and x_3 are consequently also slightly different; but the overall conclusion related to the relative values of the routing and production stores of the individual catchments remains unchanged (not shown here). As such, within the examined range, the influence of this split has only a minor influence on the actual storage parameters of the model, which are the main focus of our analysis as discussed later.

The unit hydrographs are used to simulate a time lag between rainfall events and resulting streamflow peaks by spreading effective rainfall over successive time steps (Perrin et al., 2003). The time parameter (x_4 for UH1 and twice x_4 for UH2) defines the time period of the unit hydrographs, i.e. the number of days the water is distributed over time to simulate peak flows. The smallest integers exceeding x_4 and $2*x_4$ define the number of unit hydrograph inputs for UH1 and UH2, respectively. The ordinates of the unit hydrographs are then derived from cumulative proportions of the input with time (S-curve method), thereby influencing the shape of the unit hydrographs and affecting the proportion of water distributed over the time period (for details see eq. 9-17 in Perrin et al., 2003). The non-linear routing store based on a power law is able to simulate long streamflow recessions, as the outflow reduces to very low values as the reservoir content relative to its maximum capacity declines over time (see eq. 20 in Perrin et al., 2003).

Moreover, based on the water level in the routing store, a groundwater exchange term is computed based on a water exchange coefficient x_2 and the reservoir content. This groundwater exchange term is computed for both flow components, the direct runoff and the one via the routing store. The total stream (or spring) flow is the output of the routing store and the direct runoff including (or subtracting) the exchange components. All four parameters in the model (x_1-x_4) are real numbers, where x_1 and x_3 are positive [mm]; x_2 [mm] can be zero, negative (outflow) or positive (inflow) and x_4 is greater than 0.5 [day]. Obviously, allowing more parameters to be calibrated, a model might yield a better fit; however as Perrin et al. (2003) could show, a simple model structure has to

be favored in order to avoid overparametrization of the model while still getting valuable information from model parameters about the catchment and its physical characteristics (e.g. Mouelhi et al., 2006; Wagner et al., 2013).

4. Results

4.1 Local scale – SRGcatch

The SRGcatch is simulated (calibrated and validated) using GR4J+ and the discharge data at the SEQ gauging station. The model yields acceptable model fits, which is demonstrated in Figure 5 by comparing observed and simulated runoff (spring discharge). The $\overline{NSE}$ values are given in Table 2 for calibration and validation periods. The available time series (see Table 1) were split into two equal parts (excluding a warm-up period); which were then used each for calibration and validation applying a simple split test according to Klemes (1986).

The GR4J+ and its optimal (based on $\overline{NSE}$) parameters found for the two input data sets (S-AWS and Schöner-ZAMG data sets) are compared to the median values of the study of Perrin et al. (2003) and discussed in the following (Table 3). First of all, the model allows observing the influence of solid precipitation in an alpine catchment. The model results of the snow accumulation and melt are compared to visual data available from a remote camera (S-RDC) that takes pictures of the catchment once a day. Although no quantitative information is possible, obvious snow cover changes correlate with changes in the snow accumulation of the snow module of the GR4J+ and support its functional efficiency (Figure 6). Subsequently, the storage of water from rainfall and/or snowmelt in the catchment is accomplished by a production and a routing store. Based on model calibration and validation, x_1 is rather small and seems to play a subordinate role, whereas x_3 is relatively large (especially compared to the median value from the study of Perrin et al. (2003)). Interestingly, x_4 is short and x_2 is positive, indicating that some additional water is necessary to satisfy the water balance. This deficit is especially noticeable when the S-AWS weather station data is used. This can likely be attributed to an underestimate of precipitation, especially during winter when wind and solid precipitation complicate the measurement in alpine catchments (e.g. Sevruk et al., 2009). Additional snow is deposited by the wind due to the northeast exposition of the cirque and a preferential western wind direction. Inflow into the catchment from a neighboring catchment can be excluded based on the geological settings. The short x_4 might be explained by a vadose zone that is passed rather quickly; which is consistent with the fast flow component identified by Winkler et al. (2016b). The small x_1 is related to the rather sparsely vegetated catchment with little to no soil. The rather

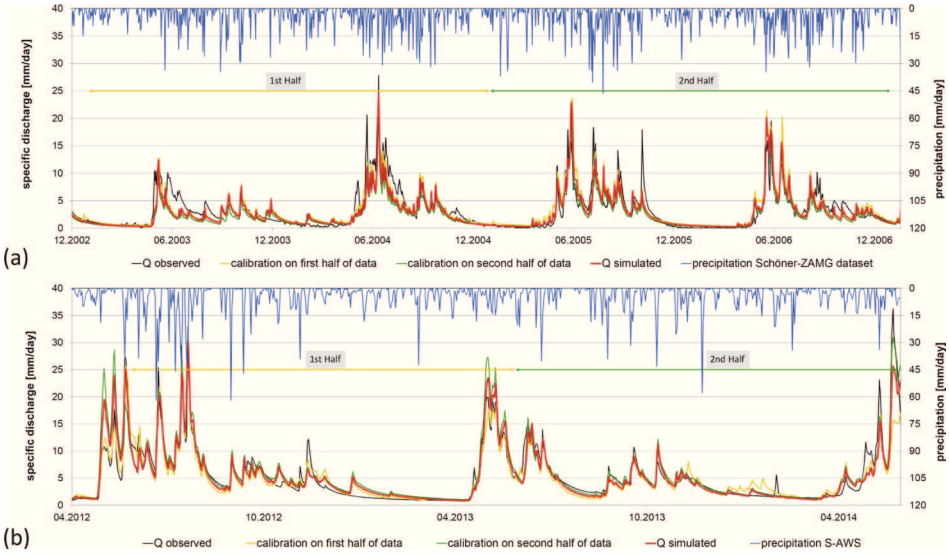

Figure 5: Comparison of observed and simulated runoff of SEQ using the GR4J+. Observed discharge is compared to simulated discharge based on calibration of different parts of the data (complete data set, first and second half) and the related validation is shown. For the time period 2002-2007, the forcing input (precipitation and air temperature) is based on the Schöner-ZAMG dataset (a); for the time period 2012-2014, the data from the S-AWS weather station is used (b).

efficiency criteria $\overline{NSE}$	complete time series		first half of data set		second half of data set	
	SchönerDS	S-AWS	SchönerDS	S-AWS	SchönerDS	S-AWS
calibration on total time series	**78.60**	**89.47**	75.89	90.73	80.05	87.41
calibration on first half of data set	74.36	84.81	**77.86**	**92.31**	71.23	73.02
calibration on second half of data set	76.20	87.50	68.82	86.02	**80.75**	**89.62**

Table 2: $\overline{NSE}$ values for calibration and validation of the first and second half of the data, respectively, and vice versa, as well as calibration of the whole time series (excluding a warm-up period; see Figure 5). Bold values are the calibration values, other values are related to the validation periods. For the time period 2002-2007, the forcing input (precipitation and airtemperature) is based on the Schöner-ZAMG dataset (SchönerDS); for the time period 2012-2014, the data directly from the S-AWS weather station is used.

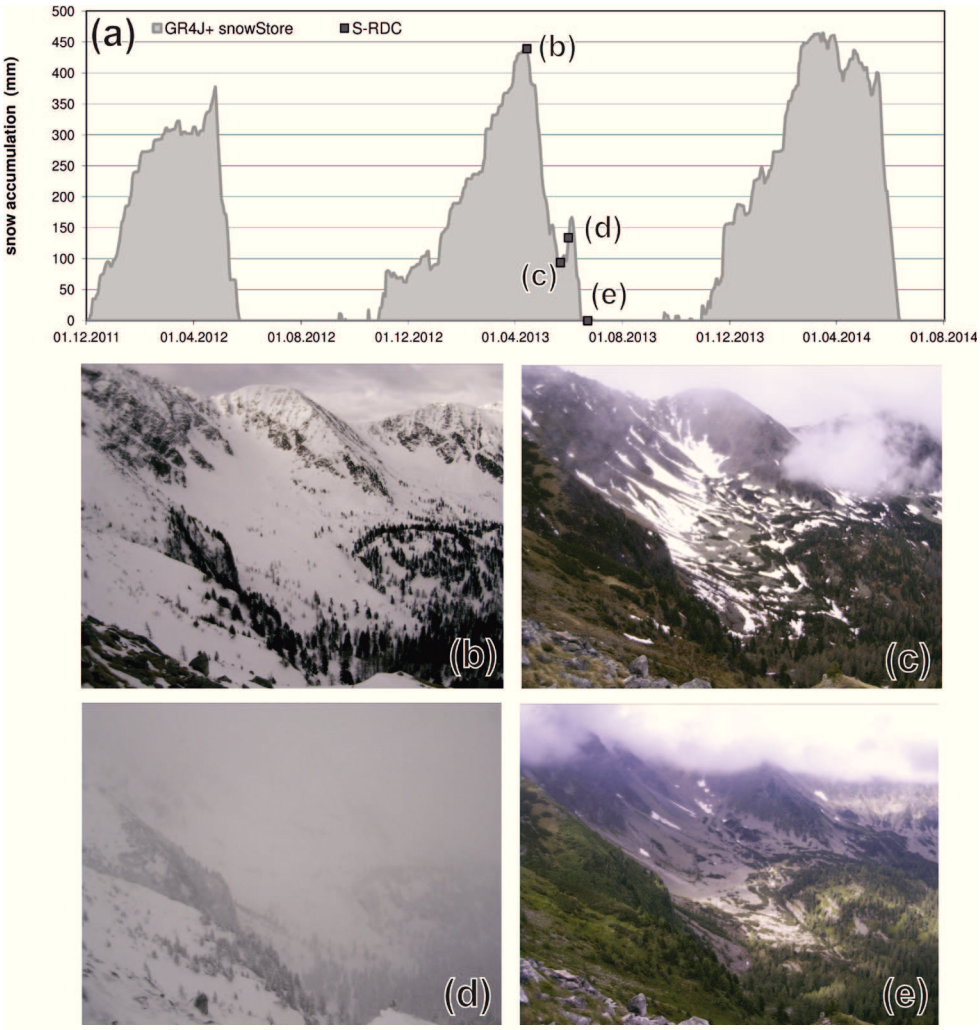

Figure 6: Comparison of snow model results and observed snow cover. (a) Modeled snow accumulation for the SRGcatch. Note the snow melt periods especially in May and June. (b-e) Extend of snow cover based on pictures of the S-RDC correlate well with the modelled snow accumulation and melt as indicated by exemplary photos related to certain time periods indicated in (a).

large x_3 indicates a substantial groundwater storage component. This is likely due to the debris accumulations of the relict rock glacier and the surrounding scree slopes, as there is not much storage in the fractured rock itself and a thick weathering zone is absent. Considering only these debris accumulations, the actual storage capacity can be assumed to be even higher, as the areal cover of the relict rock glacier makes up only 16.5 % of the total catchment while other debris accumulations cover 26.8 %. The actual volume of the sediment body representing the relict rock glacier is interestingly large with a maximum sediment thickness of more than 60 m (Winkler et al., 2016b). However, the actual storage is represented by the thickness of the saturated layer (e.g. Muir et al., 2011). Winkler et al. (2016b) suggested that the lowest 10 to 15 m are supposedly build up by finer grained sediments that act as the main aquifer. The overlaying layers seem to be

		S-AWS	Schöner/ZAMG dataset					Perrin et al. (2003)
		SRGcatch	SRGcatch	UW-fullyLump	UW-semiDistr	FL-fullyLump	FL-semiDistr	median (80 % conf. intervall)
efficiency criteria	$\overline{NSE}$ (%)	89.47	78.6	63.97	64.28	72.42	73.13	56.8
	$\overline{NSE}_Q$ (%)	89.5	76.32	59.98	60.34	64.59	65.74	51
	$\overline{NSE}_{\sqrt{Q}}$ (%)	90.1	81.41	64.7	64.98	74.42	74.89	61.9
	$\overline{NSE}_{\log Q}$ (%)	88.79	78.07	67.24	67.53	78.26	78.74	57.5
	WB (%)	97.58	90.58	97.5	98.45	96.51	96.64	79
model parameters	x_1 (mm)	89.78	14.55	1317.37	1513.38	490.26	568.46	350 (100 to 1200)
	x_2 (mm)	9.4	2.3	-0.02	0.01	-0.65	-1.03	0 (-5 to 3)
	x_3 (mm)	302.82	487.78	314.12	343.53	673.63	503.74	90 (20 to 300)
	x_4 (days)	1.15	1.33	1.26	1.43	1.65	1.41	1.7 (1.1 to 2.9)
	T_s (°C)	2.56	1.05	1.59	1.75	1.95	1.54	-
	T_m (°C)	4.61	4.1	4.18	3.5	3.4	4.08	-
	C_m (mm/°C)	3.65	3.32	2.45	1.86	2.54	2.72	-

Table 3: Model parameters and efficiency criteria (average, classical, square root-transformed and log-transformed Nash-Sutcliffe efficiency criteria, WB = water balance criterion) of the GR4J+ of the SRGcatch using the S-AWS and the Schöner-ZAMG data sets as forcing input and published median values (and 80 % confidence intervals) of the study of Perrin et al. (2003). Moreover, the model parameters and efficiency criteria of the UWcatch and the FLcatch using the GR4J+ and the GR4J+sd are displayed. WB = sum of the modelled runoff divided by the sum of the observed runoff in percent; values below 100 % indicate an underestimation of the modelled runoff, values above 100 % an overestimation.

unsaturated based on geophysical surveys (seismic refraction and ground penetrating radar; Winkler et al., 2016a,b).

The rainfall-runoff model, however, does not allow for direct identification of storage components or any hydraulic parameters. Nevertheless, a comparison of different catchments and/or sub catchments allows drawing conclusions regarding the relative importance of individual components. Compared to average parameter values from the study of Perrin et al. (2003), it is noteworthy that x_3 is rather large and x_1 rather small (Table 3). How this translates to the UWcatch and the FLcatch and the effect of relict rock glacier-influenced headwaters will be discussed later.

For the SRGcatch, it can be concluded that the GR4J+ is able to reproduce the observed runoff using both the S-AWS weather station data as well as the Schöner-ZAMG data set. Moreover, the model aids in aquifer characterization (i.e. it supports the findings of Winkler et al., 2016b). In general, the SRGcatch indicates a relatively large routing store and a rather small production store, in combination with a rather short time lag (within the vadoze zone). This might be representative for an alpine setting where relict rock glaciers and related screes are dominant.

4.2 A more regional scale – the influence of rock glaciers on downstream river flow

For the regional analysis, the forcing input parameters are extracted from the Schöner-ZAMG dataset as no meteorological data are available for the investigated catchments (besides S-AWS). For the larger catchments (FLcatch and UWcatch) it was aimed to quantify the influence of the rock glaciers in the individual catchments. In other words, is the signal of the large routing store (high storage capacities) of the SRGcatch still observable in the catchments FLcatch and UWcatch? Moreover, what is the actual contribution of the relict rock glacier sub-catchments to the total runoff of the two catchments at discrete time steps?

Table 3 shows the efficiency criteria of the model for the three different gauging stations SEQ (considering SRGcatch), FL and UW. Moreover, the hydrographs of observed versus simulated discharge (calibration and validation) of FL (7.26 km²) and UW (Liesing creek, 44.1 km²) are presented in Figure 7.

Figure 8 shows an overview of the storage parameters x_1 and x_3 of the GR4J+ of the three catchments and the relation to the fraction of rock glacier area, rock glacier-influenced catchment area, and scree area. Moreover, the median values and the 80 % confidence interval from the study of Perrin et al. (2003) are displayed. For the SRGcatch, x_1 is almost not noticeable at this scale (for values see Table 3). x_3 for the SRGcatch is additionally shown as area-corrected values, where it is assumed that the possible storage is reduced to the area of the rock glacier itself or the area of the rock glacier and the adjacent scree deposits. Moreover, for the UWcatch and the FLcatch, the storage parameters are shown

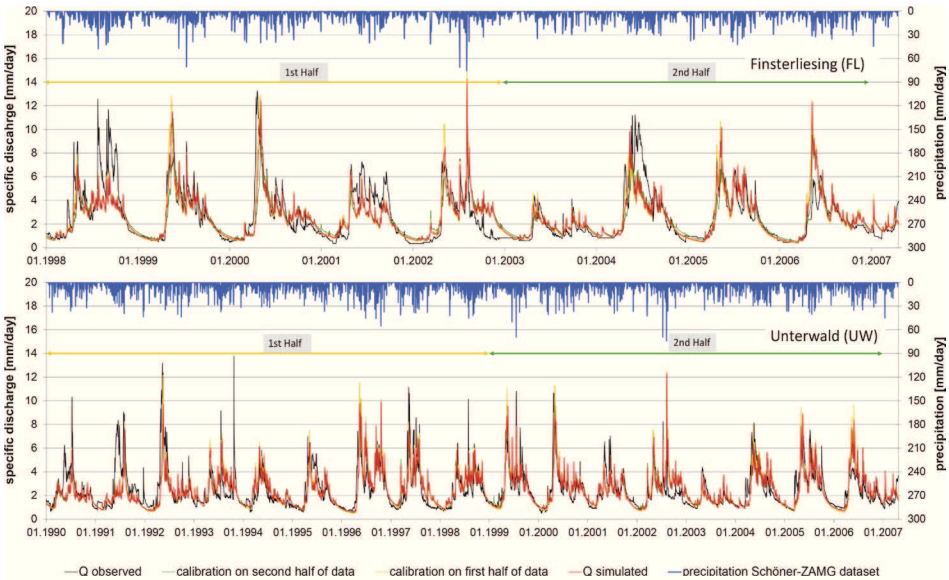

Figure 7: Observed and simulated runoffs of FL and UW using GR4J+. Observed discharge is compared to simulated discharge based on calibration on different parts of the data and the related validation is shown.

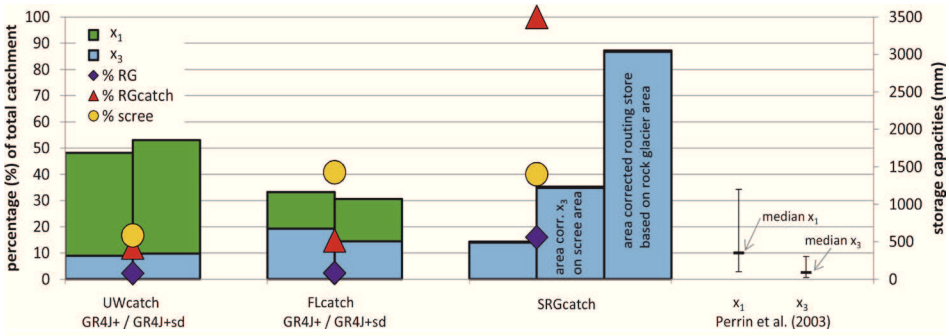

Figure 8: Graphical representation of the storage parameters x_1 and x_3 of the individual catchments considered in GR4J+ and GR4J+sd for the UWcatch and the FLcatch and in GR4J+ for the SRGcatch in comparison to the median parameters and the 80 % confidence interval from the study of Perrin et al. (2003). Moreover, SRGcatch additionally shows area-corrected values, with the possible storage reduced to the area of the rock glacier itself, and to the area of the rock glacier including the adjacent scree deposits (area corr. x_3 on scree area). Additionally, the fraction of rock glacier area (RG), rock glacier influenced catchment area (RGcatch), and scree area compared to the catchment area is displayed.

for the GR4J+ approach and for an extended semi-distributed approach (discussed in the next section).

Comparing model parameters of the GR4J+ approach with catchment characteristics shows that x_1 plays the most important role in the UWcatch. However, x_3 is also still above the median values of the study of Perrin et al. (2003) in this catchment. For the FLcatch, x_3 is more dominant than x_1, and both values are above the median of Perrin et al. (2003). For the SRGcatch, x_1 is almost negligible, while x_3 is relatively large. As much of the actual catchment is composed of bare rocks and steep cliffs, a more realistic area is used for the routing store by assuming that the contributing area where storage might take place is not the whole catchment area but is only related to the relict rock glacier area itself (area corrected routing store based on rock glacier area in Figure 8), or the area of the relict rock glacier and the adjacent scree deposits (area corr. x_3 on scree area in Figure 8). Because of the smaller considered area, the capacity of the store increases accordingly.

The simple internal model structure applied for the larger catchments is on the one hand suitable to simulate the runoff (operational mode: simulated flow acceptably agrees with observed data; Table 3), but might be too simple (not enough parameters/stores) to really reproduce the actual processes in the real catchment (principle of equifinality, e.g., Beven, 1993, 2006). However, the relatively large values of x_3 for the UWcatch and the FLcatch (Figure 8) indicate some storage component that might be related to the relict rock glacier-influenced sub-catchments (and/or other debris accumulations). However, based on these three catchments, increasing x_3 of the rainfall-runoff model seems to go hand in hand with increasing areal coverage of relict rock glaciers and/or debris accumulations within a catchment besides an obvious correlation of decreasing x_1 with increasing areal coverage of sparsely vegetated debris accumulations and bare rocks.

To elaborate on this, a semi-distributed approach was applied (GR4J+sd). The relict rock glacier-influenced parts of the UWcatch and the FLcatch are simulated separately and added to the UWcatch and the FLcatch as an external source (after the production store; see Figure 4). Therefore, the forcing input parameters of the catchments are computed only for the areas that are not influenced by the relict rock glaciers (6.2 km² and 38.7 km² for the FLcatch and the UWcatch, respectively). Table 3 compares the model fits as well as the resulting parameter sets of the UWcatch and the FLcatch using the fully lumped and the semi-distributed approach. Figure 9 compares the simulated hydrographs based on these two approaches.

Interestingly, for the semi-distributed approach, a relatively large x_3 is still needed to simulate the observed discharge accordingly for both catchments, although the influence of the relict rock glaciers is considered separately. For the FLcatch, x_3 decreases while x_1 increases. The semi-distributed approach suggests a small increase in both storage parameters of the UWcatch. However, the explicit consideration of the relict rock glaciers using GR4J+sd does not really change the storage capacities of the individual stores for both catchments. This leads to the conclusion that although the relict rock glaciers play a role in deferring the runoff, other storage components are also active and important in the UWcatch and the FLcatch. These storages are likely to be related to moraine materials and other scree deposits present in the catchments. Unfortu-

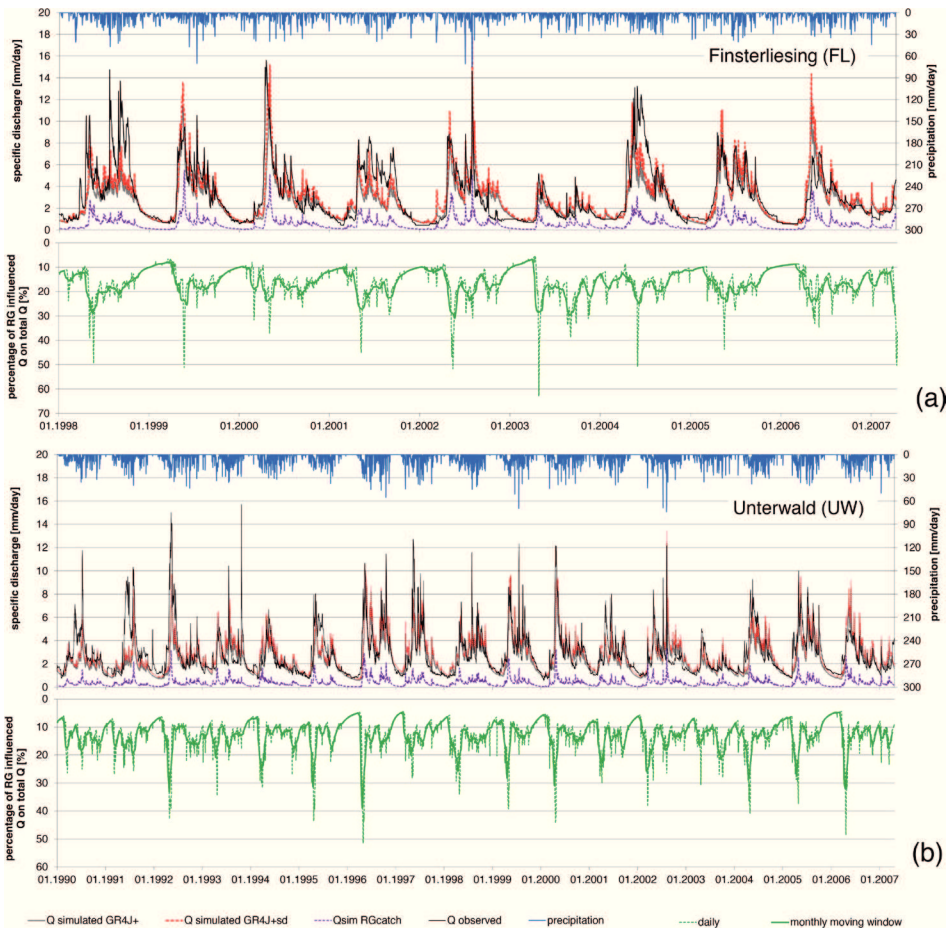

Figure 9: Observed and simulated runoff of Finsterliesing (FL) (a) and Unterwald (UW) (b) gauging stations. Simulated runoff based on the semi-distributed (GR4J+sd) and the fully lumped (GR4J+) approach and the simulated runoff from the respective rock glacier-influenced headwaters (Qsim RGcatch) is shown. In addition, the percentage of relict rock glacier (RG)-influenced headwater-runoff compared to the total runoff on a daily basis and using a one month moving window is displayed.

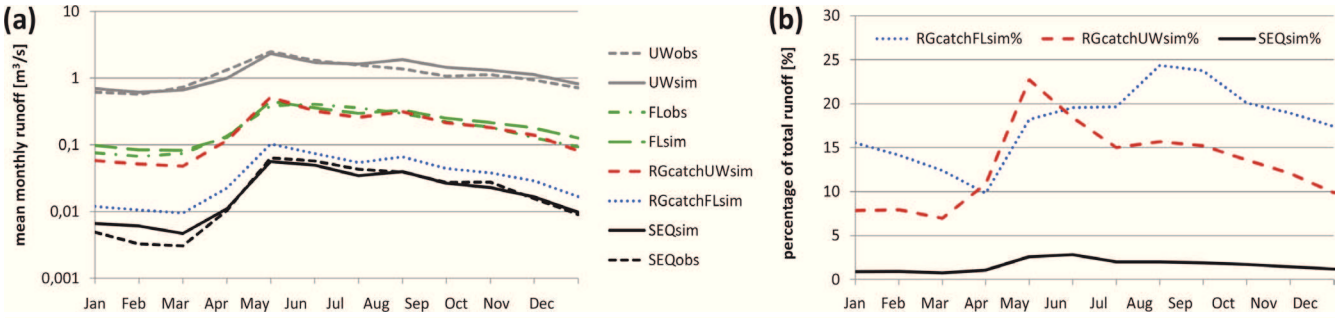

Figure10: Seasonal runoff contributions. (a) Seasonal mean monthly runoff for the time period 06/2002-04/2007 for the three gauging stations UW, FL and SEQ (observed = obs; simulated = sim), and the simulated runoff from the rock glacier-influenced headwaters within the FLcatch (RGcatchFLsim) and the UWcatch (RGcatchUWsim). (b) Percentage of simulated runoff from the relict rock glacier-influenced headwaters within the FLcatch (RGcatchFLsim %) and the UWcatch (RGcatchUWsim %) and the percentage of runoff from the SRGcatch at the SEQ gauging station within the UWcatch (SEQsim %).

nately, little is known about their storage capabilities in these particular catchments and further research is needed.

In addition to the contribution of rock glacier-influenced headwaters on the total runoff of the FLcatch and the UWcatch on a daily basis (Figure 9), Figure 10 shows the rock glacier-influenced headwater runoff versus the total runoff of the FLcatch and the UWcatch as monthly averages. Interestingly, the contribution of rock glacier influenced headwaters seems to play only a minor role during winter base flows. However, their contribution in the late snow melt period and during summer months is rather high. Based on these simulations, the average annual contribution of relict rock glacier-influenced headwaters on the FLcatch and the UWcatch is about 16 % and 13 %, respectively (note that this is slightly above the areal share, see Table 1). On a monthly average (see Figure 10b), the lowest values are in April for the FLcatch (10 %) and in March for the UWcatch (7 %) and the highest values in August (24 %) and May (23 %), respectively. On a daily basis (see Figure 9), the variation increases and ranges from about a quarter to more than four times of the areal share (runoff contribution of 6 % to 63 % for the FLcatch and 4 % to 52 % for the UWcatch compared to an areal share of 15 % and 12 %, respectively).

5. Discussion

Water resources studies in the 1990s already recognized the significance of relict rock glacier springs for the water supply for human consumption and the ecosystem in the Niedere Tauern Range (Untersweg and Schwendt 1995, 1996). The detailed understanding of the hydrogeological system/structure of relict rock glaciers such as the SRG is work in progress. Recent results are discussed by Winkler et al. (2016b). General aquifer and catchment characteristics of these alpine catchments can potentially be derived from rainfall-runoff models of different complexity. However, parsimonious models are to be favored for a more unique process-based interpretation in such alpine settings due to data limitations and the often limited information content of runoff time series (Jakeman and Hornberger, 1993). As aquifer (or catchment) characterization often leads to non-unique results (principle of equifinality; e.g. Beven, 1993, 2006), the mutual agreement of the conceptual model of Winkler et al. (2016b) and the model approach applied herein reinforce each other. Moreover, it allows to test the rainfall-runoff model in terms of its physical relevance (Mouelhi et al., 2006; Wagner et al., 2013).

To be able to quantify the storage capabilities and the influence of relict rock glaciers on stream flow further downstream, outflow from relict rock glacier catchments is computed based on simulated runoff using GR4J+ and the parameter set of the SRGcatch (ungauged basin approach). This simple approach takes all the (ungauged) relict rock glacier-influenced headwaters within the catchment into account. The simulated discharge of the rock glacier-influenced headwaters cannot be verified at the moment, but within the study area, the similarity of the SRGcatch to the other relict rock glacier-influenced catchments seems to be justified, and this can be seen as a valuable first approximation. Comparing this simulated outflow to discharge at a gauging station further downstream allows a detailed description of the impact of these landforms. Interestingly, the temporal contribution of relict rock glacier-influenced headwaters on streamflow of the FLcatch and the UWcatch at their gauging stations based on this approach indicates that in the late snowmelt period and during summer months, the contribution is a multiple of its areal share (up to 52 % for UWcatch and 63 % for FLcatch in Figure 9 related to an areal share of 12 % and 15 %, respectively). This seems to be related to the replenishing of the depleted routing (and also production) store during the snow melt period and the following summer storm events. As such, the relatively high volume of water in the routing store (x_3, representing the aquifer component) leads to a higher outflow during this time period as the outflow is related to the actual fill level of the store. Although delayed snow melt, which is common in higher parts of alpine catchments, also plays a role in delaying runoff (e.g. Hood and Hayashi, 2015), the important role of the production store is emphasized here by the fact that these observations are also made during summer time when no snow is present in the catchments. This is also in agreement with the observation of a faster aquifer response in times when the water level increases and upper, more conductive aquifer layers are

activated (Winkler et al., 2016b). The fast flow component of the relict rock glacier-influenced headwaters becomes more dominant and the buffer capabilities are reduced. However, during winter base flows, the contribution actually decreases to about half of the areal share (see Figs. 9 and 10) as storages are increasingly depleted and the outflow is further reduced. For the catchments FLcatch and UWcatch, the production store has a higher importance than for the SRGcatch, likely due to the more extensive soil cover and subsequent larger storage capacity (Figure 8).

Moreover, the comparison of the storage components of GR4J+ and GR4J+sd applied to alpine catchments which are influenced by relict rock glaciers, shows that the relict rock glaciers do not have as much of an influence on runoff during base flow as expected from field experience (e.g. Untersweg and Schwendt, 1996). The parameter sets of both approaches are rather similar, especially compared to the respective other catchment (UWcatch for FLcatch). As Hill (2006) pointed out, the use of simple models with a limited number of parameters is generally preferable over very complex models. However, this result might indicate that using only streamflow data in a relatively complex catchment, some information about catchment complexity might remain hidden. An increasing production store (x_1, representing the soil moisture accounting store) from the SRGcatch via the FLcatch to the UWcatch correlates with an increase in soil and vegetation cover. The routing store x_3 of the UWcatch is the smallest compared to the other two, but the largest values are obtained for the FLcatch. It has to be noted that there are other storage components besides relict rock glaciers in the FLcatch (and also the UWcatch) that additionally delay/buffer runoff. The role of other debris accumulations and especially one of moraine deposits needs further attention (e.g. Roy and Hayashi, 2009; Langston et al., 2011). Moreover, ambiguities are to be expected due to the fact that different debris accumulations might have different (aquifer) thicknesses and subsequent storage volumes; the differences between areal coverage (applied in the approach herein) and actual volume of the debris accumulations needs to be further examined.

Nevertheless, the hydrological response of relict rock glaciers seems to be of importance for the transformation of precipitation to runoff in alpine catchments. On the one hand, the lumped-parameter model is able to reproduce the observed runoff behavior of the SRGcatch, and on the other hand, based on a recent hydrogeological (and geophysical) study at the SRGcatch (Winkler et al., 2016b), the model can further be used to aid in catchment/aquifer characterization. However, if parts of the model region (here the catchment and especially the rock glacier itself) become better understood or the model region becomes more complex, a more distributed model is required to account for this added knowledge, or more parameters/storages are needed to account for it. This will in turn increase model complexity. However, the necessary additional input data to justify a more complex model is usually unavailable.

6. Conclusions

A simple rainfall-runoff model was able to reproduce the observed runoff from a relict rock glacier spring catchment as well as the runoff in alpine catchments that are affected by relict rock glacier-influenced headwaters.

The parameter sets of the rainfall-runoff model can be related to catchment characteristics. The relict Schöneben Rock Glacier is associated with a high storage capacity of the routing store, which fits with the current conceptual understanding of the catchment/aquifer system. However, the results are more ambiguous when catchment characteristics become more complex. Other debris accumulations, such as moraine deposits and scree slopes, also seem to play an important role in the catchments with rock glacier influenced headwaters.

Applying a simple semi-distributed approach, the runoff drained from relict rock glaciers can explicitly be accounted for in catchments further downstream. These results suggest that a significant influence on downstream river flow is observed during the late snow melt period and summer time, that reaches a multiple (more than four times) of its areal share.

Finally, it needs to be pointed out that the applied model could potentially be used to apply climate projections (precipitation rate/intensity, temperature) to study the impact of relict rock glaciers or other sediment accumulations such as moraines or scree slopes in alpine catchments in a changing environment. As precipitation patterns change and increasing temperature alters the time and duration of solid precipitation, the impact of these relict rock glacier-influenced headwaters on stream flow further downstream might become (even) more important and are subject of future research.

Acknowledgements

This study was funded by the European Regional Development Fund (ERDF) and the Federal Government of Styria. The authors are grateful to the Hydrographic Service of Styria for providing the discharge data. The digital elevation models and the topographic maps were provided by the GIS Service of the Federal Government of Styria (GIS Steiermark). The temperature and precipitation data (Schöner-ZAMG dataset and Climate Atlas Styria) were kindly provided by the Zentralanstalt für Meteorologie und Geodynamik (ZAMG). We acknowledge the very constructive suggestions by Masaki Hayashi and an anonymous reviewer that greatly improved the paper.

References

Andréassian, V., Perrin, C. and Michel. C., 2004. Impact of imperfect potential evapotranspiration knowledge on the efficiency and parameters of watershed models. Journal of Hydrology, 286, 19-35. http://dx.doi.org/10.1016/j.jhydrol.2003.09.030

Barnett, T.P., Adam, J.C. and Lettenmaier, D.P., 2005. Potential impacts of a warming climate on water availability in snow-dominated regions. Nature, 438, 303-309. http://

dx.doi.org/10.1038/nature04141

Barsch, D., 1996. Rockglaciers: Indicators for the present and former geoecology in high mountain environments. Springer Series in Physical Environment 16. Springer Verlag, Berlin, 331 pp.

Beven, K., 1993. Prophecy, reality and uncertainty in distributed hydrological modeling. Advances in Water Resources, 16, 41-51. http://dx.doi.org/10.1016/0309-1708(93)90028-E

Beven, K., 2006. A manifesto for the equifinality thesis. Journal of Hydrology 320, 18-36. http://dx.doi.org/10.1016/j.jhydrol.2005.07.007

Buttle, J.M., 1994. Isotope hydrograph separations and rapid delivery of pre-event water from drainage basins. Progress in Physical Geography 18, 16-41. http://dx.doi.org/10.1177/030913339401800102

Clow, D.W., Schrott, L., Wobb, R., Campell, D.H., Torizzo, A. and Dornblaser, M., 2003. Ground water occurrence and contributions to streamflow in an alpine catchment, Colorado Front Range. Ground Water, 41, 937-950. http://dx.doi.org/10.1111/j.1745-6584.2003.tb02436.x

Gasser, D., Gusterhuber, J., Krische, O., Puhr, B., Scheucher, L., Wagner. T. and Stüwe, K., 2009. Geology of Styria: An overview. Mitteilungen des naturwissenschaftlichen Vereins für Steiermark, 139, 5-36.

Gray, D. M., 1970. Handbook on the Principles of Hydrology. National Research Council of Canada, Secretariat, Canadian National Committee for the International Hydrological Decade, Ottawa, Canada, 625 pp.

Haeberli W., Hallet, B., Arenson, L., Elconin, R., Humulum, O., Kääb, A., Kaufmann, V., Ladanyi, B., Matsuoka, N., Springman, S. and VonderMühll, D., 2006. Permafrost creep and rock glacier dynamics. Permafrost and Periglacial Processes 17, 189-216. http://dx.doi.org/10.1002/ppp.561

Hausmann, H., Krainer, K., Brückl, E. and Ullrich, C., 2012. Internal structure, ice content and dynamics of Ölgrube and Kaiserberg rock glaciers (Ötztal Alps, Austria) determined from geophysical surveys. Austrian Journal of Earth Sciences 105/2, 12-31.

Hill, M.C., 2006. The practical use of simplicity in developing ground water models. Ground Water, 44/6, 775-781. http://dx.doi.org/10.1111/j.1745-6584.2006.00227.x

Hood, J.L. and Hayashi, M., 2015. Characterization of snowmelt flux and groundwater storage in an alpine headwater basin. http://dx.doi.org/10.1016/j.jhydrol.2014.12.041

Jakeman, A.J. and Hornberger, G.M., 1993. How much complexity is warranted in a rainfall-runoff model? Water Resources Research, 29/8, 2637-2649. http://dx.doi.org/10.1029/93WR00877

Kellerer-Pirklbauer, A., Lieb, G.K. and Kleinferchner, H., 2012. A new rock glacier inventory of the Eastern European Alps. Austrian Journal of Earth Sciences 105/2, 78-93.

Kirchner, J.W., 2003. A double paradox in catchment hydrology and geochemistry. Hydrological Processes 17, 871-874. http://dx.doi.org/10.1002/hyp.5108

Kirchner, J.W., 2006. Getting the right answers for the right reasons: Linking measurements, analyses, and models to advance the science of hydrology. Water Resources Research, 42/3, W03S04. http://dx.doi.org/10.1029/2005WR004362

Klemes, V., 1986. Operational testing of hydrological simulation models. Hydrological Sciences Journal, 31/1, 13-24. http://dx.doi.org/10.1080/02626668609491024

Krainer, K. and Ribis, M., 2012. A Rock Glacier Inventory of the Tyrolean Alps (Austria). Austrian Journal of Earth Sciences 105/2, 32-47.

Krainer, K., Kellerer-Pirklbauer, A., Kaufmann, V., Lieb, G.K., Schrott, L. and Hausmann, H., 2012. Permafrost Research in Austria: History and recent advances. Austrian Journal of Earth Sciences 105/2, 2-11.

Krainer, K., Bressan, D., Dietre, B., Haas, J.N., Hajdas, I., Lang, K., Mair, V., Nickus, U., Reidl, D., Thies, H. and Tonidandel, D., 2015. A 10,300-year-old permafrost core from the active rock glacier Lazaun, southern Ötztal Alps (South Tyrol, northern Italy). Quaternary Research 83, 324-335. http://dx.doi.org/10.1016/j.yqres.2014.12.005

Langston, G., Bentley, L.R., Hayashi, M., McClymont, A.F. and Pidlisecky, A., 2011. Internal structure and hydrological functions of an alpine proglacial moraine. Hydrological Processes 25/19, 2967-2982. http://dx.doi.org/10.1002/hyp.8144

López-Moreno, J.I. and García-Ruiz, J.M., 2004. Influence of snow accumulation and snowmelt on streamflow in the central Spanish Pyrenees. Hydrological Sciences Journal 49/5, 787-802. http://dx.doi.org/10.1623/hysj.49.5.787.55135

Majone, B., Bertagnoli, A. and Bellin A., 2010. A non-linear runoff generation model in small Alpine catchments. Journal of Hydrology, 385, 300-312. http://dx.doi.org/10.1016/j.jhydrol.2010.02.033

Millar, C.I., Westfall, R.D. and Delany, D.L., 2013. Thermal and hydrologic attributes of rock glaciers and periglacial talus landforms: Sierra Nevada, California, USA. Quaternary International, 310, 169-180. http://dx.doi.org/10.1016/j.quaint.2012.07.019

Monnier, S., Camerlunck, C., Rejiba, F., Kinnard, C., Feuillet, T. and Dhemaied, A., 2011. Structure and genesis of the Thabor rock glacier (Northern French Alps) determined from morphological and ground-penetrating radar surveys. Geomorphology 134, 269-279. http://dx.doi.org/10.1016/j.geomorph.2011.07.004

Monnier, S. and Kinnard, C., 2015. Internal Structure and Composition of a Rock Glacier in the Dry Andes, Inferred from Ground-penetrating Radar Data and its Artefacts. Permafrost and Periglacial Processes. http://dx.doi.org/10.1002/ppp.1846

Mouelhi, S., Michel, C., Perrin, C. and Andréassian, V., 2006. Stepwise development of a two-parameter monthly water balance model. Journal of Hydrology, 318, 200-214. http://dx.doi.org/10.1016/j.jhydrol.2005.06.014

Muir, D.L., Hayashi, M. and McClymont, A.F., 2011. Hydrological storage and transmission characteristics of an alpine talus. Hydrological Processes 25, 2954-2966. http://dx.doi.org/10.1002/hyp.8060

Nash, J.E. and Sutcliffe, J.V., 1970. River flow forecasting

through conceptual models. Part I – A discussion of principles. Journal of Hydrology, 10/3, 282-290. http://dx.doi.org/10.1016/0022-1694(70)90255-6

Oudin, L., Hervieu, F., Michel, C., Perrin, C., Andréassian, V., Anctil, F. and Loumagne, C., 2005. Which potential evapotranspiration input for a lumped rainfall-runoff model? Part 2 – Towards a simple and efficient potential evapotranspiration model for rainfall-runoff modeling. Journal of Hydrology, 303, 290-306. http://dx.doi.org/10.1016/j.hydrol.2004.08.026

Oudin, L., Andréassian, V., Perrin, C., Michel, C. and Le Moine, N., 2008. Spatial proximity, physical similarity, regression and ungaged catchments: A comparison of regionalization approaches based on 913 French catchments, Water Resources Research, 44/3, W03413, http://dx.doi.org/10.1029/2007WR006240.

Perrin, C., Michel, C. and Andréassian, V., 2003. Improvement of a parsimonious model for streamflow simulation. Journal of Hydrology, 279, 275-289. http://dx.doi.org/10.1016/S0022-1694%2803%2900225-7

Prettenthaler, F., Podesser, A. and Pilger, H. (eds.), 2010. Studien zum Klimawandel. Band IV: Klimaatlas Steiermark Periode 1971-2000. Eine anwenderorientierte Klimatographie. ÖAW, Vienna, 358 pp.

Roy, J.W. and Hayashi, M., 2009. Multiple, distinct groundwater flow systems of a single moraine-talus feature in alpine watershed. Journal of Hydrology, 373, 139-150. http://dx.doi.org/10.1016/j.jhydrol.2009.04.018

Schmid, S.M., Fügenschuh, B., Kissling, E. and Schuster, R., 2004. Tectonic map and overall architecture of the Alpine orogen. Eclogae Geologicae Helvetiae, 97/1, 93-117. http://dx.doi.org/10.1007/s00015-004-1113-x

Schöner, W. and Dos Santos Cardoso, E., 2004. Datenbereitstellung, Entwicklung von Regionalisierungstools und einer Schnittstelle zu den regionalen Klimamodellen (Arbeitsbericht für den Zeitraum 1.11.2003 bis 30.9.2004). Projektbericht für das Projektjahr 1, Projekt reclip:more (Research for Climate Protection: Model Run Evaluation). 44 pp, http://foresight.ait.ac.at/SE/projects/reclip/reports/report6_Regionalisierung_ZAMG.pdf

Sevruk, B., Ondrás, M. and Chvíla, B., 2009. The WMO precipitation measurement intercomparisons. Atmospheric Research, 92, 376-380. http://dx.doi.org/10.1016/j.atmosres.2009.01.016

Uhlenbrook, S., 2006. Catchment hydrology – a science in which all processes are preferential. Hydrological Processes 20/16, 3581-3585. http://dx.doi.org/10.1002/hyp.6564

Untersweg, T. and Schwendt, A., 1995. Die Quellen der Blockgletscher in den Niederen Tauern. Bericht der wasserwirtschaftlichen Planung Nr. 78, Graz, 76 pp.

Untersweg, T. and Schwendt, A., 1996. Blockgletscher und Quellen in den Niederen Tauern. Mitteilungen der Österreichischen Geologischen Gesellschaft, 87, 47-55.

Wagner, T., Themeßl, M., Schüppel, A., Gobiet, A., Stigler, H. and Birk, S., 2012. Auswirkungen des Klimawandels auf Abfluss und Wasserkrafterzeugung österreichischer Flüsse. Niederschlags-Abfluss-Modellierung basierend auf vier Klimaszenarien bis 2050. Wasserbau Symposium 2012 Tagungsband, Graz. ISBN 978-3-85125-230-9, pp. 1-8.

Wagner, T., Mayaud, C., Benischke, R. and Birk, S., 2013. Ein besseres Verständnis des Lurbach-Karstsystems durch ein konzeptionelles Niederschlags-Abfluss-Modell. Grundwasser, 18, 225-235. http://dx.doi.org/10.1007/s00767-013-0234-4

Weijs, S.V., Mutzner, R. and Parlange, M.B., 2013. Could electrical conductivity replace water level in rating curves for alpine streams? Water Resources Research 49/1, 343-351. http://dx.doi.org/10.1029/2012WR012181

Winkler, G., Pauritsch, M., Wagner, T. and Kellerer-Pirklbauer, A., 2016a. Reliktische Blockgletscher als Grundwasserspeicher in alpinen Einzugsgebieten der Niederen Tauern. Berichte der Wasserwirtschaftlichen Planung Steiermark, Band 87, 134 p.

Winkler, G., Wagner, T., Pauritsch, M., Birk, S., Kellerer-Pirklbauer, A., Benischke, R., Leis, A., Morawetz, R., Schreilechner, M.G. and Hergarten, S., 2016b. Identification and assessment of flow and storage components of the relict Schöneben Rock Glacier, Niedere Tauern Range, Eastern Alps (Austria). Hydrogeology Journal. http://dx.doi.org/10.1007/s10040-015-1348-9

Wolff, M.A., Isaksen, K., Petersen-Øverleir, A., Ødemark, K., Reitan, T. and Brækkan, R., 2015. Derivation of a new continuous adjustment function for correcting wind-induced loss of solid precipitation: results of a Norwegian field study. Hydrology and Earth System Sciences, 19, 951-967. http://dx.doi.org/10.5194/hess-19-951-2015

Zurawek, R., 2002. Internal Structure of a Relict Rock Glacier, Sleza Massif, Southwest Poland. Permafrost and Periglacial Processes 13, 29-42. http://dx.doi.org/10.1002/ppp.403

Zurawek, R., 2003. The problem of the identification of relict rock glaciers on sedimentological evidence. Landform Analysis 4, 7-15.

Received: 18 May 2015
Accepted: 12 November 2015

Thomas WAGNER[1)*)], Marcus PAURITSCH[1)] & Gerfried WINKLER[1)]
Institute of Earth Sciences, NAWI Graz Geocenter, University of Graz, Heinrichstrasse 26, 8010 Graz, Austria;
*) Corresponding author: thomas.wagner@uni-graz.at

8. Appendix

Selection of conference abstracts related to this thesis

A) Pauritsch M, Wagner T, Winkler G, Birk S (2016) A numerical groundwater model to assess the hydrogeological behavior of a relict rock glacier aquifer (Niedere Tauern Range, Austria), Geophysical Research Abstracts Vol. 18, EGU2016-15561, 2016

B) Pauritsch M, Hergarten S, Winkler G, Birk S (2015) Analytical solutions for recession analyses of sloping aquifers in alpine catchments, Geophysical Research Abstracts Vol. 17, EGU2015-14986, 2015

C) Pauritsch M, Wagner T, Winkler G, Birk S (2015) Hydrogeological assessment of a relict glacier aquifer using a numerical groundwater model (Niedere Tauern Range, Austria)

D) Pauritsch M, Birk S, Hergarten S, Kellerer-Pirklbauer A, Winkler G (2014) Analytical solutions for recession analyses of sloping aquifers –applicability on relict rock glaciers in alpine catchments Geophysical Research Abstracts Vol. 16, EGU2014-11682, 2014

E) Pauritsch M, Winkler G, Kellerer-Pirklbauer A, Birk S (2013) Hydraulic properties and inner structure of a relict rock glacier in the Eastern Alps, Austria, Geophysical Research Abstracts Vol. 15, EGU2013-8394, 2013

F) Pauritsch M, Kellerer-Pirklbauer A, Birk S, Winkler G (2012) Discharge dynamics of a relict rock glacier in a crystalline catchment in the Seckauer Tauern, Austria, Geophysical Research Abstracts Vol. 14, EGU2012-7546, 2012

A

A numerical groundwater model to assess the hydrogeological behavior of a relict rock glacier aquifer (Niedere Tauern Range, Austria)

A three dimensional numerical groundwater model representing a relict rock glacier with an extent of 0.17 km², located in the Eastern Alps (Schöneben rock glacier, Niedere Tauern Range, Austria) is used to highlight the impact of the major internal aquifer structures and the morphology of the aquifer base on the discharge behavior. The model is implemented in MODFLOW and calibrated using the discharge data of the spring. The recharge is determined based on precipitation and evapotranspiration which is calculated using a simple soil water balance model in combination with the monthly potential evapotranspiration. Data are provided by an automatic weather station on the Schöneben rock glacier where precipitation and air temperature are continuously measured. It is renounced to use a snow model in order to keep the model as simple as possible. Therefore the investigation is limited to the time periods from late summer to the beginning of the snowmelt in spring. The aquifer geometry and in particular the morphology of the aquifer base are based on geophysical investigations (ground penetrating radar and seismic refraction). However, due to gaps of the geophysical investigations the interpolation of the aquifer base at the margin of the rock glacier is related to uncertainties. Therefore, two different morphologies of the aquifer base were used which mainly differ in the slope of the south-eastern margin. Several model setups with increasing complexity of the internal structure (from homogeneous to heterogeneous) were applied to demonstrate the effects of the vertical (layering) and horizontal (preferential flow) aquifer heterogeneity on the discharge behavior. The results show that a model with a homogeneous setup cannot satisfyingly reproduce the discharge dynamics observed at the Schöneben rock glacier. With a heterogeneous setup, the model fit greatly improves but shows differences between the horizontally and vertically heterogeneous setups. The morphology of the aquifer base is important for the discharge behavior, especially when a simple internal structure is considered. However, with a more complex internal structure including a higher number of parameters, the impact of the aquifer base can be compensated through the calibration of the other aquifer parameters. Among the investigated model setups the best fit to the observed discharge is achieved in the calibration as well as in the validation by a combination of vertical and horizontal heterogeneities, which are related to differences in hydraulic conductivities of about three orders of magnitude (in the range of 10-2 to 10-5 m/s). This indicates that relict rock glaciers cannot be considered as simple homogeneous aquifer systems but as highly heterogeneous and that their consideration in alpine catchments is not straightforward.

B

Analytical solutions for recession analyses of sloping aquifers in alpine catchments

Analytical solutions for the discharge recession of sloping aquifers are commonly used to simulate the runoff of shallow aquifers with slope angles of a few degrees and in particular hillslopes. However, in alpine catchments, potentially deeper aquifers represented by debris accumulations such as relict rock glaciers can be found in areas with much steeper slope angles. These aquifers might be important for flood reduction and drought prevention and the discharged water can be used for drinking water supply and small hydroelectric power plants. Here it is attempted to reproduce the recession behavior of such highly inclined aquifers by applying existing analytical solutions for sloping aquifers.

More specifically, an analytical solution for the discharge recession of a sloping aquifer is compared to a numerical model (MODFLOW) for a variety of slope angles. In addition a sensitivity analysis is made to reveal the effects of the various approximations introduced in the analytical solution, such as homogeneity, parallel side boundaries and a straight profile.

The results show that the deviation between the analytical solution and the numerical model depends on the hydraulic properties and is in general acceptable for all tested slope angles. However, the sensitivity analysis shows that the simplifying assumptions and especially the initial condition have great impact on the discharge recession. Therefore, only the long-term behavior of the analytical solution should be considered if the model is employed for aquifer characterization. In summary, the combined use of analytical solutions and simple numerical models helps to better understand the opportunities and limitations of the recession analysis of sloping aquifers.

C

Hydrogeological assessment of a relict glacier aquifer using a numerical groundwater model (Niedere Tauern Range, Austria)

A three dimensional numerical groundwater flow model (implemented in MODFLOW) of the relict Schöneben-rock glacier, located in the Styrian Niedere Tauern Range is used to highlight the impact of the major internal structure of the aquifer and the topography of the aquifer base on the discharge behavior. The aquifer geometry and in particular the topography of the aquifer base is identified using geophysical investigations (ground penetrating radar and seismic refraction). Due to gaps of the geophysical investigations the interpolation of the aquifer base margin is related to uncertainties. Therefore two different shapes of the aquifer base were determined which differ mainly in the slope of the south-eastern margin. The recharge is determined based on precipitation and air temperature data, which are continuously measured on the Schöneben-rock glacier and a calculated evapotranspiration. As there are no piezometers on the rock glacier and also no other information about the groundwater level, the model is only calibrated using the discharge data of the spring. Several model setups with increasing complexities (from homogeneous to heterogeneous internal structure) were applied to demonstrate the effects of the vertical and horizontal aquifer heterogeneity on the discharge behavior. In general the discharge behavior is better reproduced with a layered internal structure supporting the current conceptual understanding of relict rock glaciers. However, none of the model setups succeed in simulating the observed long-term baseflow recession. Therefore, an alternatively shaped aquifer base with a lower slope angle in the south-eastern part was additionally applied yielding better results. This suggests that not only the internal structure but also the aquifer base topography highly impacts the discharge behavior of such aquifers.

D

Analytical solutions for recession analyses of sloping aquifers – applicability on relict rock glaciers in alpine catchments

Rock glaciers as aquifer systems in alpine catchments may strongly influence the hydrological characteristics of these catchments. Thus, they have a high impact on the ecosystem and potential natural hazards such as for example debris flow. Therefore, knowledge of the hydrodynamic processes, internal structure and properties of these aquifers is important for resource management and risk assessment. The investigation of such aquifers often turns out to be expensive and technically complicated because of their strongly limited accessibility. Analytical solutions of discharge recession provide a quick and easy way to estimate aquifer parameters. However, due to simplifying assumptions the validity of the interpretation is often questionable. In this study we compared results of an analytical solution of discharge recessions with results based on a numerical model. This was done in order to analyse the range of uncertainties and the applicability of the analytical method in alpine catchment areas. The research area is a 0.76 km² large catchment in the Seckauer Tauern Range, Austria. The dominant aquifer in this catchment is a rock glacier, namely the Schöneben Rock Glacier. This relict rock glacier (i.e. containing no permafrost at present) covers an area of 0.11 km² and is drained by one spring at the rock glacier front. The rock glacier consists predominantly of gneissic sediments (mainly coarse-grained, blocky at the surface) and extends from 1720 to 1905 m a.s.l.. Discharge of the rock glacier spring is automatically measured since 2002. Electric conductivity and water temperature is monitored since 2008. An automatic weather station was installed in 2011 in the central part of the catchment. Additionally data of geophysical surveys (seismic refraction and ground penetrating radar) have been used to analyse the base slope and inner structure of the rock glacier. The measured data are incorporated into a numerical model implemented in MODFLOW. The numerical model was then compared to the analytical solution based on the one dimensional Boussinesq equation for unconfined flow in sloping aquifers. Field observations as well as results from the numerical model suggest that the rock glacier has a complex internal structure with zones of low hydraulic conductivity and a high conductive layer on top. The analytical solution attempts to represent this heterogeneous aquifer by an equivalent homogeneous medium. However, as the relative contribution of the different aquifer components varies throughout the recession, the parameter estimates are not easily interpreted in terms of actual aquifer properties. Employing analytical solutions for recession analysis in this type of setting therefore requires a sound understanding of the internal structure and its influence on the flow and storage processes within the rock glacier.

E

Hydraulic properties and inner structure of a relict rock glacier in the Eastern Alps, Austria

Water economic studies in 1990s documented the importance of the springs draining relict rock glaciers for water supply and human consumption as well as for the ecosystem in alpine catchments in the Niederen Tauern Range, Austria. Recent studies confirm the hydrologic importance and show that in the easternmost subunit, the Seckauer Tauern Range, more than 40% of the area above 2000 m a.s.l. and up to 20% of the area above 1500 m a.s.l. drain through relict rock glaciers. Thus, the hydraulic properties of these alpine aquifers are considered to be important controls on the hydrology of these areas. Nevertheless their hydraulic properties and their inner structure are still poorly understood. Our hydrogeological research is carried out at the Schöneben Rock Glacier, located in Seckauer Tauern Range, Austria. This rock glacier is presumably relict although patches of permafrost might exist particularly in the upper part of the landform. The rock glacier covers an area of 0.11 km² and drains a total catchment of 0.76 km² with a maximum elevation of 2282 m a.s.l.. The rock glacier consists predominantly of gneissic sediments (mainly coarse-grained, blocky at the surface) and extends from 1720 to 1905 m a.s.l.. Discharge of the rock glacier spring is recorded since 2002. Electrical conductivity and water temperature used as natural tracers are continuously monitored since 2008. Furthermore, a tracer test with simultaneous injection of the fluorescent dyes naphthionate and fluoresceine at two injection points (one close to the front and one close to the rooting zone of the rock glacier) was performed. Recession analysis of the spring hydrograph reveals similarities to the flow dynamics of karst springs. The results exhibit on the one hand a slow base flow recession indicating a high storage capacity and on the other hand sharp discharge peaks immediately after rainfall events referring to a high hydraulic conductivity. Applying different analytic runoff models, the hydrograph analysis provides two possible conceptual aquifer models: (1) an aquifer with multiple overlapping exponential runoff components and (2) a single homogeneous aquifer with a runoff following a power law function triggered by diverging recharge pulse durations. Best fits to the analysed hydrographs were achieved with a 25 days recharge pulse and a base flow coefficient of 0.002 d-1. The recession coefficients of the multiple exponential runoff components range from 0.04 to 0.001 d-1. The derived hydraulic conductivity indicates a sandy, poorly silty aquifer for the base flow component. The peak of the fluoresceine breakthrough curve was observed after approximately 90 days, fitting well to the reciprocal of the base flow recession coefficient. The spring responds within a few hours to recharge events with sharp discharge peaks and negative electric conductivity and temperature peaks. Discharge separation based on electrical conductivity data reveals that only 20% of the discharge peak is recently recharged water. The natural and artificial tracers thus support the hydraulic model of two diverging storage components building up

the aquifer of the relict rock glacier. While a fine grained (sandy, poorly silty although with larger embedded blocks) inner zone provides the base flow component, a coarse grained, blocky upper zone lacking fine-grained sediments provides the fast run off component.

F

Discharge dynamics of a relict rock glacier in a crystalline catchment in the Seckauer Tauern, Austria

The discharge dynamics of rock glaciers is still poorly understood. In particular studies about springs of relict rock glaciers are rare. However, particularly in crystalline mountain regions (relict) rock glaciers form important aquifers drained by springs with discharge up to several tens of litres. Thus, they are essential for the local ecology and can be used for drinking water supply or hydroelectric power production. This study focuses on the relict Schöneben Rock Glacier in the Seckauer Tauern Range, Austria (E14°40'26'', N47°22'31''). The relict rock glacier covers an area of 0.11 km² extending between 1720 and 1905 m a.s.l.. It consists predominantly of coarse-grained gneissic sediments and is covered with blocks up to a size of several cubic metres. The entire spring catchment, including the relict rock glacier, covers 0.76 km² with a maximum elevation of 2282 m a.s.l.. The discharge of the rock glacier spring has been recorded since 2002. Furthermore, electrical conductivity and water temperature have been recorded since 2008. These data were used to analyse the recession behaviour of the spring, to separate the discharge components and to characterize the hydraulic aquifer properties. Furthermore, a tracer test with simultaneous injection of the fluorescent dyes naphtionate and fluorescein at two injection points (one close to the front and one close to the rooting zone of the rock glacier) was conducted in order to obtain information about the travel times of the water through the rock glacier.

The observed spring hydrograph exhibits a slow base flow recession but sharp discharge peaks after rainfall events comparable to karst aquifers. This similarity is also indicated by the electrical conductivity and temperature of the spring water responding strongly and only slightly delayed after the rise in discharge. The spring hydrograph can be decomposed in three exponential recession functions with different recession coefficients depending on the range of discharge: (a) discharge >40 l/s = 0.2-0.07 [1/d], (b) discharge 10-40 l/s = 0.07-0.03 [1/d], (c) discharge <10 l/s = 0.02-0.006 [1/d]. In the artificial tracer experiment, the peak of the fluorescein breakthrough curve was observed between 79 and 108 days after the tracer injection, which agrees well with the (reciprocal of the) recession coefficient of the base flow (α=0.02-0.006 [1/d] corresponding to a response time of 50-

167 days). Naphtionate, which was injected close to the front, was not detected during an observation period of 6 months. As opposed to the long travel times of the artificial tracers, the hydrograph separation based on the electrical conductivity of the spring water reveals that soon (approximately 3 hours) after the rise in discharge a significant portion (up to 50 %) of the discharging water originates from rapid recharge. The water temperature shows a sharp negative peak after recharge events, which might indicate some small remaining permafrost bodies in the rock glacier. A first conceptual model of the relict rock glacier assumes a coarse-grained mantle with high hydraulic conductivity, capable to transport the rapid recharge and a core with lower hydraulic conductivity, resulting in a slow base flow recession.